# ADSORPTION OF CHLOROMETHANES FROM WATER USING ACTIVATED CARBON / METAL OXIDES NANOPARTICLES

BY

MOHAMMED SALAH AHMED ABDELBASSIT

A Thesis Presented to the

DEANSHIP OF GRADUATE STUDIES

**KING FAHD UNIVERSITY OF PETROLEUM & MINERALS**

DHAHRAN, SAUDI ARABIA

In Partial Fulfillment of the
Requirements for the Degree of

# MASTER OF SCIENCE

**In**

CHEMISTRY

MAY, 2014

KING FAHD UNIVERSITY OF PETROLEUM & MINERALS

DHAHRAN- 31261, SAUDI ARABIA

**DEANSHIP OF GRADUATE STUDIES**

This thesis, written by MOHAMMED SALAH AHMED ABDELBASSIT under the direction his thesis advisor and approved by his thesis committee, has been presented and accepted by the Dean of Graduate Studies, in partial fulfillment of the requirements for the degree of **MASTER OF SCIENCE IN CHEMISTRY.**

Dr. Khalid Alhooshani
(Advisor)

Dr. Abdullah J. Al-Hamdan
Department Chairman

Dr. Abdulaziz Alsaadi
(Member)

Dr. Salam A. Zummo
Dean of Graduate Studies

Dr. Tawfik A. Saleh

29/5/14
Date

عمادة الدراسات العليا
DEANSHIP OF GRADUATE STUDIES

# Dedication

This thesis is dedicated to my great parents for their unconditional love, prayers, endless support and encouragement, my dearest wife, who leads me through the valley of darkness with light of hope and support and my beloved brother and sisters.

# ACKNOWLEDGMENTS

I am extremely grateful to Allah who gave me the health and ability to accomplish this work. I would like to thank King Fahd University of Petroleum and Minerals (KFUPM) for giving me the opportunity to complete my master's degree.

I would never have been able to finish my thesis without the guidance of my committee members, help from friends, and support from my family and wife. I would like to express my deepest gratitude to my advisor Dr. Khalid Alhooshani for his excellent guidance, caring, patience, and providing me with an excellent atmosphere for doing research and directions as well as the other committee members: Dr. Abdulaziz Alsaadi and Dr. Tawfik A. Saleh. My special thanks to the chemistry department presented by Dr. Abdullah J. Al-Hamdan and my graduate advisor Dr. Bassam Al-Ali for their assistance and help during my studies. And all of my thanks to the chemistry department faculty and staff.

# TABLE OF CONTENTS

# LIST OF TABLES

# LIST OF FIGURES

# LIST OF ABBREVIATIONS

**AC** : Activated Carbon

**$CeO_2$-NP/AC** : Ceria Nanoparticles Activated Carbon

**Cl-VOCs** : Chlorinated Volatile Organic Compounds

**EDX** : Energy Dispersive X-ray analysis

**FT-IR** : Fourier Transform Infra-red Spectroscopy

**HS-GC-MS** : Headspace Gas Chromatography Mass Spectrometer

**NMOsNPs** : Nonionized Metal Oxides Nanoparticles

**MOS** : Metal Oxide Semiconductor

**SEM** : Scanning Electron Microscope

**SIM** : Selected Ion Monitoring

**TIC** : Total Ion Chromatogram

**$SiO_2$-NP/AC** : Silica Nanoparticles Activated Carbon

**ZnO-NP/AC** : Zinc Oxide Nanoparticles Activated Carbon

# ABSTRACT (ENGLISH)

Full Name : Mohammed Salah Ahmed Abdelbassit

Thesis Title : Adsorption of chloromethanes from water using activated carbon / metal oxides nanoparticles

Major Field : Chemistry

Date of Degree : May, 2014

In the presented work, four adsorbents: activated carbon derived from waste tire rubber, activated carbon loaded with zinc oxide nanoparticles (ZnO/AC), silica nanoparticles and Ceria nanoparticles were prepared and examined for removal of chloromethanes namely: dichloromethane, trichloromethane and carbon tetrachloride from aqueous solutions. Nanoporous carbon (NC) prepared from waste tires by pyrolysis. Further surface-modification was carried out by successive treatment with $H_2O_2$ and $HNO_3$ and the composites were prepared by co-precipitation methods followed by calcinations at high temperature. The produced adsorbents were characterized using different techniques such as scanning electron spectroscope (SEM), energy dispersive X-ray spectroscope (EDX), FTIR spectrophotometer, and X-ray diffraction. Batch experiments were performed by using different adsorbent dosages, initial concentrations, and contact time. The kinetics of the adsorption for these pollutants onto the adsorbents was undergo to the pseudo second-order kinetic model, Freundlich and Langmuir models were abide to the adsorption process and the hydrophilic fraction adsorption fitted the intraparticle diffusion model. The order of the sorption efficiency is as following: $SiO_2$-NP/AC > ZnO-NP/AC > $CeO_2$-NP/AC > AC.

# ABSTRACT (ARABIC)

## ملخص الرسالة

**الاسم الكامل: محمد صلاح أحمد عبدالباسط**

**عنوان الرسالة: إدمصاص مركبات الكلوروميثان من الوسط المائي بإستخدام الكربون المنشط/أكاسيد المعادن النانوية.**

**التخصص: كيمياء**

**تاريخ الدرجة العلمية: مايو 2014**

**لقد تم في هذا البحث تحضير أربعة أنواع جديدة من الممتزات وهي كما يلي: الكربون المنشط المشتق من مخلفات إطارات السيارات المستعملة ، الكربون المنشط/أكسيد الزنك النانوي،الكربون المنشط/أكسيد السليكون النانوي والكربون المنشط/أكسيد السيريوم النانوي. المرحلة الثانية هي إختبار مدي كفاءة هذه الممتزات في إمتزاز مركبات الكلوروميثان والتي تعتبر من الملوثات البيئية وبالتحديد تم إستخدام ثلاثة مركبات محضرة في الوسط المائي بتراكيز مختلفة وهي ثنائي كلوروميثان، ثلاثي كلوروميثان ورباعي كلوروميثان. إن الكربون المنشط ذو المسام النانوي تم تحضيره عبرعدة خطوات وهي التفكك الحراري في جو خامل من غاز الهليوم ومن تم التنشيط الفيزيائي واخيرا الكيميائي بواسطة بيروكسيد الهيدروجين وحمض النيتريك.**

**بالنسبة للممتزات الأخري تم تحضيرها عن طريق الترسيب المشترك ومن ثم تسخين الناتج عند درجة حرارة عالية. هنالك عدة طرق تشخيصية أستخدمت لتحديد شكل وتركيب الممتزات وأيضا الثبات الحراري. حركية الإدمصاص لقد تم دراستها ووجد أنها تتبع للرتبة الثانية الكاذبة كما تم دراسة أيزوثريم الإدمصاص والنتائج خضعت للانغمور أيزوثيرم كما تم إعادة إستخدام الممتزات لثلاثة مرات وأعطت نفس الكفاءة الامتزازية. من خلال المقارنة بين الممتزات الأربعة وجد أن ترتيبها من حيث الكفاءة الإمتزازية كالأتي: ،الكربون المنشط/أكسيد السليكون النانوي > الكربون المنشط/أكسيد الزنك النانوي > الكربون المنشط/أكسيد السيريوم النانوي > الكربون المنشط.**

# CHAPTER 1

# INTRODUCTION

Hazardous volatile organic compounds (VOCs) which are typically used as solvents, cleaning agents, coating agents, and extractants in different industries, are released from various chemical and pharmaceutical industries (J. Lemus, 2012). Chloromethanes are considered hazardous waste materials and are produced in large amounts for different applications (C. S.-F. B. de Rivas 2012). The proper disposal and monitoring of these compounds is of significant concern on the environment due to their stability, and the accumulation in of these compounds in the environment also contributes to the contamination of groundwater, which threatens living beings and can be considered dangerous and toxic organic pollutants ((ATSDR) 1997). Additionally, these compounds cause a depletion in the ozone layer of the atmosphere and act in conjunction with photochemical smog to increase global warming (E. Dobrzynska, 2010). Furthermore, the chloromethanes are used in large-scale quantities by industries and are then released as industrial effluent waste (Yu J.-J. C.-Y., 2000; Shawwa A. S., 2001) Most of the chloromethanes are classified as carcinogenic and toxic (R. Iranpour 2005). These compounds, when released into the environment via industrial exhausting gases or wastewater streams, present direct and serious impendence to all living organisms. Thus, it is important to eliminate these compounds before discarding the wastewater to the environment. Therefore, chloromethanes were classified as highly harmful compounds,

and the emission monitoring and regulation was begun by the U.S. Environmental Protection Agency. Adsorption technology is one of the most commonly used techniques in the elimination of chlorinated volatile organic compounds (Cl-VOCs). Activated carbon is most frequently used material among the different adsorbents due to large surface area, unique microporosity and low cost (Lillo-Ródenas et al 2005). Different methods for removal of Cl-VOCs have been reported. For example, cryogenic condensation (Gupta, 2002), biofiltration (Xie, 2009), wet absorption methods (Chungsiriporn, 2006) as well as catalytic oxidation (Palacio, 2010) and thermal oxidation connected with recuperation are a few example methods (Salvador, 2006). Volatile organic compounds (VOCs) are expressed by the US EPA as compounds which have high stability and possess a vapor pressure higher than 0.1 mmHg (13.332Pa) (Arjan Giaya 2000). Chloromethanes compounds are one of the VOCs containing at least one covalently bonded chlorine atom. The environmental pollution produced by industrial wastewaters from many industries including herbicide, pesticide, paint, solvent, pharmaceutical, pulp, and paper (Sonoyama 2001). The maximum solubility of dichloromethane (17,220mg$L^{-1}$) which is higher compared to the chloroform and carbon tetrachloride 8250 and 825 mg$L^{-1}$, respectively (Rexwinkel 1999). Chlorinated hydrocarbons are absorbed readily via the digestive system and lungs when breathed and transferred to body in the blood. They can be collected in the liver, kidneys, brain, or fatty tissues in short time. In liver, it changes into other compounds and finally passes out of the body. Generally most of these compounds are discarded from the body within few days after the exposure. High dosage was observed to cause dizziness, decrease the ability to concentrate and remember, damage the nervous system, and lead to an irregular

heart beat that are exposed in the work place and in laboratory animals (Parker 1997, V. Hecht 1995, R.F. Dunn 1994).

## 1.1 Statement of the problem

Many Cl-VOCs are harmful compounds to human health and the environment. The chloromethanes have been considered as contaminants for the ground water. These compounds must be monitored under serious environmental regulations due to their toxicity, carcinogenicity (J.W. Lee 2005 ). These compounds are also causes decaying of the stratospheric ozone layer, global warming and the photochemical smog formation, and the effect on human tissues (J. Pires 2001 ). As a results enhanced adsorption must be used by designing more efficient adsorbents.

## 1.2 Objectives of the study

- Development of some nanocomposits adsorbent prepared from activated carbon with some metal nanoparticles like ZnO/AC and $CeO_2$/AC. The activated carbon was prepared from waste materials.
- Characterization of the prepared adsorbents by using different analytical techniques like scanning electron microscope (SEM), (EDX), (TGA),(XRD) and spectroscopic characterization by FT-IR.
- Treatment of the chloromethanes (dichloromethane, chloroform and carbon tetrachloride) by the developed materials.
- Evaluating the performance by applying the kinetic order models and adsorption isotherm models such as Langmuir, Frundlich and Temkin isotherms.

## 1.3 The significance of the study

It is a worldwide problem nowadays to get a clean source of drinking water. Thus, this study will develop a process for water treatment. The focus will be on chloromethanes, mainly three compounds (dichloromethane, chloroform and carbon tetrachloride).

# CHAPTER 2

# LITERATURE REVIEW

Desalinated water it can be used for different purposes its use for drinking and other related domestic purposes. Thus, it is important to introduce a safe water supply. Chloromethanes have a wide applications in the chemical and pharmaceutical industries, they have been used as solvents and in aerosols, dry cleaning, adhesives, etc. (Z.M. de Pedro 2006). The toxicity of Cl-VOCs is related to their difficulty to biodegradation and, accumulation in the environment. They classified as carcinogenic or toxic and exhibit potential hazard under exposed (R. Iranpour 2005).

## 2.1 Methods for removal of chlorinated hydrocarbons

Depending on their concentration in water and on the usage of the treated water, different methods have been used for the removal of chloromethanes and their recycling treatment (V. Janda 2004). These methods include photocatalytic degradation, ultraviolet (UV) oxidation, biological treatment, air stripping, and thermal treatment (Jin Chul Joo 2013). Other methods for removal of Cl-VOCs have been reported, such as cryogenic condensation (Gupta 2002), biofiltration (Xie 2009), wet absorption methods (Chungsiriporn 2006) as well as catalytic oxidation (Palacio 2010) and thermal oxidation connected with recuperation (Salvador 2006). There are different porous materials that can be used as adsorbents like: zeolites (J. A. Pires 2002), clays (López-Cortés 2008), MCM-48 (W.G. Shim 2006), silica and spherical silicas (Hung 2009), organically

modified silica adsorbents and activated carbon from various precursors (Rafał Janus 2011).

Adsorption technology is one of the most widely used methods for the treatment of Cl-VOCs. (Lillo-Ródenas et al 2005). Adsorption by activated carbon provides high efficiency for the removal of organic, inorganic heavy metal ions, and volatile chlorinated hydrocarbons contaminants from industrial wastewater and drinking water (Sotelo 2002, Yun 1998). Nowadays, activated carbon is the most commonly used material for the removal of VOCs due to its high surface area, unique microporous structure, and low cost (Pan, 2013). The main method for the removal of chloromethanes is incineration, but the problem is producing other compounds which are more hazardous than the target contaminants, like phosgene, dioxins and furans (D. Verhulst et al 1996 , A. Buekens et al 1998). Different treatments are being investigated for the removal of chloromethanes, such as hydrodechlorination by using different kinds of the catalysts, like Pt or Pd. The hydrodechlorination with Pt or Pd method is promising due to the high conversions, but the deactivation of the catalyst is its limitation (Jesus Lemus 2012). Non-destructive techniques like adsorption, condensation and absorption are the most frequently applied for the removal/recovery of chloromethanes from gas streams (A. Anfruns 2011, X. Ren 2011 ).

## 2.2 Metal oxide nanoparticles

Metal oxides nanoparticles represent a high surface area with nano-sized building blocks (H. M. K. Yogesh Kumar 2013). The most important factors for these surfaces are the size and shape of nonionized metal oxides nanoparticles NMOsNPs, which can affect their adsorption efficiency. Many studies have been conducted on the synthesis of metal

oxide nanomaterials, and these studies managed to prepare nanomaterials which were of different shapes, highly stable, and nonagglomerated. There are two types of the methods for the synthesis : (1) physical methods, which include high-energy ball milling with severe plastic deformation and (2) chemical methods, including chemical vapor condensation, controlled chemical co-precipitation, pulse electrode position, liquid flame spray, liquid-phase reduction, gas-phase reduction, etc (L. Li 2006 ). In addition to the the widely used aforementioned techniques, others methods include co-precipitation (A.L. Willis 2005, B.L. Cushing 2004), thermal decomposition and/or reduction (J. Park 2004), and hydrothermal synthesis (X. Wang 2005 ), which produced the metal oxides nanoparticles with high yield percent (Y. Ju-Nam 2008).

### 2.2.1 Zinc oxide nanoparticles

Zinc oxide nanoparticles are environmentally friendly and have many applications in photocatalysis (H.B. Zeng 2008, G.H Chen 2008), gas sensors (Z.H. Jing et al 2008), solar cells (T.P. Chou 2007 ). As an adsorbent, ZnO has been primarily used for removal of $H_2S$. However, recently ZnO nanoparticles have been used with high efficiency in the removal of heavy metals (W. C. X.B. Wang 2010). For example, Lee et al, (J.H. Lee 2005 ) synthesized (ZnO) nanoparticles powder via "solution-combustion method (SCM)" which was tested on the removal of $Cu^{2+}$ ions from the solution and resulted in high adsorption capacity. There are several different methods by which high surface area ZnO nanoparticles can be created, such as the following: hydrothermal (T.M. Shang 2007, F. Xu 2006 , X.L Cao 5267–5270), solvothermal (T. Ghoshal 2007), chemical vapor deposition (N. Zhang 2009, C. Xu 2006 ), electrochemical deposition (B.Q. Cao 2007 , B. Illy 2005), and microwave methods (Z.H. Jing et al 2008). ZnO

nanoplates exhibit properties like $TiO_2$, and has advantages that include being an inexpensive material, easy preparation, and suitable to tailor morphologically (X.F. Ma 2010). More specifically, the solvothermal method for preparation of ZnO nanoplates (W. C. X.B. Wang 2010) contains two non-polar terminal planes with several micrometers in the planar direction and is 10–15 nm in thickness. To summarize, zinc oxide nanoparticles impregnated on activated carbon (ZnO-NP-AC) are non-toxic and thus suitable for being a "green" adsorbent (H.B. Senturk 2009 ).

### 2.2.2 Cerium oxide nanoparticles

Ceria is an inexpensive, nontoxic, and highly stable material. Therefore, ceria has been used as a component to prepare composite oxides (J.R. Xiao 2006, Y.H. Xu 2006). Ceria is a rare earth metal oxide which is commonly used in the industry as a catalyst, UV protectant, and in many applications as adsorbents, shielding materials, fuel cells, gas sensors, polishing materials, and luminescence (S. Yabe 2003, L.Y. Wang 2007, E.L. Brosha 2002). The adsorption capacity of ceria depends significantly on the surface morphologies, sizes, shapes, and areas. Ceria nanoparticles has shown new properties for catalytic activity (S. Carrettin 2004 ), blue shift in absorption spectra (T. F. S. Tsunekawa 2000), lattice expansion (K. I. S. Tsunekawa 2000), phase transformation, and photovoltaic response (A. Corma 2004 ). Cerium oxide nanoparticles were prepared by converting $Ce^{3+}$ to $Ce^{4+}$ with an oxidizing agent under alkaline conditions and stabilized by hexamethylenetetramine (HMT) (F. Zhang 2004). During this process, $CeO_2$ nanocrystals can be stabilized by HMT which prevents agglomeration of nanoparticles through formation of double electrical layer. The mean size of the prepared material was 12 nm. The development of new synthesis

approaches and the application of highly dispersed cerium oxide nanoparticles on activated carbon materials has been studied intensively. Namely, $CeO_2$/AC composite was synthesized by the chemical co-precipitation through impregnation method with cerium nitrate salt (J.C. Serrano-Ruiz 2008, E. Ramos-Ferna´ndez 2008).

### 2.2.3 Silicon oxide nanoparticles

Silica is a widely available in the earth's crust, but it has low reactivity and thus, is limited in its direct use (Uhrlandt, 2006). On the other hand, the crystalline shape and microstructure of various silica products have many uses. The amorphous silica, which has high specific surface area (porous material with a small size of the particle), is widely used in many applications, such as absorbents, thermal insulators, and catalyst supports (J. L. Gurav 2010, GM 2003, Adam 2012). Furthermore, silica has unique properties due to its stability, possibility to be regenerated, fast equilibrium, high mechanical resistance, and high surface area; therefore it is considered distinguish adsorbents (A.R. Cestari, 2006 ), also it can decorated by different surface groups (M.A. Hassanien, 2006). Many studies have been conducted using functionalized silica materials as adsorbent in pollutant removal (V.K. Gupta S. , 2009 ; N.M. Mahmoodi, 2011).

Many studies produced silica nanoparticles, but a silicon source is needed as a precursor, and silicon alkoxides are a commonly used material for such a precursor (Soleimani Dorcheh 2008, Vivero-Escoto 2010). Silicon alkoxides (such as tetraethoxysilane) can be produced from the carbothermal reduction raw sand (RM Laine 1991, Rösch 2000). Silica nanoparticles are commonly used nanomaterial for many industrial applications such as, packaging, high-molecule composite materials, and ceramics production (Xifei Yang 2013). Silica nanoparticles can also be used as

hardening agent and in different medical applications because it is biocompatible and non-toxic (L. Yang 2013). The silica nanoparticles can be used as an impregnated medium for the synthesis of surface-modified silica, which means it works well as an adsorbent and high capacity cation exchange (J. Wang 2010 , R. Serna-Guerrero 2010).

## 2.3 Activated carbon

Adsorption is a highly efficient processes that can be used for removing certain organic and inorganic contaminants from wastewater. Carbonaceous adsorbents, like activated carbon and granular carbon, have been used in the treatment of the wastewater because it is a cost-effective material, has a high capacity of adsorption, and is generally available locally (Wang 2007). Due to the aforementioned properties, activated carbon has a applicable for industrial uses, especially in the water purification and industrial wastewater treatment (Jankowska 1991, Gonzalez-Serrano 2004). Furthermore, carbonaceous adsorbents are most commonly applied toward the treatment and removal of species from aqueous effluents. Additionally, granular activated carbons have been investigated for their ability to uptake volatile compounds and have been shown to be highly efficient at reducing the contaminants to undetectable levels, which prevents the disposal of harmful volatile compounds into the atmosphere (Stenzel 1995, Bansode 2003). Adsorption via activated carbon (AC) has been commonly used for the up taking of gaseous organic contaminants (P. Navarri, 2001; X. Zhang, 2011 ).

The ability of commercially available activated carbons (GAC 1240, GCN 1240, RB 1, pK 1-3, ROW 0.8 SUPRA) to remove chloromethanes from wastewater was investigated, and the best adsorbent was reported to be GAC 1240 granulated activated

carbon (Pavonia et al., 2006). Commercial activated carbon (CAC) has limitations for its usual as material that can be used for removal of environmental contaminants because of its high cost, and for this reason, researchers have developed cost-effective adsorbents and have investigated different raw starting materials (eg: bagasse sugar, starch xanthenes, sawdust of *Pinus sylvestris*, chitosan, bentonite, and discarded automobile tires) for activated carbon synthesis (C. J. V.K. Gupta 2003, W.S. Wan Ngah 2005, G. Bereket 1997, F. Calisir 2009). Tire rubber is one of the promising materials in the synthesis of activated carbon; it is composed from different elastomers, such as butadiene rubber, natural rubber, and styrene butadiene rubber besides other additives such as sulfur, carbon black, and zinc oxide (R. Murillo 2006). About 32% by mass of the rubber tire is the carbon black; therefore, the total carbon content between 70–75 wt % (B. G. V.K. Gupta 2011 ). Production of activated carbon from waste tires for aqueous phase treatment of contaminants has recently received more interest (Miguel 2002, Ariyadejwanich 2003, Hamadi 2004, Mui 2010).

# CHAPTER 3

# Experimental

## 3.1 Chemicals and materials

Three chloromethanes standards were used in this study: dichloromethane ($CH_2Cl_2$, 99 %, 84.93 g/mol), chloroform ($CHCl_3$, 99% , 119.38 g/mol) and carbon tetrachloride ($CCl_4$, 99%, 153.82 g/mol). These chloromethane standards as well as the Zinc nitrate and ammonia were obtained from Sigma-Aldrich.

## 3.2 Preparation of the adsorbents

### 3.2.1 Preparation of Activated Carbon (AC)

The procedure for the synthesis of activated carbon (AC) from waste rubber tire material is explained by Gupta et al, (Vinod Kumar Gupta 2013 ). The waste of rubber tire was heated to 300 ˚C to isolate the black oil and yellow diesel oil. Then, the granules were carbonized by thermal pyrolysis under helium gas at 500˚C for 3h. The carbonaceous material was heated with steam at 900˚C for 2h to develop its porosity system. The chemical activation was performed via $HNO_3$ and $H_2O_2$ treatment in order to develop oxygen groups on the surface of the material. The carbonaceous material was treated with $HNO_3$ (4M concentration) with a ratio of 1g of carbon to 20 mL of $HNO_3$ and then heated at 60˚C for 24h. Next, the product was washed and dried at 100˚C and then followed by

treatment by $H_2O_2$ (6%) with a ratio of 1 g/20mL carbon/$H_2O_2$. Again, it was washed and dried at 100˚C.

### 3.2.2 Preparation of ZnO-NP/AC

ZnO nanoparticles loaded with AC were prepared via thermal co-precipitation. 6.0g of the prepared AC was suspended in 150 mL of deionized water and dispersed with a sonicator. A 6.975g of Zn $(NO_3)_2.6H_2O$ was dissolved in 50 mL of deionized water and then added gradually to the previous mixture. The mixture was stirred for 2h. The pH of the mixture was adjusted between 8-9. Next, that the solution was refluxed at 90˚C for 6h with constant stirring. The precipitate was collected by filtration and thenwashed and dried at 110˚C overnight. The composite was calcined at 350˚C for 4h.

### 3.2.3 Preparation of $SiO_2$-NP/AC

The composite of $SiO_2$–NP/AC was prepared via co-precipitation method. 6.0g of AC was dispersed in 150mL of suitable media by the use of sonicator. A 50mL solution containing 3.8g of sodium meta silicate was prepared and then added drop-wise into the AC mixture. This new mixture was stirred for 24h at 50$^o$C. The mixture was pH-controlled while being heated under reflux at 90$^o$C for 12h with stirring. The precipitate was then cooled, filtered, washed and dried at 110$^o$C overnight. The product was calcined at 350$^o$C for 4h.

## 3.3 Characterization of the adsorbents

The characterization of the adsorbents was achieved by using a combination of various techniques and analyses, which included: 1. scanning electron microscope (SEM) to show the morphology of the developed adsorbents, 2. energy dispersive X-ray

spectroscopy (EDX) and X-ray diffraction spectroscopy (XRD) for compositional analysis, and 3. thermogravimetric analysis (TGA) to reflect the physical and chemical structure changes during the conversion and to provide thermal stability information. Some spectroscopic techniques like infrared spectroscopy were used to determine the functional groups present on the surface of the adsorbents.

### 3.3.1 Fourier Transform Infrared spectroscopy (FT-IR)

FT-IR (Nicolet 6700 spectrometer-Thermo electron, USA) was provided by OMNIC software, and verified with a deuterated triglycine sulfate (DTGS) detector. The samples were prepared via the solid KBr pellet techniques, and the spectra were obtained by using the transmittance mode with wave number over range between (4000-400 $cm^{-1}$). The background correction of the spectra was performed by 16 scans with resolution 2 $cm^{-1}$ for the correction of background noise.

### 3.3.2 Field Emission Scanning Electron Microscope (FE-SEM)

Field emission scanning electron microscope (TESCAN LYRA 3 FEG) model was used for identification of the surface morphology and nanostructure of the prepared adsorbents.

### 3.3.3 Energy Dispersive X-ray Analysis (EDX)

Energy dispersive X-ray spectroscopy (EDX) instrument model ( Oxford-England and X-Max detector) was used for the determination of the chemical composition of the adsorbents.

### 3.3.4 X-ray Diffraction Analysis (XRD)

X-ray diffraction results were obtained by using (Shimadzu XRD Model 6000, Japan) diffractometer (Kα radiation of Cu); the instrument was operated at 40kV and 30mA.

### 3.3.5 Thermogravimetric Analysis (TGA)

Thermogravimetric analysis was performed using SDT analyzer (Q 600) that is manufactured by TA instruments (USA). The sample being tested (usually 6mg) was placed in an aluminum crucible. The temperature was raised at a uniform rate of 15$^{o}$C /min. The analyses were made over a temperature range of 20–900$^{o}$C in a nitrogen atmosphere flowing at a rate of 50 ml/min.

## 3.4 Batch sorption procedure

The equilibrium adsorption isotherm was studied by using batch adsorption procedures. These batch equilibrium studies were conducted by using the composite materials within a solution of chlorinated hydrocarbons in a series of 125mL conical, airtight Pyrex glass flasks. A few different parameters were recorded, such as 1. the effect of the composite dosage in a range between (0.25-5 g/L), and 2. the effect of initial concentration and contact time. Each flask contained 50ml of a chlorinated hydrocarbons solution with the desired pH and temperature being adjusted. A predetermined amount of the composite was added to each flask and placed in an isothermal shaker at 150 rpm until equilibrium was achieved. The chlorinated hydrocarbon adsorption at a certain time, t, ($q_t$, mg/g) was identified by equation (1):

$$q_t = (C_o - C_t) \times \frac{V}{m} \qquad (3.1)$$

Where V is the volume of chlorinated hydrocarbons solution in liters, $C_o$ (mg/L) and $C_t$ (mg/L) are the initial and final concentrations at time t of chlorinated hydrocarbons in solution, respectively and m (grams) is the weight of adsorbent.

## 3.5 Data analysis

The data were collected from the batch study at different adsorbent dosages, and concentrations (20,10,5 ppm) were analyzed by using kinetic study and applying (pseudo-first order, pseudo-second order and intra-particle diffusion). Also, different adsorption isotherm models were conducted (langmiur isotherm, Freundlich isotherm and Temkin isotherm) to identify the adsorption capacity.

## 3.6 Analysis of chloromethanes

The analysis of chlorinated hydrocarbons was carried out by using the Headspace Gas Chromatography Mass Spectrometer (HS-GC/MS). Sample analysis was conducted by using an Agilent 7890A GC interfaced with an Agilent 5975C network mass selective detector. Direct headspace automated injection was performed by using 2.5 ml-HS syringe with and injection of 250 µL of the headspace vapor. The incubation temperature was optimized in the range between 40-70℃ for 1-20min, and the optimum temperature and time were found to be 60℃ and 15 min respectively. Additionally, 10 ml vials were used, and the optimum volume was found to be 1mL. The agitation speed was 250 rpm, syringe temperature 50˚C, and the injection speed was 500 µL/sec. GC–MS conditions were optimized and adjusted, as measured by maximum sensitivity, according to the baseline separation of analyte and Gaussian peak shapes. The inlet of the GC was operated in split 50:1 mode at 180˚ C. The oven temperature program was as follows:

35℃ for 10 min, then increased at a rate of 5℃/min to 40℃ for 1 min, then 15℃/min to 120℃ for 2 min, then 20℃ /min held at 120℃ for 11 min (total run time 17.33min). The helium was maintained at a constant flow of 1.4 ml/min by using a capillary column, HP-5 (5% phenyl methyl siloxan) 30m x 320 µm x 0.25 µm. The analytes were determined by using a mass spectrometer in electron impact (EI) ionization mode at 70 eV. The mass spectrometer quadruple temperature was set at 150℃ and the mass spectrometer source at 230℃. Optimization experiments were performed in total ion chromatogram (TIC) mode between m/z 40 and 550. Quantification of dichloromethane, trichloromethane, and carbon tetrachloride were performed in selected ion monitoring (SIM) mode, and suitable fragments of the compounds were (the base peaks used for quantification are boldfaced): 49,84,86,88 for dichloromethane; 83,85,47 m/z for trichloromethane and 117,119,121,82 m/z for carbon tetrachloride.

## 3.7 Desorption and regeneration of the adsorbents

Desorption experiments were performed in batch equilibrium procedure as well. All of the experiments started by dispersing used adsorbent 0.1gram into 50 ml of 10ppm chlorinated hydrocarbons mixture after evaporation of the adsorped molecules at 100℃ for 24 hours and then agitating at 25℃ for 120 min with agitation speed 150 rpm for which three recycles were done by repeating the same procedure.

# CHAPTER 4

# Sorption by activated carbon

## 4.1 Characterization of activated carbon

Fourier transform infrared spectroscopy fig (4.1) is the most useful technique to identify the presence of a functional group in the prepared material. The band located around 1640 $cm^{-1}$ represents the enhancement in the aromatic C=C groups (carbonization). The broad band at 3400 $cm^{-1}$ represent O–H mode, and the band at 2900 $cm^{-1}$ is C–H aliphatic mode. Lastly, the band at 1054$cm^{-1}$ is representative of the C-O stretching vibration. The activated carbon morphology was investigated by SEM technique fig (4.2). The SEM image illustrates the porosity of the activated carbon. The image shows two different morphologies. One of them is granular in its structure (0.5µm in diameter). High resolution shows different pore structures on the surface of the adsorbent. EDX analysis was conducted to identify the chemical composition of the adsorbent. The spectrum in fig (4.3) illustrates the presence of carbon and oxygen in the rubber tires carbon. Table (4.1) shows the EDX analysis of prepared activated carbon. The XRD pattern of the carbon exhibits a weak diffraction peak, which can be attributed to the aromatic carbon sheets fig (4.4). The thermal stability was examined by TGA analysis under nitrogen gas as shown in fig (4.5), which shows that the material was stable up to 400˚C.

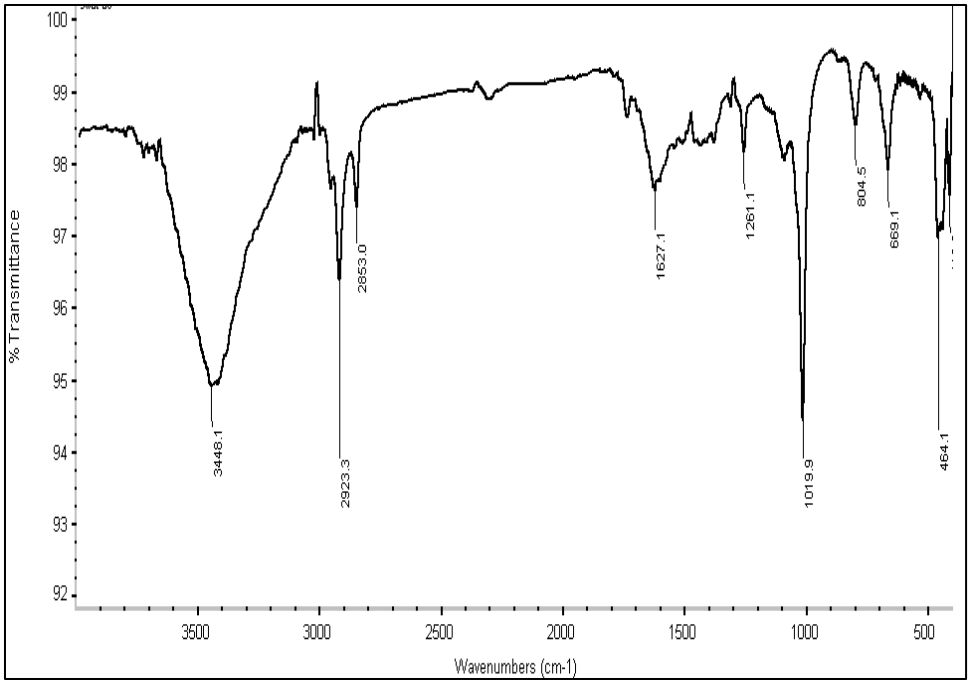


**Figure 4. 1 IR of the AC**

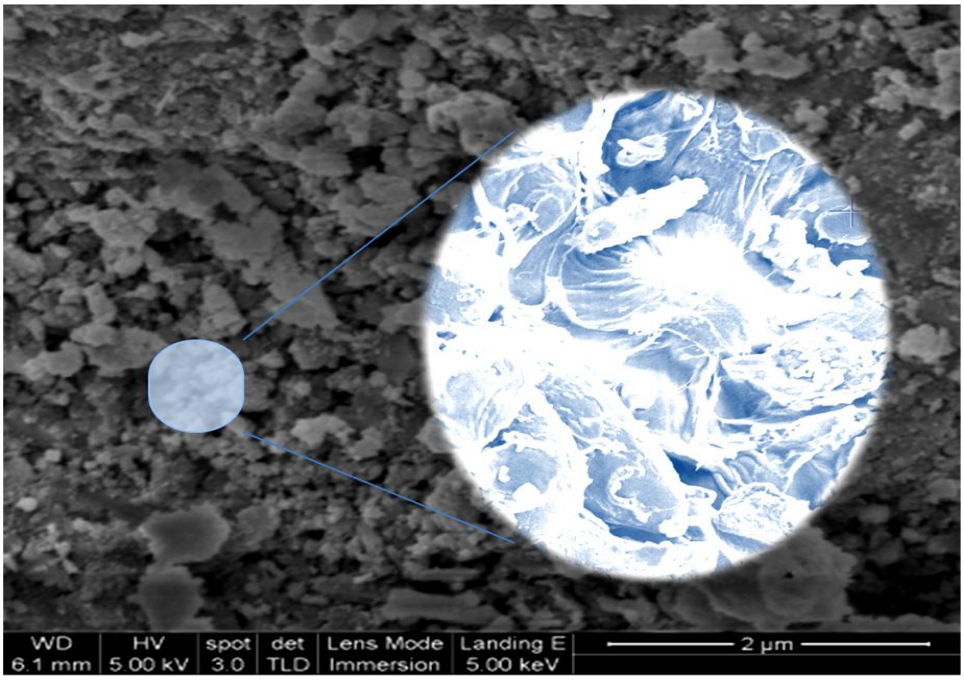


**Figure 4. 2 SEM image of AC**

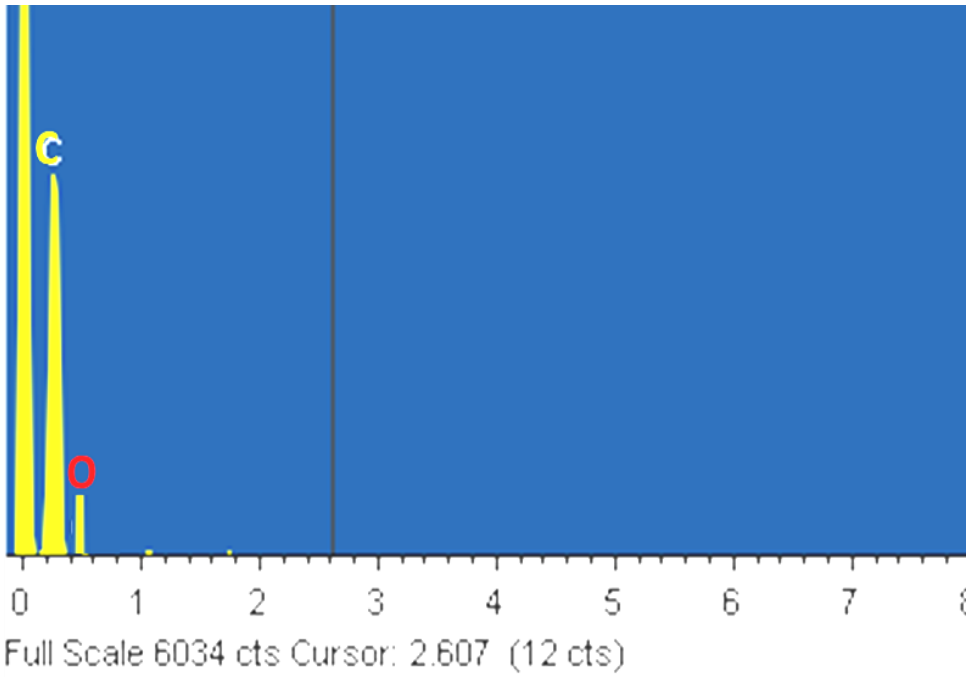


**Figure 4. 3 EDX analysis of AC**

**Table 4. 1 Chemical composition of AC adsorbent.**

| Element | Weight% | Atomic% |
|---|---|---|
| C | 93.95 | 95.39 |
| O | 6.05 | 4.61 |
| Total | 100.00 | |

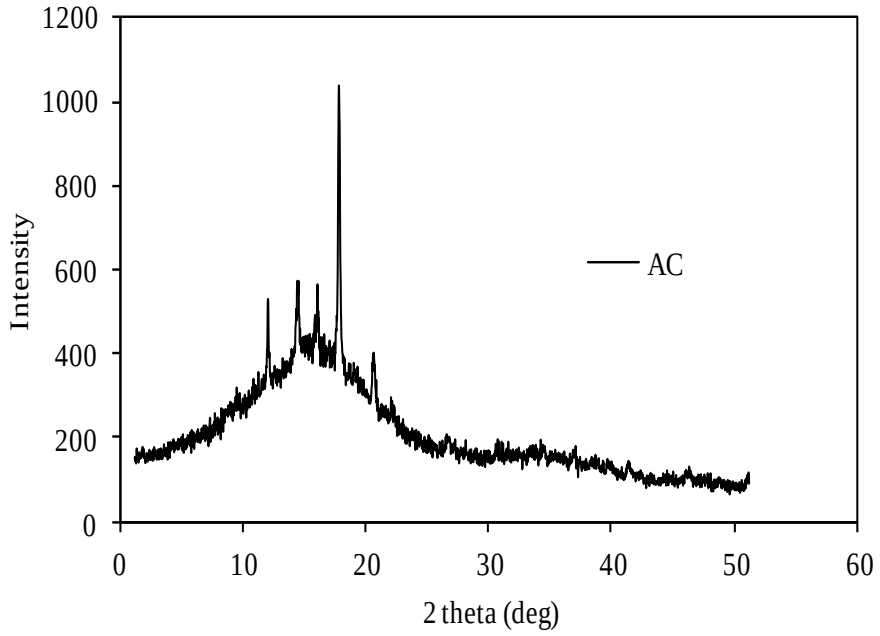


**Figure 4. 4 XRD pattern of AC**

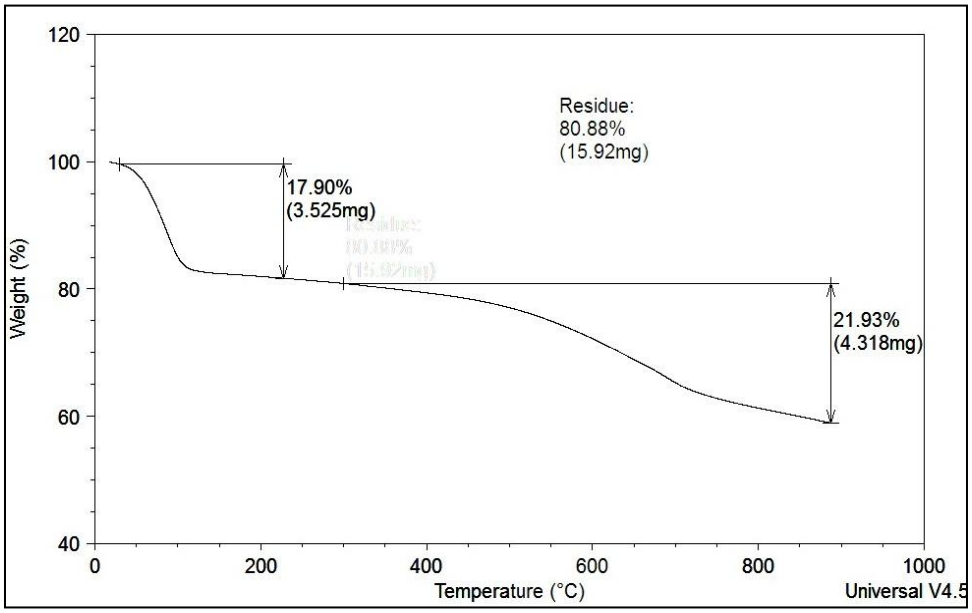


**Figure 4. 5 TGA curve of AC**

## 4.2 Effect of activated carbon dosage and contact time

Adsorbent dosage has a significant effect on the efficiency of the adsorption, depending on the initial concentration of the adsorbate. The effect of activated carbon dose on the adsorption of chlorinated hydrocarbons is illustrated in fig (4.6). Different adsorbent dosages were applied for dichloromethane, trichloromethane, and carbon tetrachloride at initial concentrations 2.0,1.0,0.5 mg/L respectively, at 25˚C with a shaking time of 60 min. Results show that as the adsorbent dosage increased, the percent removal of chlorinated hydrocarbons was increased from 45.35% to 86.96% for dichloromethane, from 79.65% to 98.13% for chloroform and from 95.90% to 99.80% for carbon tetrachloride, with an increase in the amount of adsorbent from 0.5 to 5.0 g/L. This can be attributed to the increase in surface area with an increase in adsorbent amount for a certain concentration of chlorinated hydrocarbons. It can be clearly seen that the increase in chlorinated hydrocarbons removal percentage increases dramatically when the adsorbent mass increase from 0.5 to 5.0 g/L. Finally, the increase of percent removal of chlorinated hydrocarbons was slow when activated carbon dose was greater than 5.0 g/L because some parts of active sites have become saturated by chlorinated hydrocarbons, which diminishes the adsorption process and results in a lower adsorption capacity (Ali 2013). It is obvious from fig (4.7) that the adsorbed amount of chloromethanes was increased by increasing the contact time. Therefore, the adsorption was very fast in the first 10 min and then decrease to a constant at the equilibrium point. The time of saturation is almost reached at 20 min. The percent removal of chlorinated hydrocarbons in solution is calculated by Eq (4.1) as follow:

$$\% \text{ Removal } = \frac{C_\circ - C_e}{C_\circ} \times 100 \qquad (4.1)$$

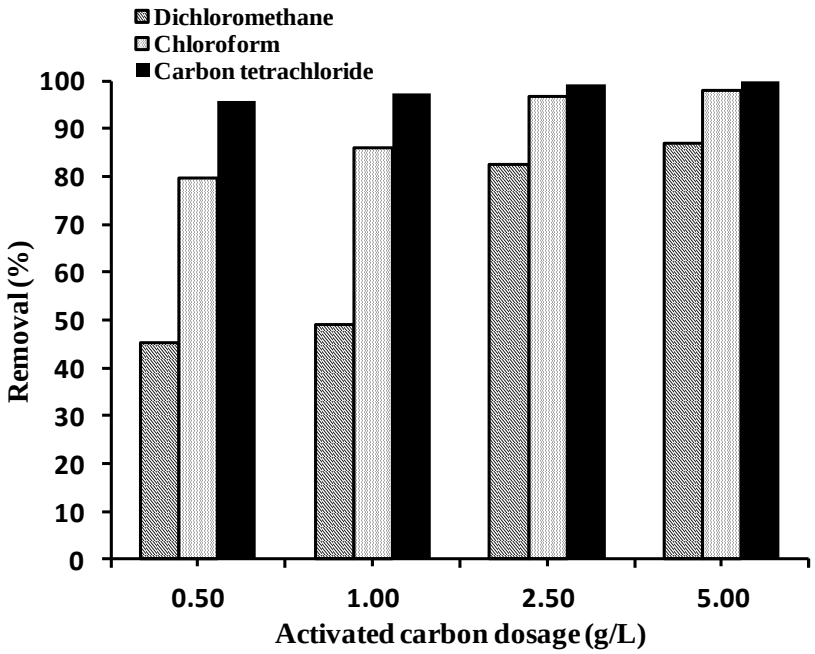


**Figure 4. 6 Effect of adsorbent dosage on the adsorption of dichloromethane, trichloromethane and carbon tetrachloride, time 20 min, temperature 25°C.**

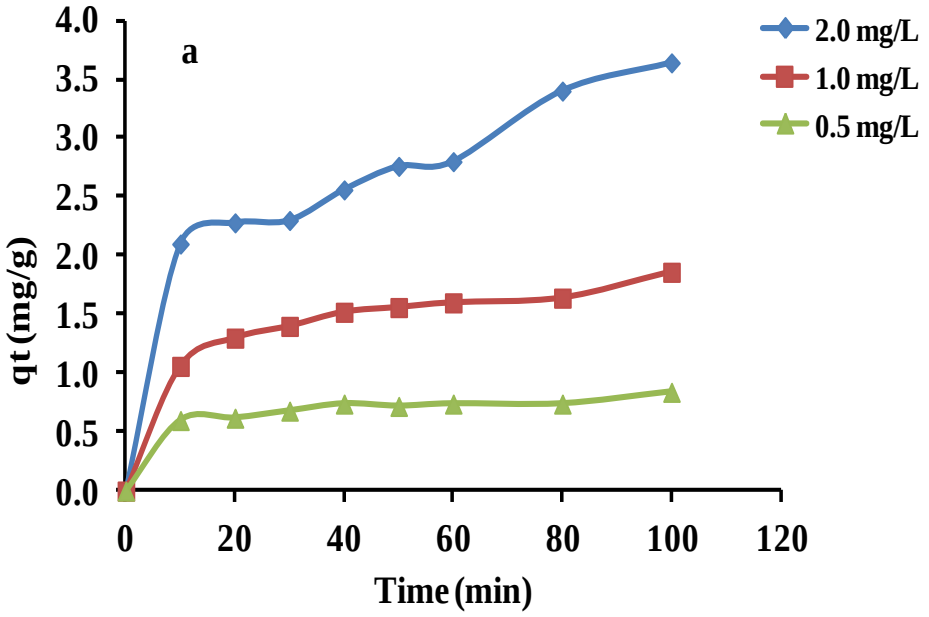

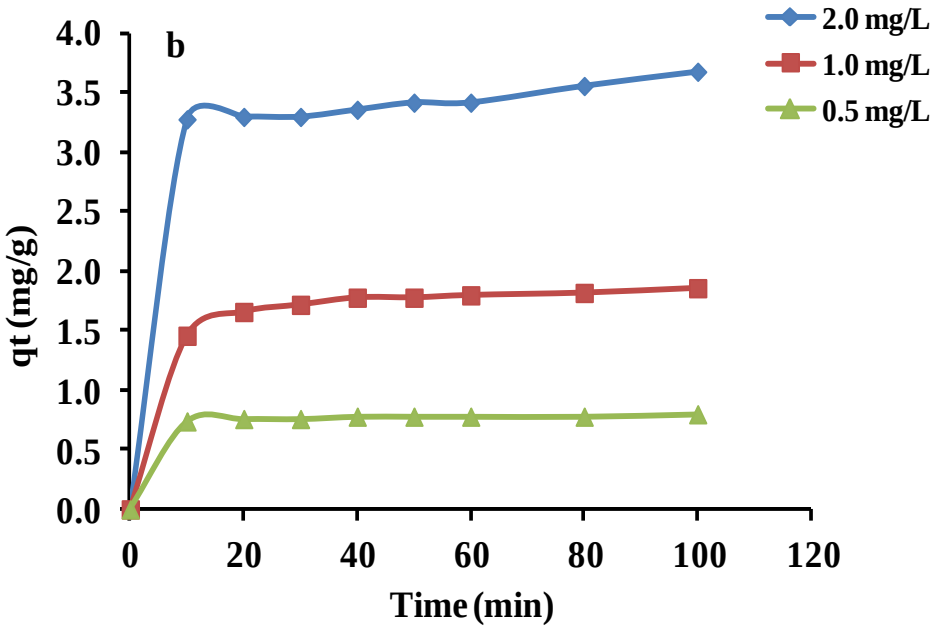


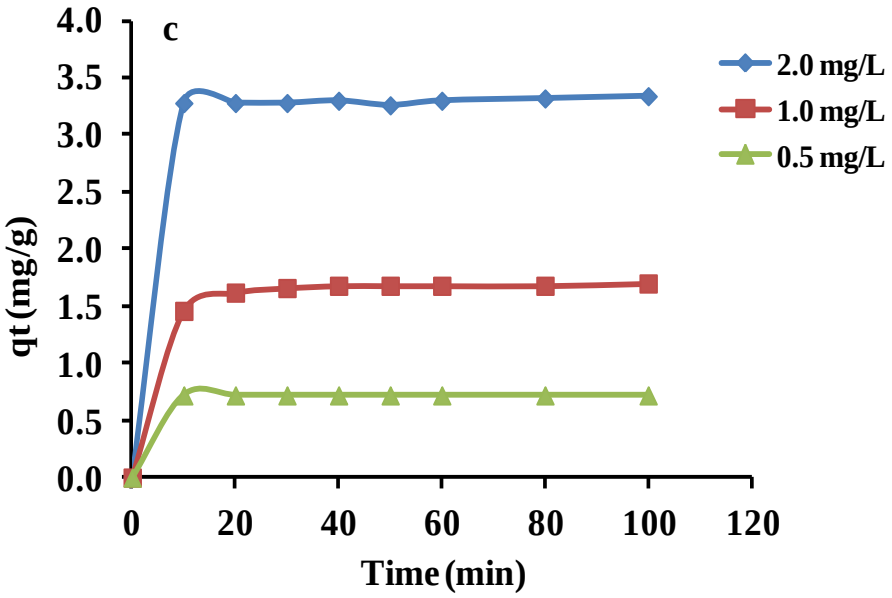


**Figure 4. 7 Effect of contact time on adsorption of (a) dichloromethane, (b) trichloromethane and (c) carbon tetrachloride at different AC dosage and temperature 25˚C.**

## 4.3 The pseudo-first-order model

The pseudo-first-order kinetic model is generally used to express the adsorption kinetics for solid-liquid systems (A. A. B.H. Hameed 2007). It is expressed as:

$$\log(q_e - q_t) = \log q_e - \frac{k_1}{2.303}\, t \qquad (4.2)$$

Where $k_1$ is the Lagergren rate constant (1/min), $q_e$ and $q_t$ are the quantity of chlorinated hydrocarbons (mg/g) at contact time t and at equilibrium, respectively. The plots of log ($q_e$-$q_t$) versus t illustrated in fig (4.8) give the values of the rate constant $k_1$ and adsorption quantity $q_e$ at equilibrium, which were calculated from the slopes and intercepts, and table (4.2) illustrates these values. The correlation coefficients ($R^2$) were low for different adsorbent dosages, which illustrates bad linearity. The agreement between the calculated $q_e$ from the equation (4.2) and observed $q_e$ is very poor. These results demonstrate that the adsorption process of chlorinated hydrocarbons does not fit well to the pseudo-first-order kinetic equation and that the mechanism of the adsorption may not obey the pseudo-first-order model.

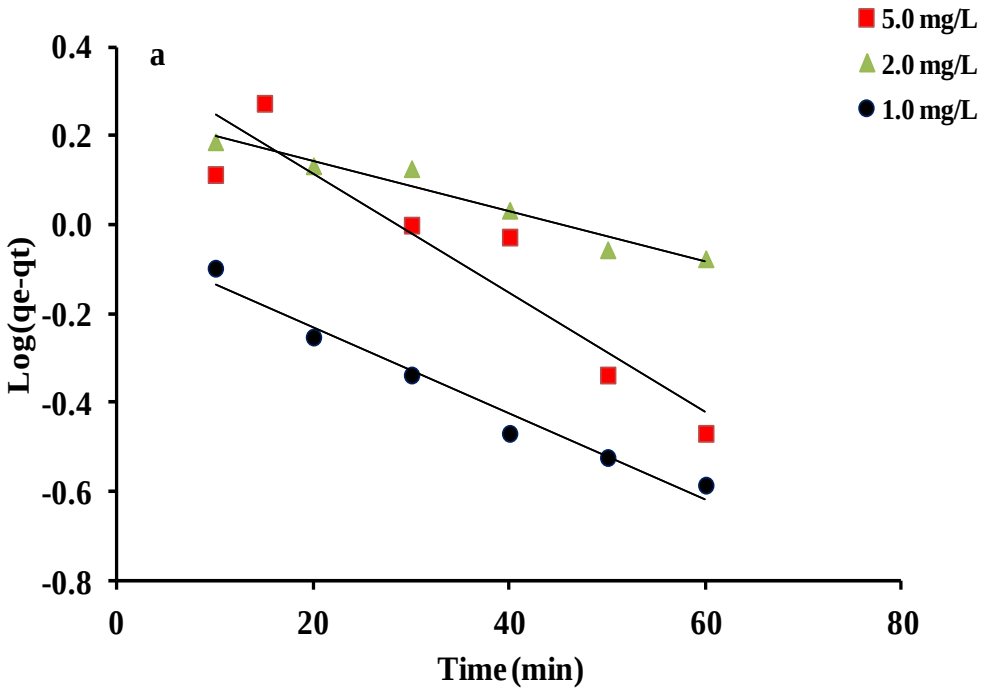
a
5.0 mg/L
2.0 mg/L
1.0 mg/L
0.4
0.2
0.0
-0.2
-0.4
-0.6
-0.8
Log(qe-qt)
0
20
40
60
80
Time (min)

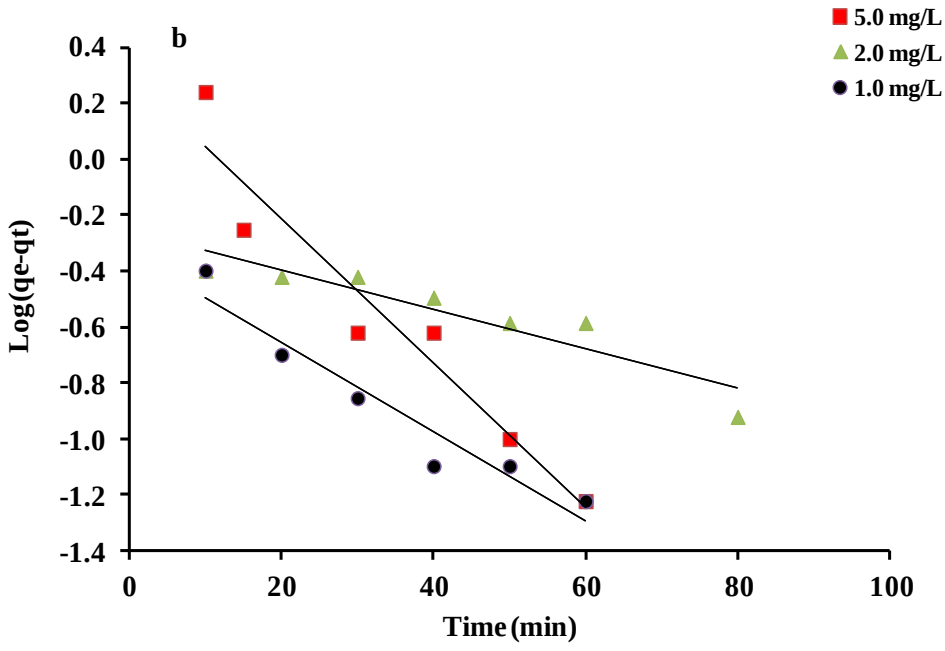
b
5.0 mg/L
2.0 mg/L
1.0 mg/L
0.4
0.2
0.0
-0.2
-0.4
-0.6
-0.8
-1.0
-1.2
-1.4
Log(qe-qt)
0
20
40
60
80
100
Time (min)

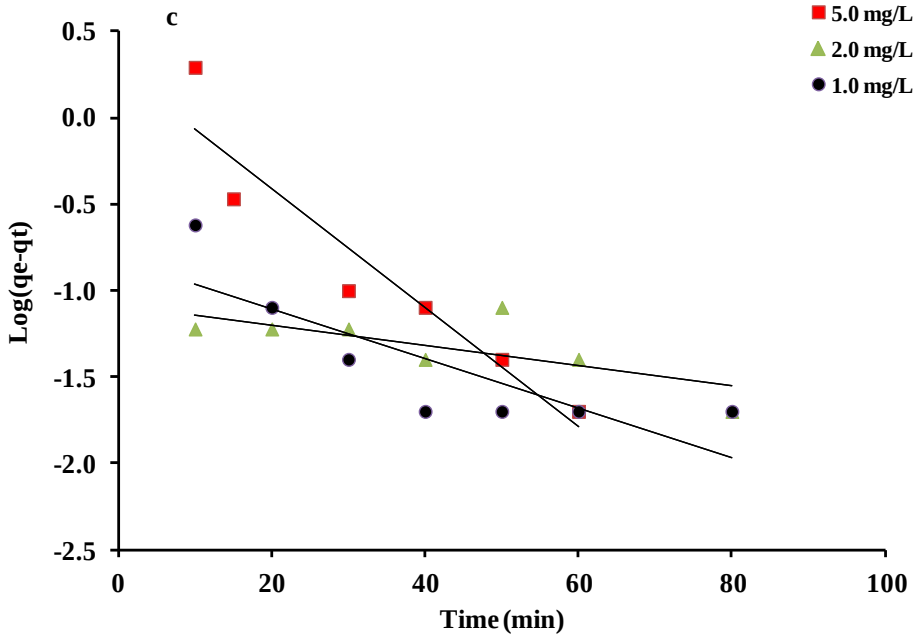


**Figure 4. 8 Lagergren first order plot for adsorption of (a) dichloromethane,(b) trichloromethane and (c) carbon tetrachloride at different AC dosage and temperature 25°C.**

## 4.4 The pseudo-second-order kinetics

The adsorption kinetic of pseudo second-order is described as (M. S. Chiou 2002, Y. S. Ho 2001, S. P. Karthikeyan 2008):

$$\frac{dq_t}{dt} = k_2(q_e - q_t)^2 \qquad (4.3)$$

Where $k_2$ is the rate constant (g/mg.min), and $q_e$ and $q_t$ are the amount of adsorbate in milligram per gram of the adsorbent at equilibrium and time t, respectively. By applying the integration at the boundary conditions t=0 to t=t and $q_t$=0 to qt=qe, the form of the equation (4.3) becomes:

$$\frac{1}{q_e - q_t} = \frac{1}{q_e} + k_2 t \qquad (4.4)$$

Equation (4.4) represents the pseudo-second-order equation in its integrated form and can be written in the linear form as below :

$$\frac{t}{q_t} = \frac{1}{k_2 q_e^2} + \frac{t}{q_e} \qquad (4.5)$$

Where h is the initial adsorption rate at t = 0 , h (mg/g.min) can be described as :

$$h = k_2 q_e^2 \qquad (4.6)$$

Therefore equation (4.6) can be written in a form as:

$$\frac{t}{q_t} = \frac{1}{h} + \frac{t}{q_e} \qquad (4.7)$$

According to the above equation, the plots of $t/q_e$ against t produced linear plots fig (4.9). Different parameters of the adsorption , such as $q_{e,}$ cal, and $k_2$ were calculated from the intercepts and slopes of the plots, respectively which are shown in table (4.2). The correlation coefficients ($R^2$) of the linear regression were higher than 0.99 for all adsorbent dosages. Additionally, the expected equilibrium adsorption capacities ($q_{e,}$ cal) calculated from Eq (4.5) coincided very well with the experimental equilibrium adsorption capacities. These results demonstrate the that fit of the experimental data to is as expected based on all of the aforementioned equations and expected equilibriums (Y. Nuhoglu 2009).

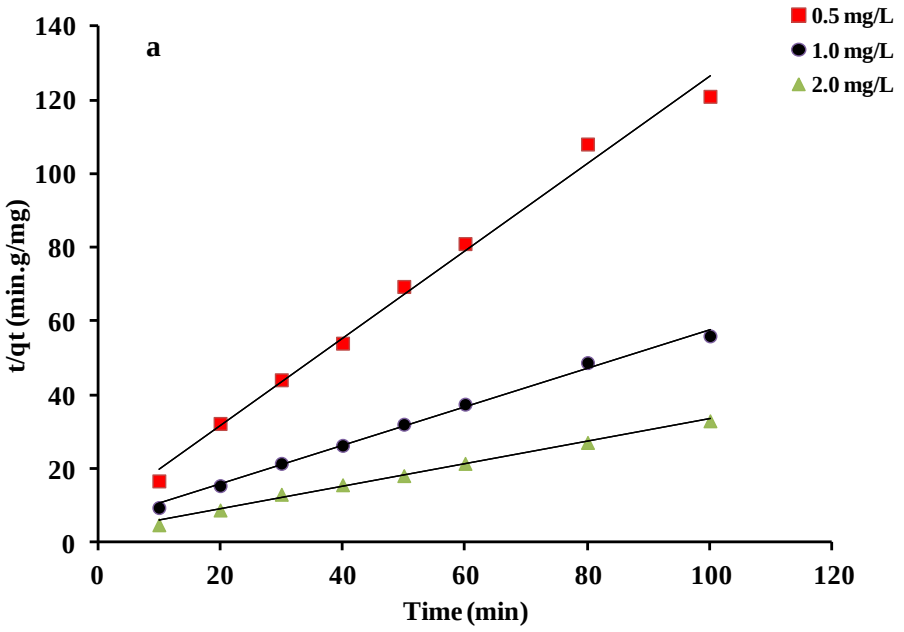
a
0.5 mg/L
1.0 mg/L
2.0 mg/L
t/qt (min.g/mg)
Time (min)
0
20
40
60
80
100
120
140

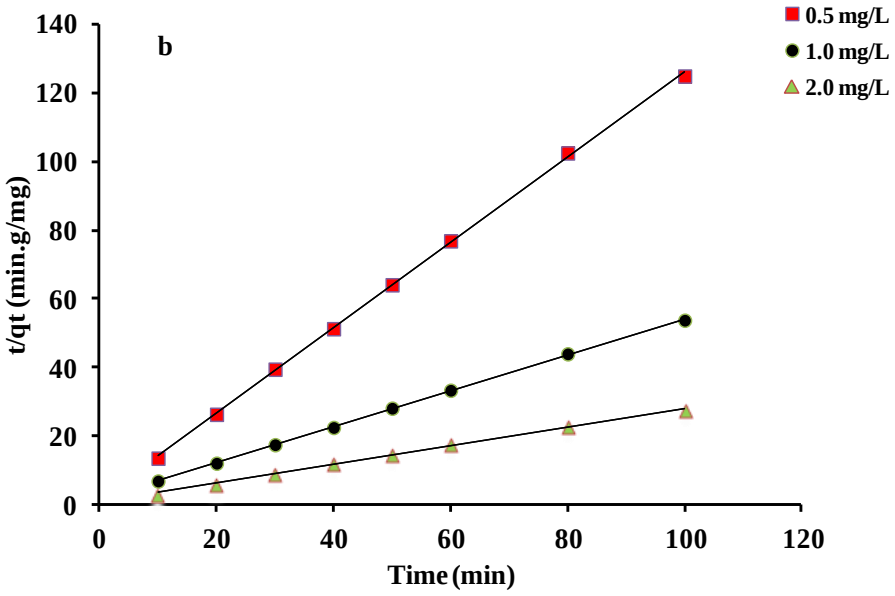
b
0.5 mg/L
1.0 mg/L
2.0 mg/L
t/qt (min.g/mg)
Time (min)
0
20
40
60
80
100
120
140

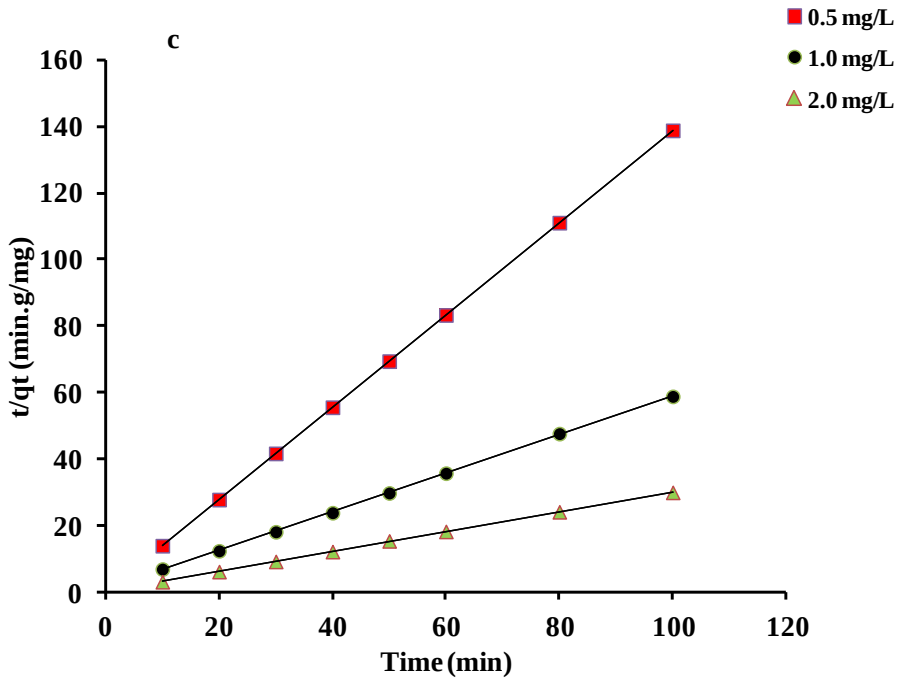


**Figure 4. 9 Linear regression of kinetics Plot: pseudo second order for (a)dichloromethane, (b)trichloromethane and (c) carbon tetrachloride at different AC dosage and temperature 25˚C.**

## 4.5 The intraparticle diffusion model

The Weber and Morris model is a typially used to determine the rate controlling step (L. Wang 2010, W.J. Weber 1963). The rate constants of intra-particle diffusion ($k_{id}$) can be investigated by using the following equation:

$$q_t = k_{id} t^{\frac{1}{2}} + C \qquad (4.8)$$

Where $q_t$ is the amount adsorbed chloronated hydrocarbons at time t, $t^{1/2}$ is the square root of the time, C is the intercept. The value of C refers to the thickness of the boundary layer. The plots of $q_t$ versus $t^{1/2}$ at different adsorbent dosages show multilinearity characterizations fig (4.10 ).The lines of the different concentrations do not go through the point of origin, which means the mechanism did not illucidate the rate of the overall

process and that there is  a complicated mechanism underlying the adsorption and intra-particle diffusion (G. Cunha 2010).

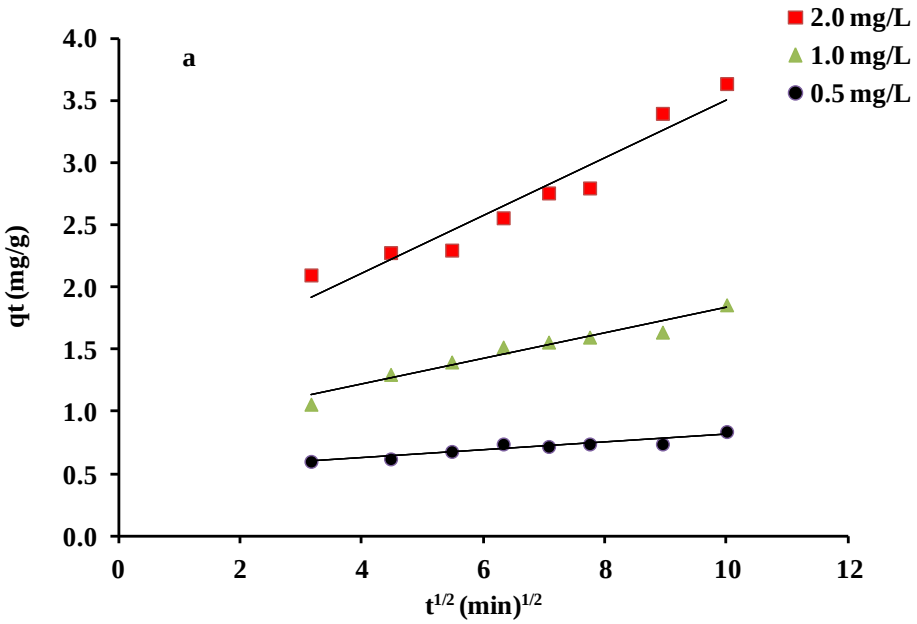


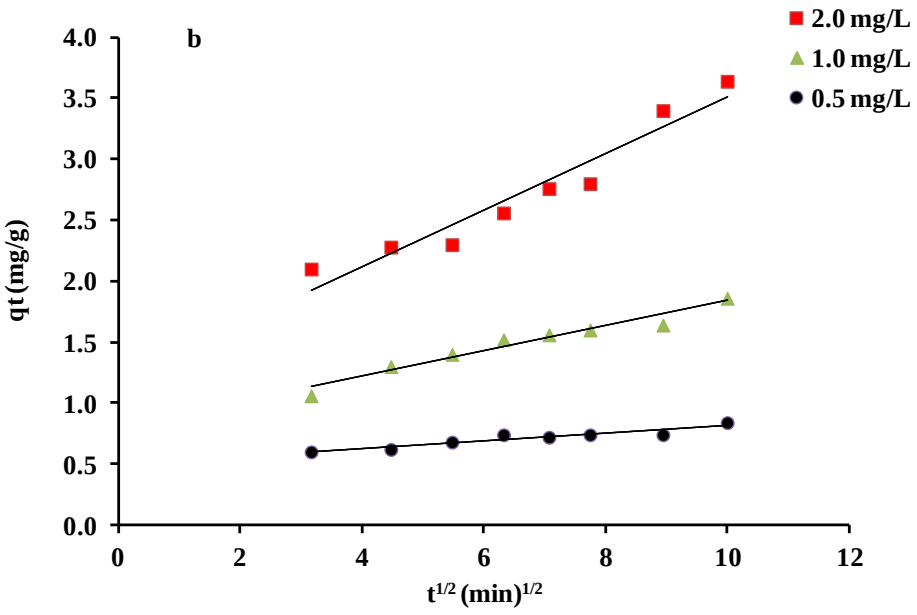

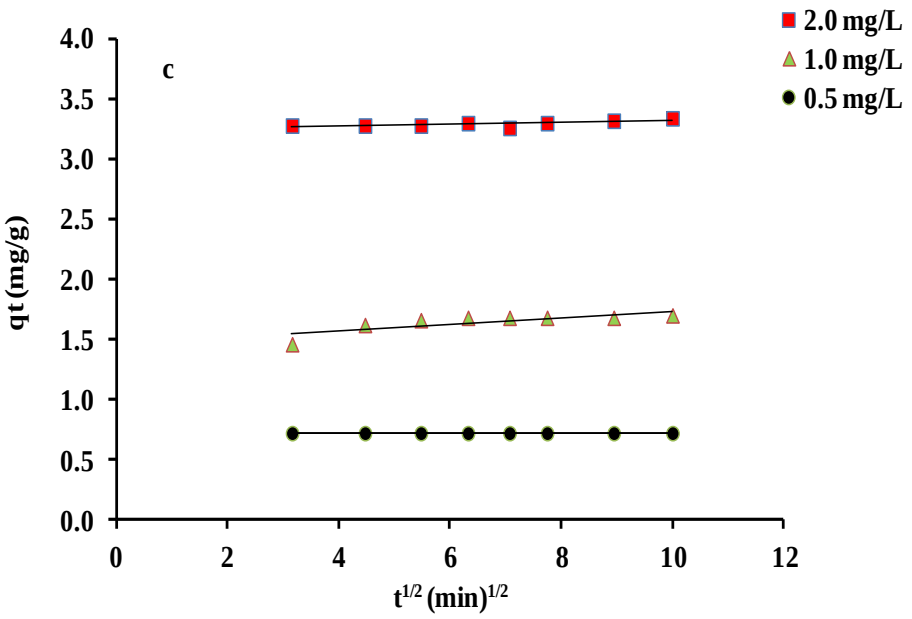


**Figure 4. 10 Intraparticle diffusion kinetic plot for (a) dichloromethane, (b) trichloromethane and (c) carbon tetrachloride at different AC dosage and temperature 25˚C.**

**Table 4. 2 Kinetic constant parameters obtained for chlorinated hydrocarbons adsorption on AC.**

| Compound | | Pseudo-first order | | | | Pseudo-second order | | | Intraparticle diffusion model | | | |
|---|---|---|---|---|---|---|---|---|---|---|---|---|
| | $C_i$ (mg/L) | $q_e$exp (mg/g) | $K_1(10^2)$ ($min^{-1}$) | $q_e$cal (mg/g) | $R^2$ | $K_2(10^{-2})$ (g/mg min) | $q_{e,cal}$ (mg/g) | h (g/min) | $R^2$ | $K_{id}(10^{-2})$ (mg/gmin) | C (mg/g) | $R^2$ |
| | 2.0 | 3.64 | 1.29 | 1.80 | 0.95 | 3.31 | 3.27 | 0.33 | 0.99 | 23.20 | 1.19 | 0.93 |
| $CH_2Cl_2$ | 1.0 | 1.86 | 2.20 | 1.09 | 0.97 | 5.40 | 1.89 | 0.19 | 0.99 | 10.32 | 0.81 | 0.95 |
| | 0.5 | 0.84 | 3.06 | 2.41 | 0.88 | 17.88 | 0.84 | 0.13 | 0.99 | 3.16 | 0.49 | 0.89 |
| | 2.0 | 3.68 | 1.61 | 1.81 | 0.85 | 8.14 | 3.72 | 1.13 | 0.99 | 5.80 | 3.03 | 0.89 |
| $CHCl_3$ | 1.0 | 1.86 | 3.66 | 2.18 | 0.93 | 16.44 | 1.91 | 0.60 | 0.99 | 5.05 | 1.40 | 0.82 |
| | 0.5 | 0.80 | 1.99 | 1.99 | 0.93 | 96.36 | 0.80 | 0.62 | 0.99 | 0.75 | 0.72 | 0.88 |
| | 2.0 | 3.34 | 1.29 | 1.80 | 0.51 | 53.68 | 3.34 | 5.99 | 0.99 | 0.83 | 3.24 | 0.54 |
| $CCl_4$ | 1.0 | 1.70 | 3.06 | 2.41 | 0.69 | 44.30 | 1.72 | 1.31 | 0.99 | 2.73 | 1.46 | 0.63 |
| | 0.5 | 0.72 | 2.23 | 1.09 | 0.90 | 45.28 | 0.72 | 0.23 | 1.00 | 72.00 | 0.00 | 0.00 |

## 4.6 Adsorption isotherm

The adsorption isotherm describes the adsorption process in terms of the interaction between the molecules in the solution of the adsorbate and the adsorbent when the adsorption process is in the equilibrium stage (Hameed 2006).

### 4.6.1 Langmuir isotherm model

The Langmuir adsorption model is given by:

$$\frac{C_e}{q_e} = \frac{1}{k_L q_m} + \frac{C_e}{q_m} \qquad (4.9)$$

Where $K_L$ is Langmuir equilibrium constant (liters/miligrams), and $q_m$ (mg/g) is the maximum adsorption capacity produced by monolayer of adsorbate. The parameters can be calculated from a plot $C_e/q_e$ versus $C_e$ fig (4.11). The most important parameter of Langmuir equation is the separation factor, $R_L$, defined by Weber and Chakkravorti (Weber T.W. 1974):

$$R_L = \frac{1}{1 + K_L C_o} \qquad (4.10)$$

Where $C_o$ is the highest initial concentration of the solute. The value of separation factor gives an indication for the type of the isotherm. Considering the $R_L$ value, adsorption is defined as either being unfavorable ($R_L>0$), linear ($R_L=1$), favorable ($0<R_L<1$) or irreversible ($R_L=0$) (S. Karagoz 2008). In our study, the $R_L$ values were 0.0118, 0.1869 and 0.1645 for dichloromethane, chloroform, and carbon tetrachloride, respectively, and these values confirmed that the prepared activated carbon from the rubber waste material exhibits the expected favorable adsorption for these compounds.

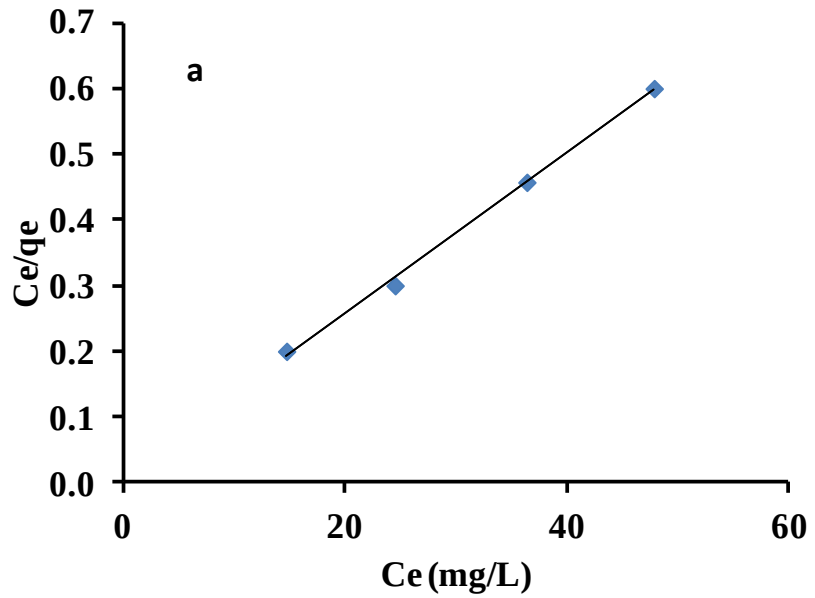
a
0.7
0.6
0.5
0.4
0.3
0.2
0.1
0.0
Ce/qe
0
20
40
60
Ce (mg/L)

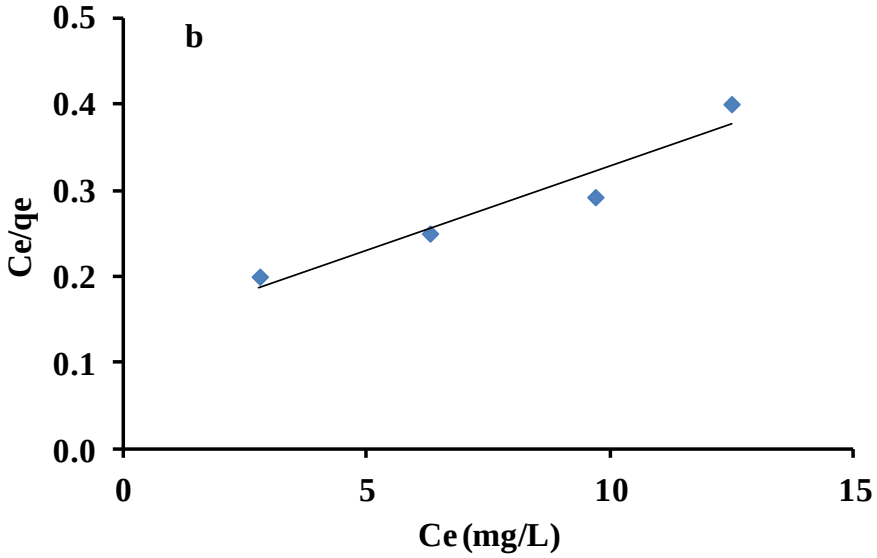
b
0.5
0.4
0.3
0.2
0.1
0.0
Ce/qe
0
5
10
15
Ce (mg/L)

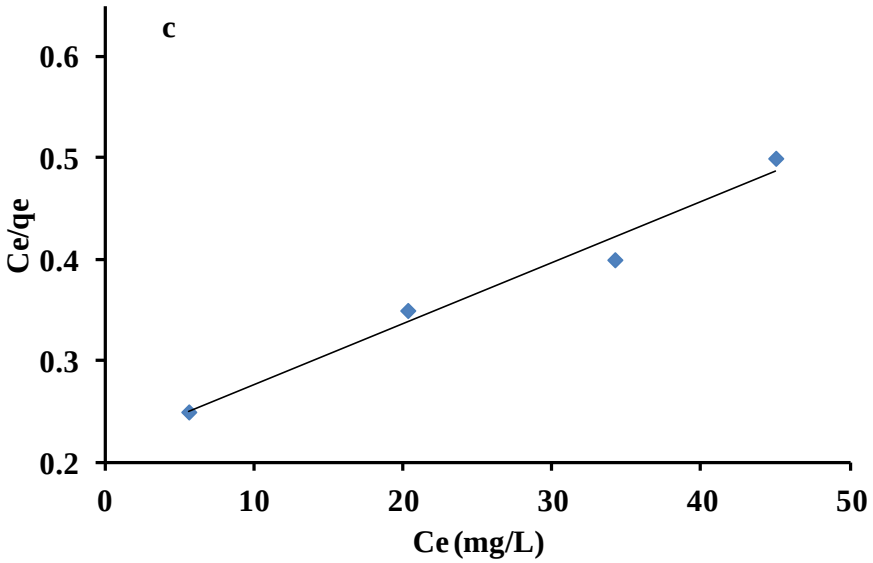


**Figure 4. 11 Langmuir model for adsorption of (a) dichloromethane, (b) trichloromethane and (c) carbon tetrachloride at different AC dosage and temperature 25˚C.**

### 4.6.2 Freundlich isotherm model

The Freundlich model is a theoretical equation can be applied to the adsorption on a heterogeneous surface of an adsorbent. The well-known Freundlich model as described by the logarithmic form is defined by the following equation:

$$\ln q_e = \ln K_f + \frac{1}{n} \ln C_e \qquad (4.11)$$

Where $k_F$ (L/g) is the adsorption capacity and, n is adsorption intensity, respectively. The plost of $\ln(q_e)$ versus $\ln(C_e)$ is shown in fig (4.12). The values of Freundlich parameters were determined and listed in table (4.3). The correlation coefficients, $R^2$, indicate that the adsorption isotherm data follow the Freundlich model well. The calculated n values from the slope indicate the adsorption capacity. Generally, when the values of n fall in the range from 2 to 10, it is a good adsorption indicator. However, those values that range from, 1-2 are moderate, and less than 1 are poor adsorption characteristics. Our n values were between 1 and 2, which indicated that the adsorption is moderate.

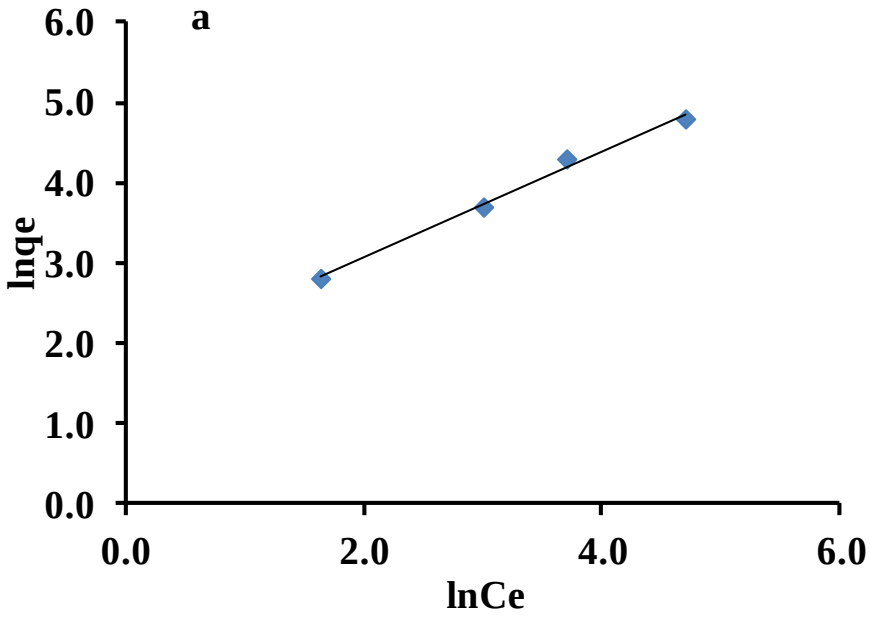
a
6.0
5.0
4.0
3.0
2.0
1.0
0.0
lnqe
0.0
2.0
4.0
6.0
lnCe

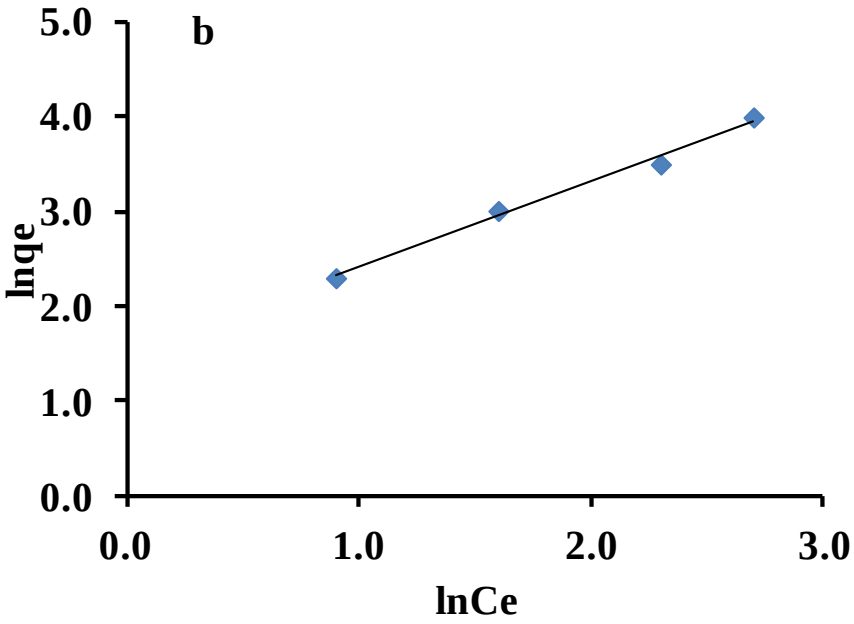
b
5.0
4.0
3.0
2.0
1.0
0.0
lnqe
0.0
1.0
2.0
3.0
lnCe

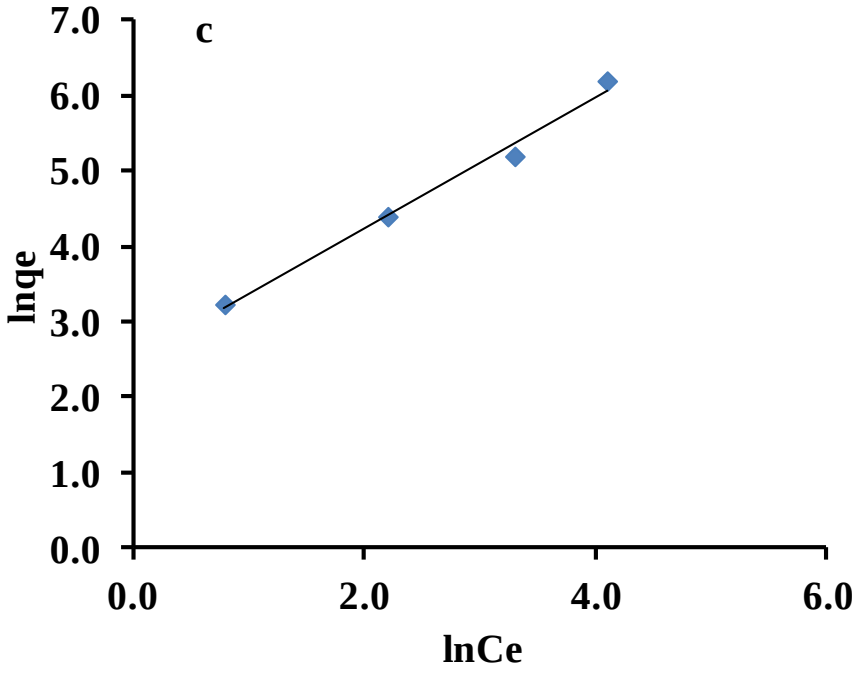


**Figure 4. 12 Langmuir model for adsorption of (a) dichloromethane, (b) trichloromethane and (c) carbon tetrachloride at different AC dosage and temperature 25˚C.**

### 4.6.3 Temkin isotherm model

The Temkin isotherm model exhibits the total amount of heat of the molecules in one layer on the surface of the adsorbent during the adsorption process. The linear decrease of adsorbent with coverage is referred to as adsorbent-adsorbate interaction. The linear form of the Temkin model is expressed as:

$$\ln q_e = \frac{RT}{b_T} \ln K_T + \frac{RT}{b_T} \ln C_e \qquad (4.12)$$

Where $b_T$ is the Temkin constant and is related to the heat of sorption (kilojoules per mole). The $k_T$ parameter is the equilibrium binding constant ,which is equal to the maximum binding energy (L/g), and R is the universal gas constant ($8.314 \times 10^{-3}$). T is the absolute temperature (degrees Kelvin) (Mohd Nazri Idrisa 2011). The isotherm parameters for the adsorption of the chloronated hydrocarbons are given in table (4.3). The correlation coefficient, $R^2$, for $q_e$ versus $\ln(C_e)$ shows that the Temkin isotherm does not flow the adsorption data.

.

Table 4.3 parameters of the Langmuir , Freundlich and Temkin models for adsorption of dichloromethane, chloroform and carbon tetrachloride at different AC dosage and temperature 25˚C.

| Compound | T (k) | Langmuir isotherm constants | | | Freundlich isotherm constant | | | | Temkin isotherm constants | | |
|---|---|---|---|---|---|---|---|---|---|---|---|
| | | $q_m$ (mg/g) | $K_L$ (L/mg) | $R^2$ | 1/n | N | $K_F$ | $R^2$ | $K_T$ (L/gm) | $b_T$ ($10^{-3}$) (KJ/mol) | $R^2$ |
| $CH_2Cl_2$ | 298 | 81.9 | 0.95 | 0.99 | 0.66 | 1.51 | 5.74 | 0.99 | 3.56 | 61.86 | 0.34 |
| $CHCl_3$ | 298 | 51.3 | 0.15 | 0.92 | 0.92 | 1.09 | 4.47 | 0.99 | 1.69 | 99.90 | 0.47 |
| $CCl_4$ | 298 | 166.7 | 0.04 | 0.97 | 0.89 | 1.15 | 12.19 | 0.99 | 1.26 | 36.1 | 0.52 |

# CHAPTER 5

# Sorption by ZnO-NP/AC

## 5.1 Characterization of ZnO-NP/AC

The shape and surface morphology of the ZnO-NP/AC nanoparticles were investigated with ascanning electron microscope (SEM), fig (5.1). The SEM images indicate the homogeneous and relatively smooth surface of the activated carbon that had been loaded with ZnO nanoparticles. The EDX analysis, fig (5.2), of the ZnO-NP/AC composite reveals that the composition of the nanoparticles corresponds to zinc and oxygen elements as in table (5.1). BET surface area of ZnO-NP/AC was found to be 15 $m^2/g$ with pore size of 0.3 $cm^3/g$ and adsorption average pore width of 802 Å. The low specific surface area and total pore volumes could be due to the loading of ZnO nanoparticles on the carbon surface. Fourier transform infrared spectroscopy fig (5.4) is the useful technique to identify the presence of functional group in the prepared material. The band laying around 1640 $cm^{-1}$ represents the enhancement in the aromatic C=C groups (carbonization). The strong and broad band at 3400 $cm^{-1}$ represent O–H mode, and the band at 2900 $cm^{-1}$ is C–H aliphatic mode. The band at 1054 $cm^{-1}$ can be attributed to C-O stretching vibration. In addition to the previously mentioned bands, there is a band at 490 $cm^{-1}$ that may be attributed to the stretching vibrational mode of

ZnO. The TGA analysis fig (5.5) shows the enhancement of the thermal stability of ZnO-NP/AC.

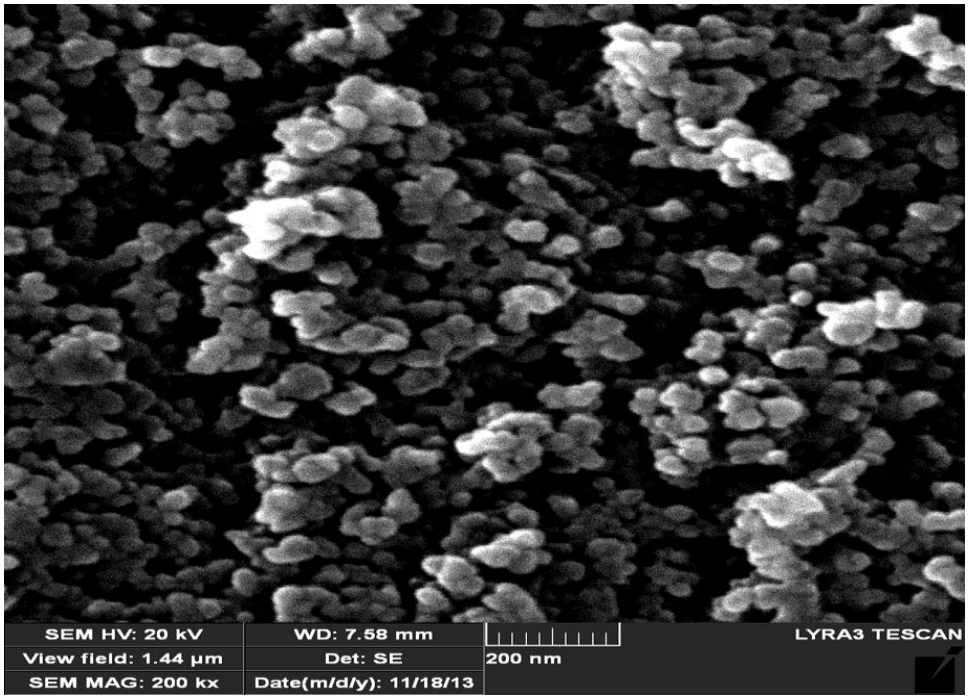


**Figure 5. 1 SEM images of the surface structure of the ZnO-NP/AC.**

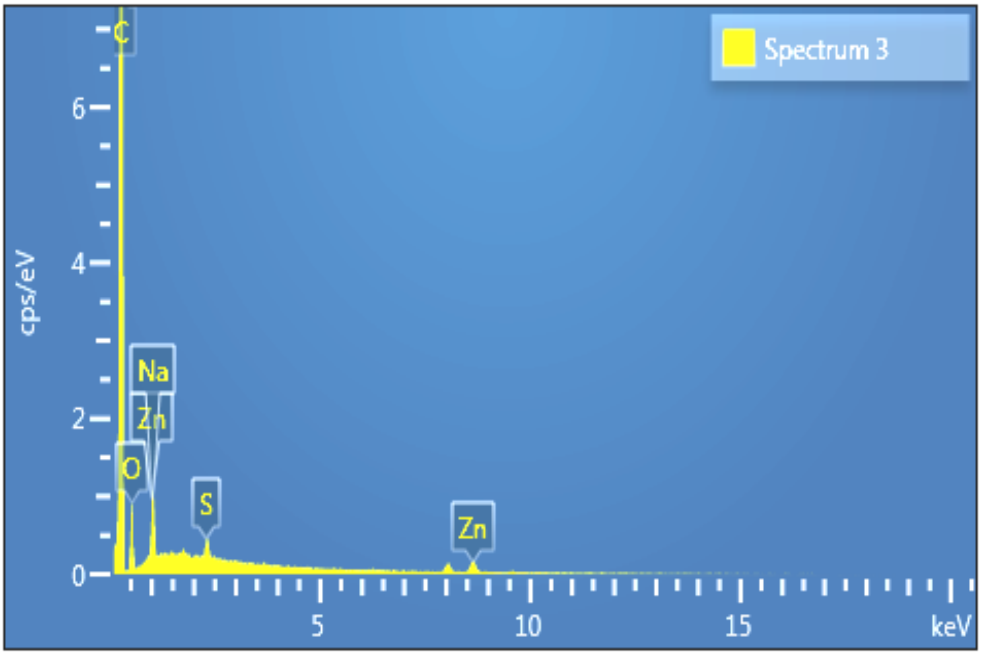


**Figure 5. 2 EDX analysis of the ZnO-NP/AC.**

**Table 5. 1 Energy dispersive X-ray analysis (EDX) quantitative microanalysis of ZnO-NP/AC.**

| N# | Element | Weight% |
|---|---|---|
| 1 | C | 88.74 |
| 2 | O | 10.58 |
| 3 | Zn | 0.68 |
| Total | | 100 |

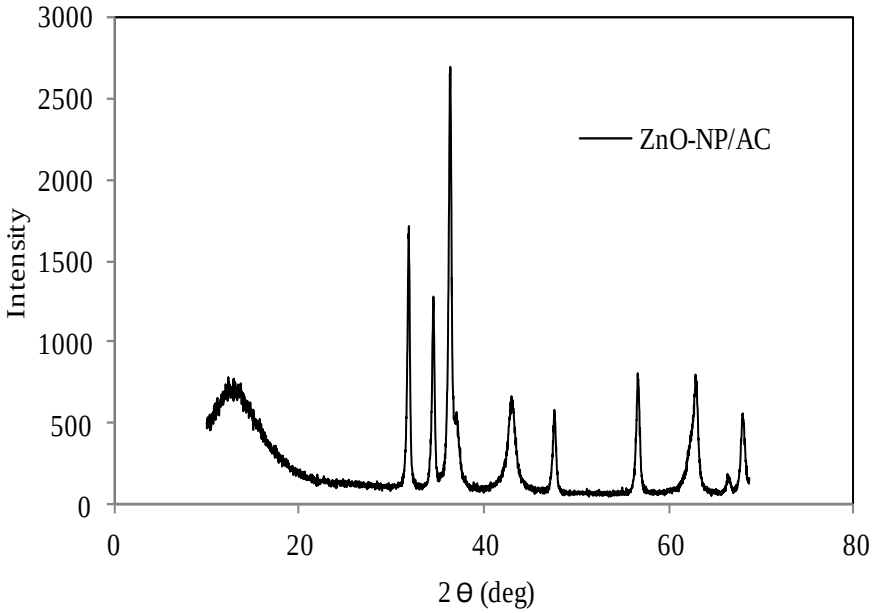


Figure 5. 3 The XRD pattern of ZnO-NP/AC.

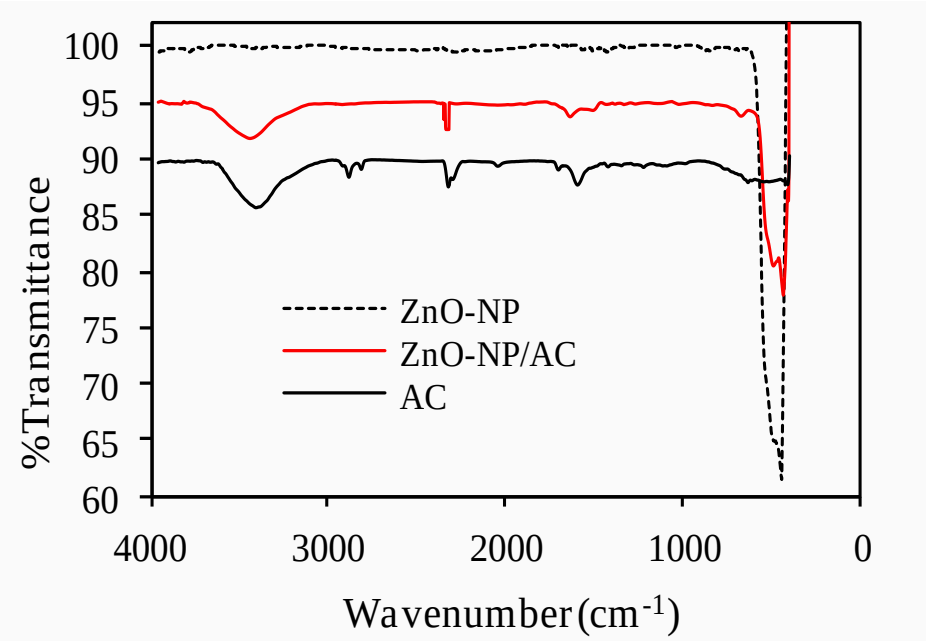


**Figure 5. 4 FTIR spectrum of the ZnO-NP/AC.**

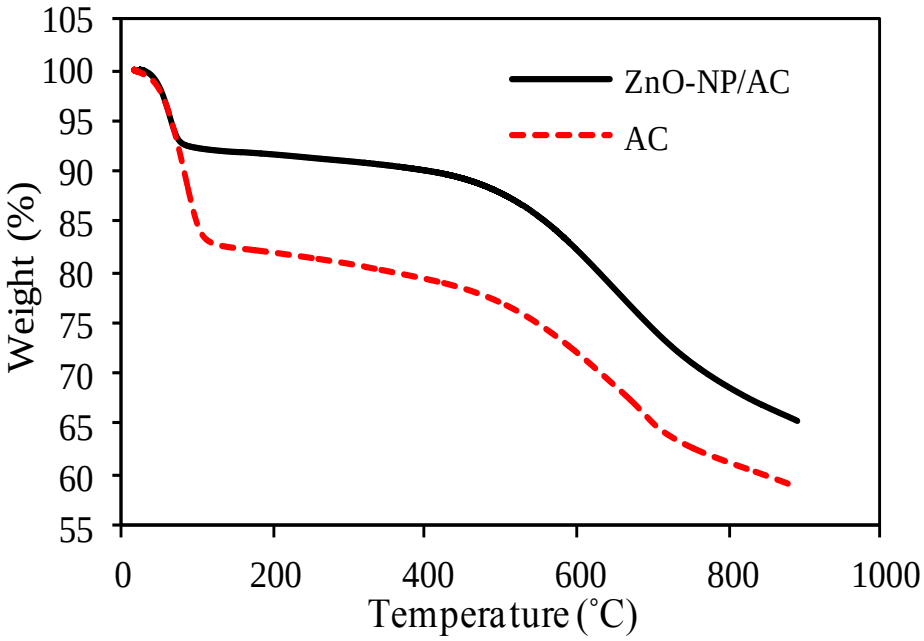


**Figure 5. 5 TGA curve of the ZnO-NP/AC.**

## 5.2 Effect of contact time and initial concentration

The adsorption profile of chlorinated hydrocarbons can be described by the effect of contact time by using ZnO-NP/AC (derived from rubber tires waste) composite at three different initial concentrations and is illustrated in fig (5.6). It can be clearly seen that the adsorption of chlorinated hydrocarbons rapidly increased with the increasing of contact time, and then decreased until the equilibrium was achieved. The resulting rate is related to the adsorption process becauase it takes place by fast rate at the initial step and is then followed by a slower internal diffusion process (Gialamouidis D. 2010). The fast adsorption at the initial step is due to the presence of a large number of vacant active sites, but after a lapse of time, the unoccupied surface sites cannot accommodate the solute molecules. This can be attributed to the repulsion between the solute molecules of the solid and bulk solution phases, so it takes a long time to reach the equilibrium. When the initial concentration is increased, the difference between the amount of the adsorbates of the solution and adsorbent phases increases because of increasing the driving force for mass transfer between the phases (Srivastava 2005). The adsorption capacity of chlorinated hydrocarbons after 10 min increased from 2.11 to 6.67 mg/g for dichloromethane, 4.67 to 11.91 mg/g for chloroform and from 3.60 to 16.10 mg/g for carbon tetrachloride as the initial chlorinated hydrocarbons concentration was increased from 5 to 20 mg/L. Therefore the adsorption was rapid in the first 10 min and then decreased until the equilibrium point. The time until saturation is nearly 20 min.

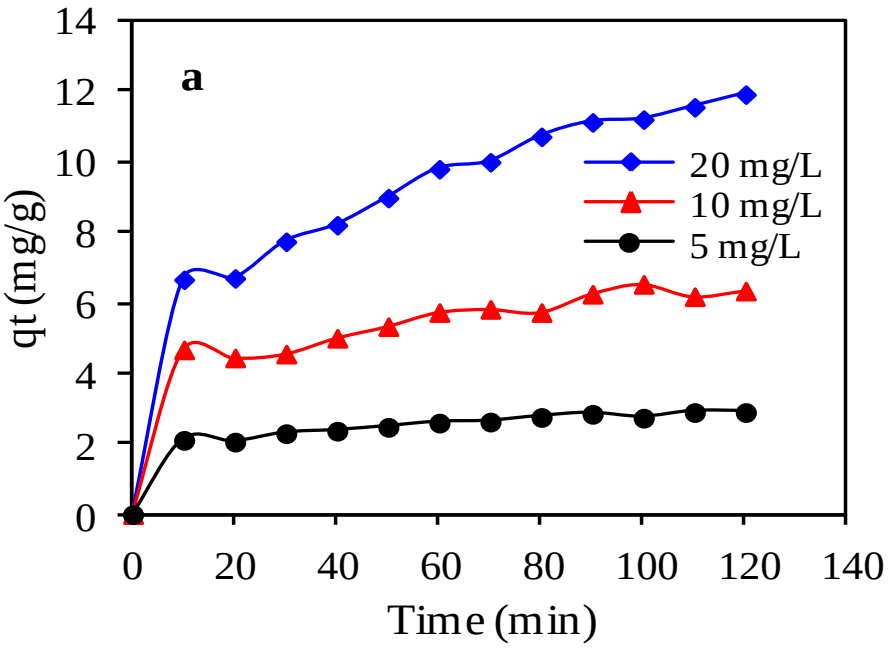
a
qt (mg/g)
Time (min)
20 mg/L
10 mg/L
5 mg/L
0
2
4
6
8
10
12
14
0
20
40
60
80
100
120
140

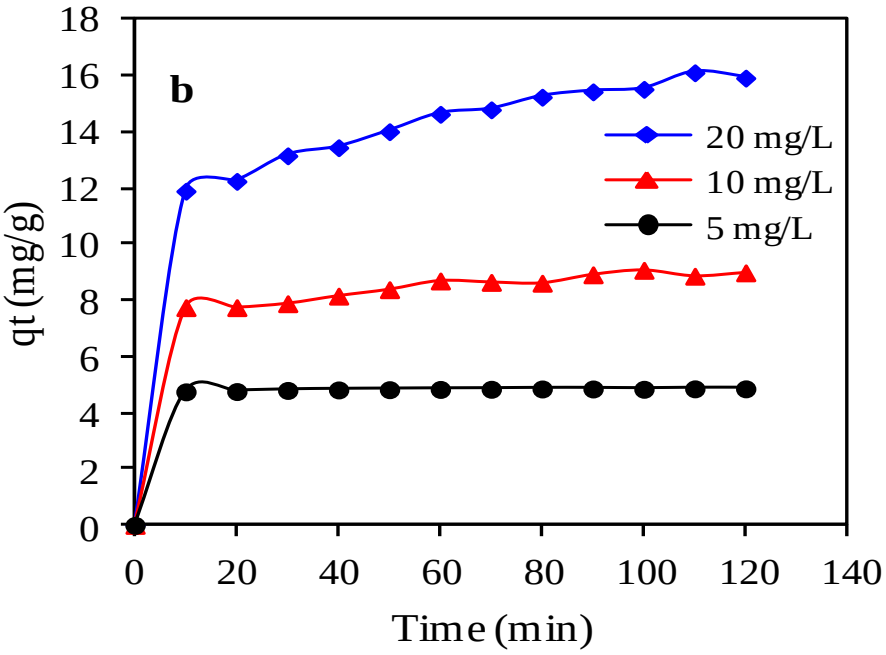
b
qt (mg/g)
Time (min)
20 mg/L
10 mg/L
5 mg/L
0
2
4
6
8
10
12
14
16
18
0
20
40
60
80
100
120
140

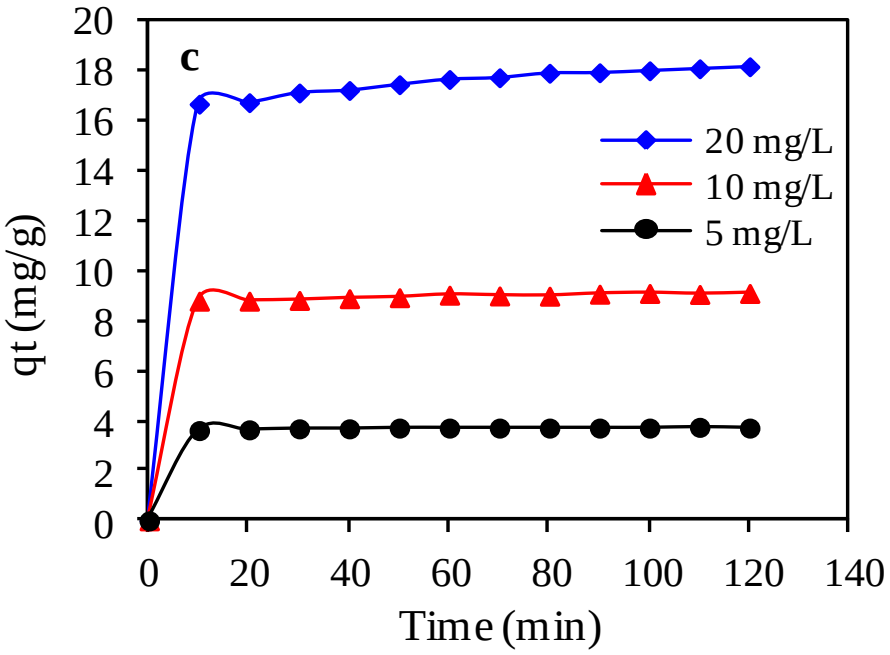


**Figure 5. 6 Effect of contact time on adsorption of (a) dichloromethane, (b) chloroform, (c) carbon tetrachloride at different concentrations,and temperature 25˚C.**

## 5.3 Effect of adsorbent dosage

The amount of the adsorbent is a significant factor because it determines the efficiency of an adsorbent (Ouazene N 2010). The effect of ZnO-NP/AC dosage on the adsorption of chlorinated hydrocarbons is illustrated in fig (5.7). Different adsorbent dosages were applied for dichloromethane, chloroform and carbon tetrachloride with initial concentration 10 mg/L at 25˚C and shaking for 60 min. The results indicate that as the adsorbent dosage increased, the percent removal of chlorinated hydrocarbons was increased from 32.24 % to 85.01 % for dichloromethane , from 80.72% to 99.4 % for chloroform and from 81.56% to 95.41 % for carbon tetrachloride with an increase in adsorbent dosage from 0.25 to 5.00 g/L. These results can be explained by the large surface area that results from an increase in the adsorbent amount or higher adsorption vacant sites for a constant concentration of chlorinated hydrocarbons (Panda L 2011, Zhang H 2010). It has been found that the increase in percent removal of chlorinated hydrocarbons was slow when the adsorbent dose was over 3 g/L (P. R. Gupta VK 2003, M. A. Gupta VK 2006). The percent removal of chlorinated hydrocarbons in solution is calculated by Eq. (5.1) as follow:

$$\% \text{ Removal} = \frac{C_\circ - C_e}{C_\circ} \times 100 \qquad (5.1)$$

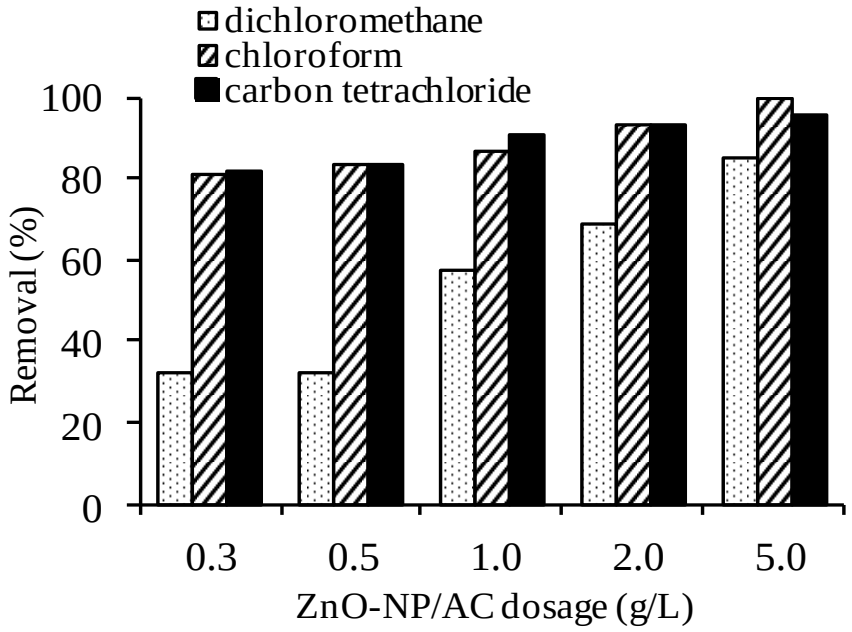


**Figure 5. 7 Effect of adsorbent dosage on the adsorption of dichloromethane, chloroform and carbon tetrachloride at different adsorbent dosage, and temperature 25˚C.**

## 5.4 Adsorption kinetics

Adsorption kinetics illustrates the interaction between solid-solution interface, and it can determine the mechanism of the reactions. In order to estimate the adsorption mechanism, the following three models can be applied: the pseudo first-order, the pseudo second-order rate equation, and finally, the intraparticle diffusion models (Singh VK 1997, Ho YS 2000, Srivastava SK 1995). The correspondence between the adsorption data and the model expected values was represented by the values of correlation coefficient ($R^2$).

### 5.4.1 The pseudo-first order model

The pseudo-first-order kinetic model is a common model applied for understanding the mechanisims of solid liquid system (A. A. B.H. Hameed 2007). It is expressed as:

$$\log(q_e - q_t) = \frac{k_1}{2.303}\, t \qquad (5.2)$$

Where $k_1$ is the Lagergren rate constant (1/min), and $q_e$ and $q_t$ are the quantity of chlorinated hydrocarbons (mg/g) at contact time t and at equilibrium, respectively. The plots of log ($q_e$-$q_t$) versus t demonstrated in fig (5.8), give the values of the rate constant $k_1$ and adsorption quantity $q_e$ at equilibrium, which were calculated from the slopes and intercepts table (5.2). The correlation coefficients ($R^2$) were low for different concentration, illustrating bad linearity. The correspondence between the calculated $q_e$ from the equation (5.2) and observed $q_e$ were very poor. This demonstrated that the adsorption of chlorinated hydrocarbons deviated from this model and the mechanism of the adsorption on the surface of the ZnO-NP/AC may not fit the pseudo-first-order model.

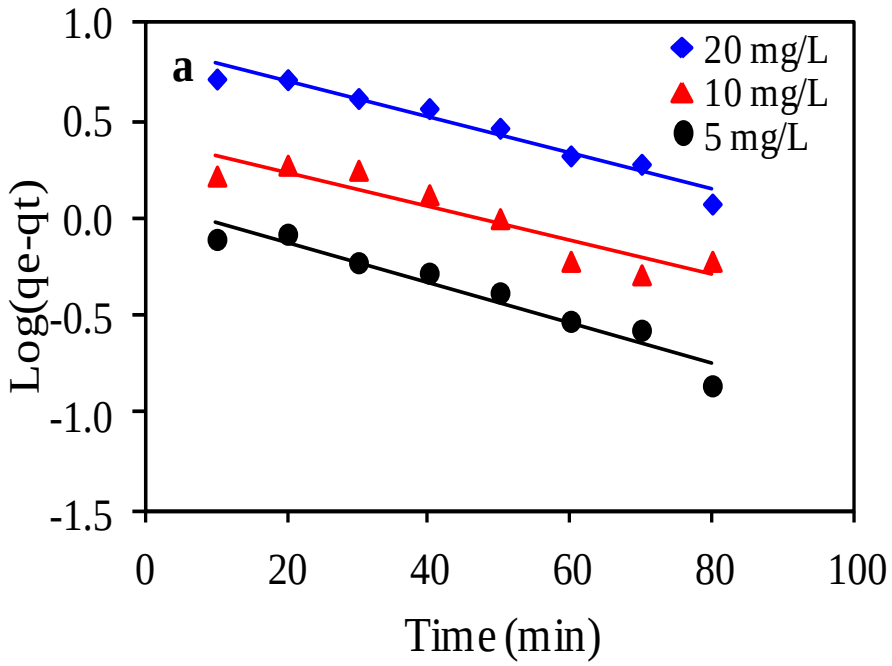

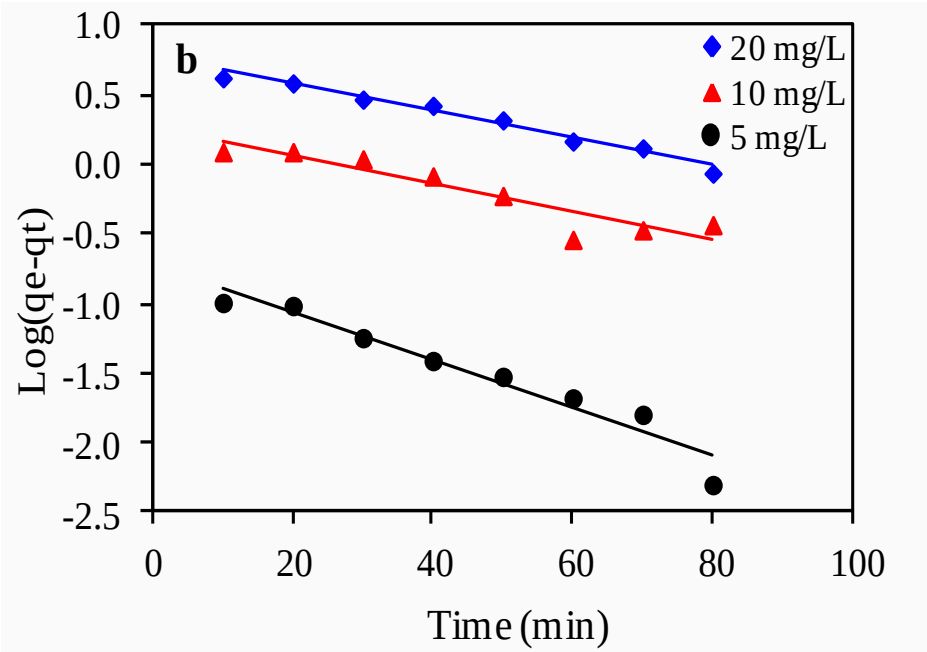


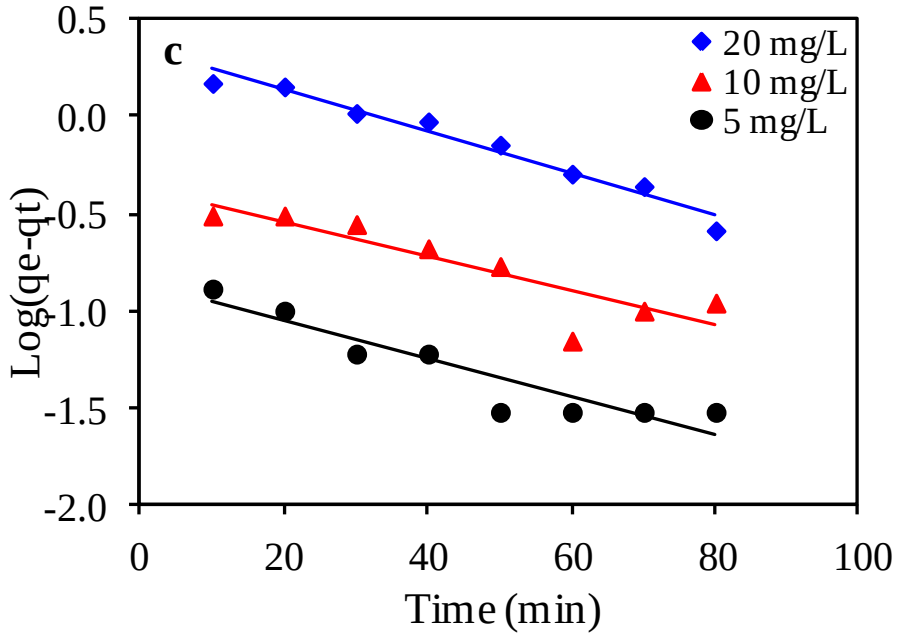


**Figure 5. 8 Lagergren first order plot for adsorption of (a) dichloromethane (b) chloroform (c) carbon tetrachloride at different concentrations and temperature 25°C.**

### 5.4.2 The pseudo-second order model

The pseudo second-order kinetic rate equation of the adsorption is expressed as (M. S. Chiou 2002 , Y. S. Ho 2001, S. S. Karthikeyan 2008):

$$\frac{dq_t}{dt} = k_2(q_e - q_t)^2 \quad (5.3)$$

Where $k_2$ is the rate constant (g/mg.min) , $q_e$ and $q_t$ are the adsorption capacity at equilibrium and time t respectively. By applying the integration at the boundary conditions t=0 to t=t and $q_t$=0 to qt=qe, the form of the equation (5.3) becomes:

$$\frac{1}{q_e - q_t} = \frac{1}{q_e} + k_2 t \quad (5.4)$$

Equation (5.4) can be written as below:

$$\frac{t}{q_t} = \frac{1}{k_2 q_e^2} + \frac{t}{q_e} \quad (5.5)$$

Where h is the initial adsorption rate at t = 0 , h (mg/g.min) can be described as :

$$h = k_2 q_e^2 \quad (5.6)$$

Therefore equation (5.6) can be written in a form as:

$$\frac{t}{q_t} = \frac{1}{h} + \frac{t}{q_e} \quad (5.7)$$

The plots of $t/q_t$ against t of equation (5.7) at different concentrations of the chlorinated hydrocarbons are illustrated in fig (5.9). The adsorption parameter $q_e$, cal and $k_2$ were calculated from the slope and the intercept, respectively table (5.2). The high linearity of the plots indicated by the correlation coefficient values ($R^2$) ( > 0.99) means that the adsorption kinetics between ZnO-NP/AC composite and the chlorinated hydrocarbons belong to the pseudo-second order. In addition, the correspondence between the $q_e$, cal and $q_e$, gives further evidence for the fitting of the adsorption data, meaning that that the

adsorption rate of chlorinated hydrocarbons adsorption seems to be controlled by a chemisorption mechanism through the sharing of electrons or by covalent bonds between the surface of adsorbent and adsorbate (Y. Nuhoglu 2009 ).

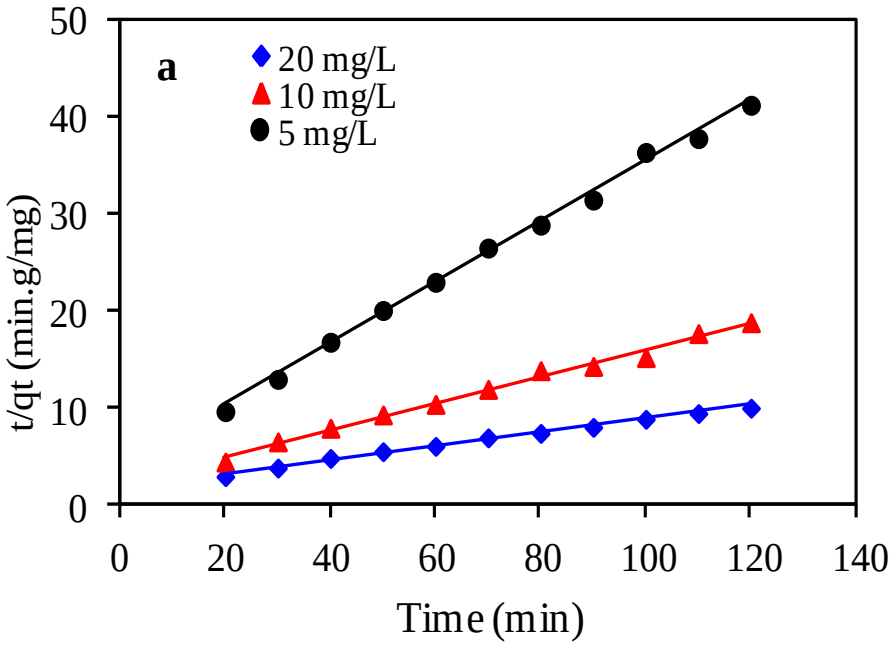


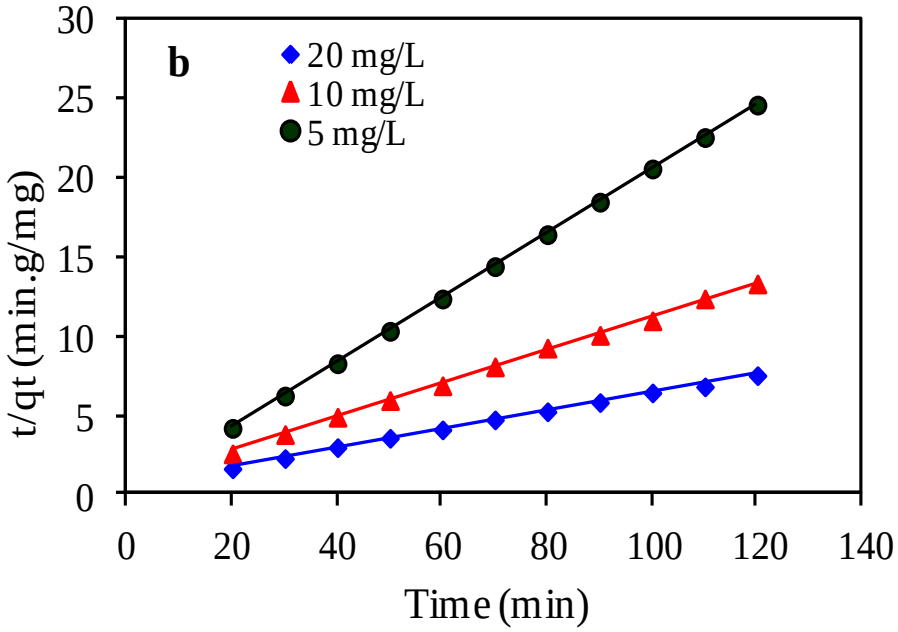

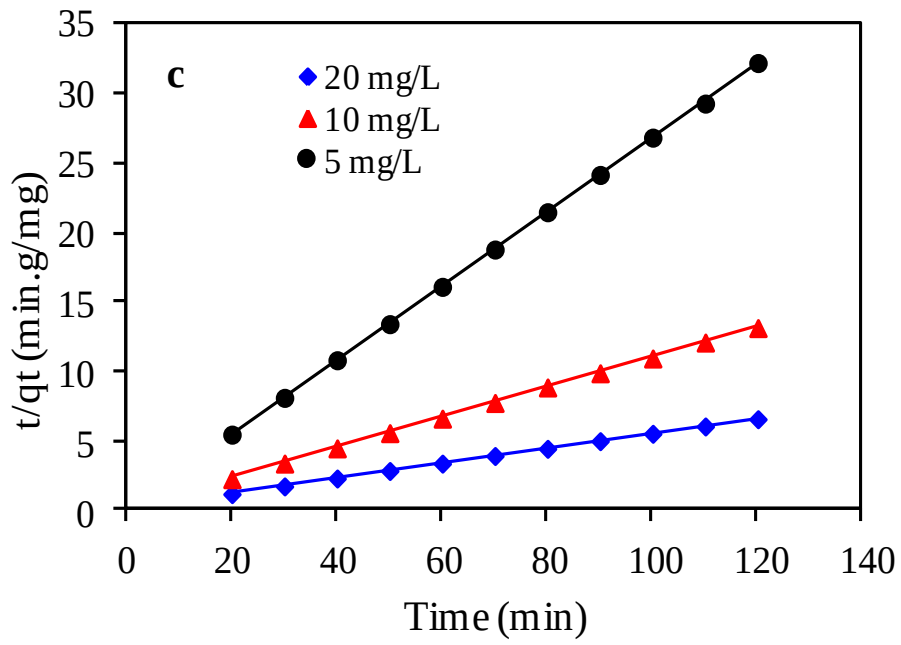


**Figure 5. 9 Linear regression of kinetics Plot: pseudo second order for (a) dichloromethane (b) chloroform (c) carbon tetrachloride at different concentrations and temperature 25˚C.**

### 5.4.3 The intraparticle diffusion model

Weber and Morris model is a usually used applied to predict the intra-particle diffusion rate controlling step (L. Wang 2010, W.J. Weber 1963). The rate constants ($k_{id}$) can be determined by using the following equation:

$$q_t = k_{id} t^{\frac{1}{2}} + C \qquad (5.8)$$

The plots of $q_t$ versus $t^{1/2}$ are illustrated in fig (5.10). The lines of the different concentration do not go through the origin, which means the mechanism does not determine the rate of the overall process, and there must therefore exist a complicated mechanism included in adsorption and intra-particle diffusion (G. Cunha 2010).

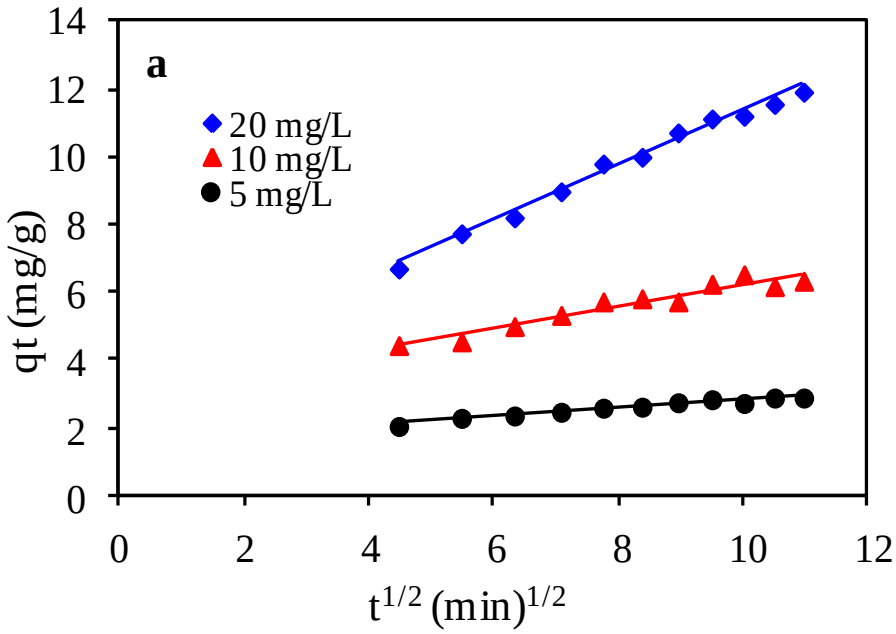
a
20 mg/L
10 mg/L
5 mg/L
qt (mg/g)
t^1/2 (min)^1/2
0
2
4
6
8
10
12
14

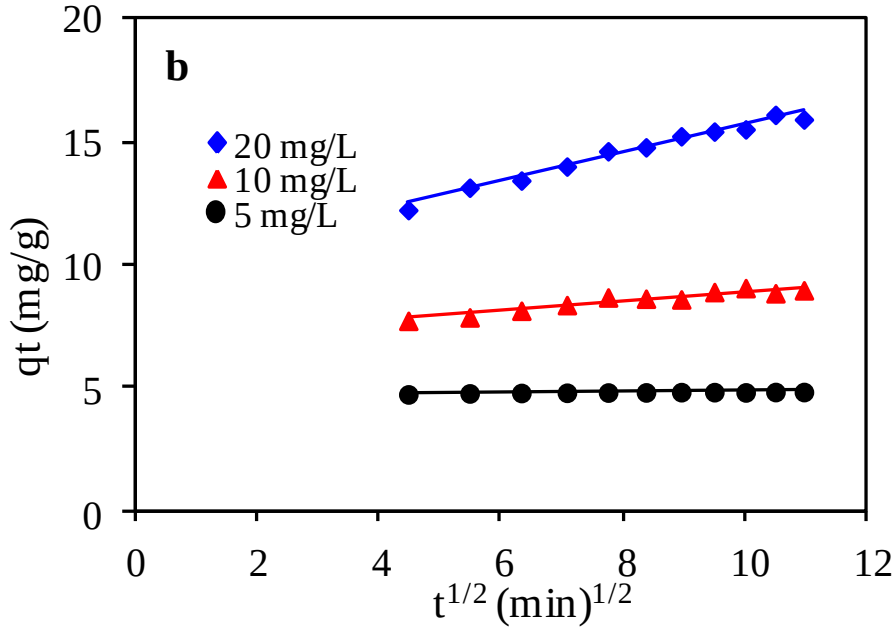
b
20 mg/L
10 mg/L
5 mg/L
qt (mg/g)
t^1/2 (min)^1/2
0
5
10
15
20
0
2
4
6
8
10
12

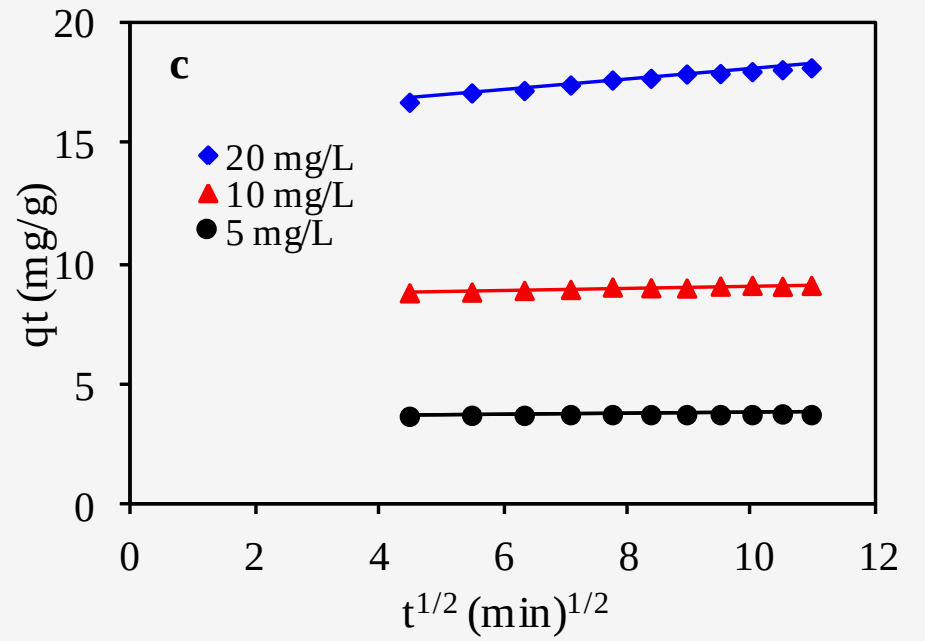


**Figure 5. 10 Intraparticle diffusion kinetic plot for (a) dichloromethane (b) chloroform (c) carbon tetrachloride at different concentrations and temperature 25˚C.**

Table 5. 2 Kinetic constant parameters obtained for chlorinated hydrocarbons adsorption on ZnO-NP/AC.

| Compound | | Pseudo-first order | | | | Pseudo-second order | | | | Intraparticle diffusion model | | |
|---|---|---|---|---|---|---|---|---|---|---|---|---|
| | $C_i$ (mg/L) | $q_e$exp (mg/g) | $K_1$ ($10^{-3}$) ($min^{-1}$) | $q_e$cal (mg/g) | $R^2$ | $K_2$ ($10^{-2}$) (g/mgmin) | $q_{e,cal}$ (mg/g) | h (g/min) | $R^2$ | $K_{id}$ (mg/gmin) | C (mg/g) | $R^2$ |
| $CH_2Cl_2$ | 20 | 11.93 | 20.96 | 7.64 | 0.954 | 0.25 | 14.39 | 0.52 | 0.995 | 0.807 | 3.276 | 0.989 |
| | 10 | 6.35 | 20.27 | 2.62 | 0.866 | 0.86 | 7.22 | 0.45 | 0.992 | 0.328 | 2.9776 | 0.932 |
| | 5 | 2.90 | 23.95 | 1.24 | 0.934 | 2.40 | 3.18 | 0.25 | 0.997 | 0.126 | 1.5769 | 0.957 |
| $CHCl_3$ | 20 | 16.13 | 22.34 | 5.88 | 0.975 | 0.56 | 17.27 | 1.69 | 0.998 | 0.581 | 9.889 | 0.979 |
| | 10 | 9.00 | 23.03 | 1.82 | 0.860 | 1.98 | 9.39 | 1.74 | 0.999 | 0.204 | 6.9046 | 0.920 |
| | 5 | 4.86 | 39.84 | 1.18 | 0.940 | 4.3 | 4.88 | 1.02 | 1.000 | 0.013 | 4.7372 | 0.841 |
| $CCl_4$ | 20 | 18.21 | 24.64 | 2.24 | 0.964 | 1.99 | 18.55 | 6.85 | 1.000 | 0.214 | 15.938 | 0.975 |
| | 10 | 9.12 | 20.49 | 2.31 | 0.782 | 9.24 | 9.19 | 7.80 | 1.000 | 0.050 | 8.5984 | 0.919 |
| | 5 | 3.75 | 22.79 | 7.23 | 0.863 | 55.76 | 3.74 | 7.79 | 1.000 | 0.010 | 3.6271 | 0.709 |

## 5.5 Adsorption isotherm

The adsorption isotherm describes the adsorption process in terms of the partition of adsorbate molecules between the two phases of adsorbent and the solution of the adsorbate at the equilibrium stage (Hameed 2006). Several isotherm models were used for investigation of adsorption capacity in adsorption of chlorinated hydrocarbon from aqueous solution. The three models were introduced in this study are Langmuir, Freundlich, and Temkin isotherms.

### 5.5.1 Langmuir isotherm model

The Langmuir assumes that the adsorption process occurs between a homogeneous adsorbent that has a certain active sites,energies, and monolayer of adsorbate. The linear equation is given by:

$$\frac{C_e}{q_e} = \frac{1}{k_L q_m} + \frac{C_e}{q_m} \qquad (5.9)$$

Where $K_L$ is Langmuir equilibrium constant (L/mg), and $q_m$ (mg/g) is the maximum amount of the monolayer adsorbate in the adsorbent. They are calculated from a plot of $C_e/q_e$ versus $C_e$ fig (5.11). The Langmuir model can be characterized by $R_{L,}$ known as the separation factor and defined by Weber and Chakkravorti:

$$R_L = \frac{1}{1 + K_L C_o} \qquad (5.10)$$

The plots of $C_e/q_e$ versus $C_e$ shows high linearity which is confirmedconfirmed by the correlation coefficient values in which $R^2$ >0.99, thus giving indication that the isotherm data fit this model well. The Langmuir parameters were calculated and listed in table (5.3).

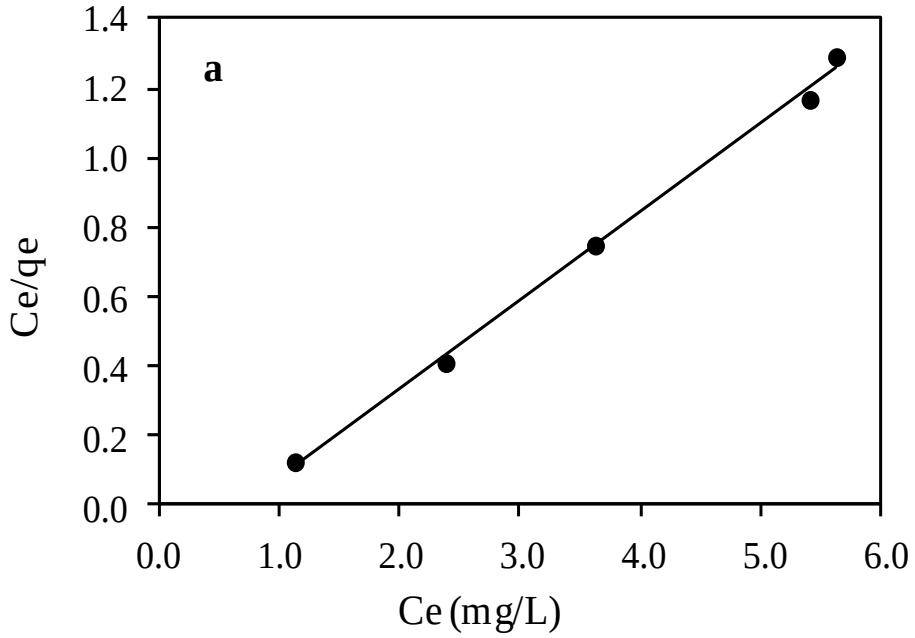
a
1.4
1.2
1.0
0.8
0.6
0.4
0.2
0.0
Ce/qe
0.0
1.0
2.0
3.0
4.0
5.0
6.0
Ce (mg/L)

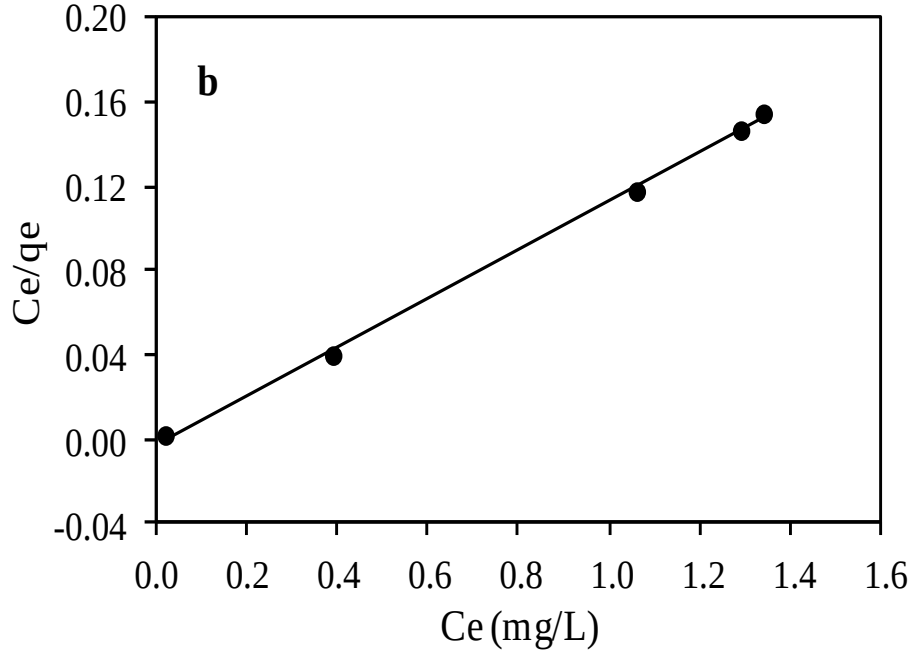
b
0.20
0.16
0.12
0.08
0.04
0.00
-0.04
Ce/qe
0.0
0.2
0.4
0.6
0.8
1.0
1.2
1.4
1.6
Ce (mg/L)

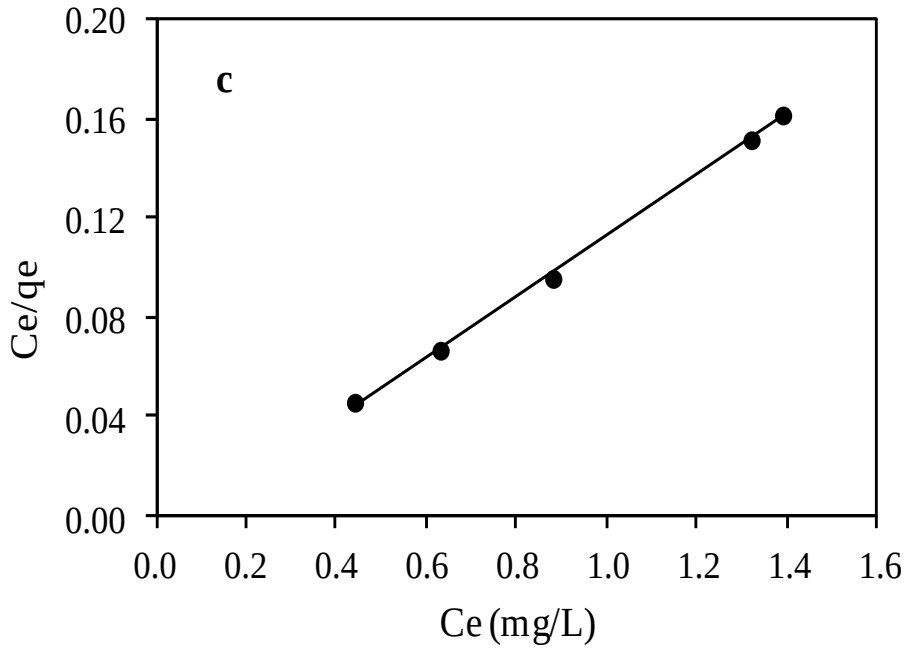


**Figure 5. 11 Langmuir model for adsorption of (a) dichloromethane (b) chloroform (c) carbon tetrachloride at different concentrations, and temperature 25˚C.**

### 5.5.2 Freundlich isotherm model

The Freundlich model is an empirical equation and that considers how the adsorption process occurs on heterogeneous surface of an adsorbent (Freundlich 1906). The Freundlich equation is defined by the following:

$$\ln q_e = \ln K_f + \frac{1}{n} \ln C_e \qquad (5.11)$$

Where $k_F$ (L/g) and n are the adsorption capacity and adsorption intensity, respectively., and can be obtained by plotting $\ln q_e$ versus $\ln C_e$ fig (5.12). The Freundlich isotherm constants $K_F$ and n were calculated table (5.3). The n values gives an indication for the favorability of the adsorption process. The values of n > 1 represent favorable adsorption conditions (Treybal 1968, V.J.P. Poots 1978, Y.S. Ho 1998). The values of the correlation coefficient of Freundlich indicate that the linearity is very poor.

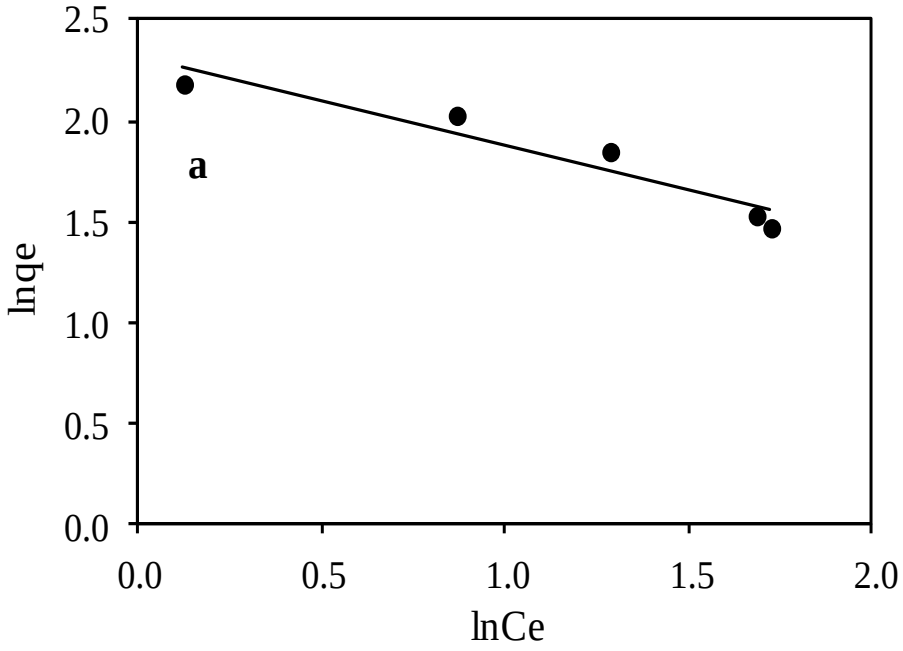
2.5
2.0
1.5
1.0
0.5
0.0
a
lnqe
0.0
0.5
1.0
1.5
2.0
lnCe

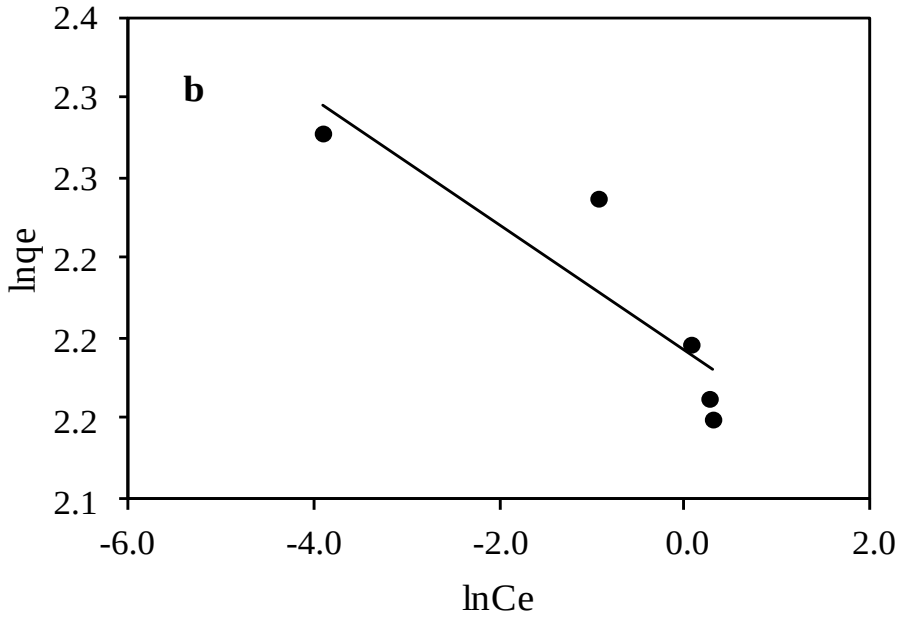
2.4
2.3
2.3
2.2
2.2
2.2
2.1
b
lnqe
-6.0
-4.0
-2.0
0.0
2.0
lnCe

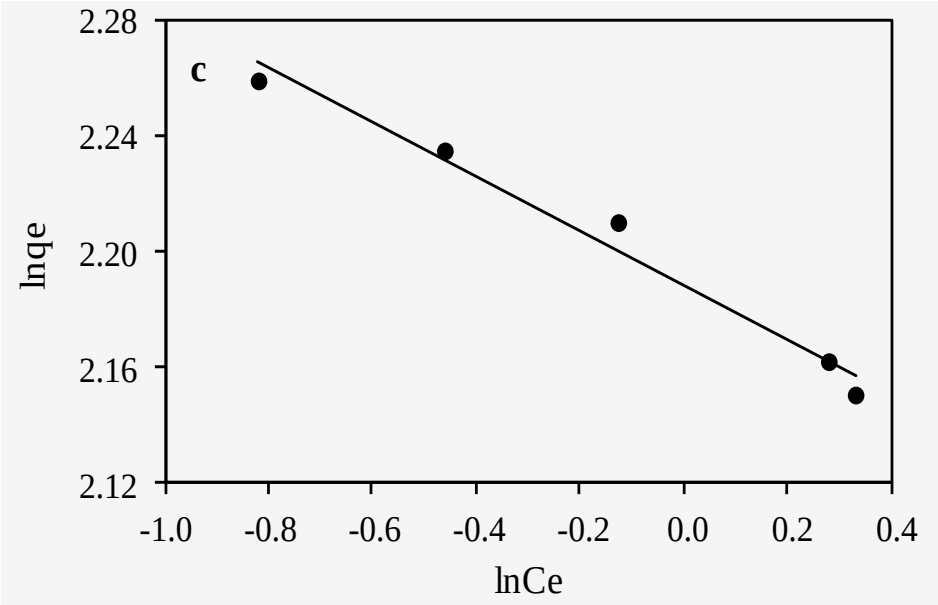


**Figure 5. 12 Freundlich model for adsorption of (a) dichloromethane (b) chloroform (c) carbon tetrachloride at different concentrations, and temperature 25˚C.**

### 5.5.3 Temkin isotherm model

The Temkin isotherm represents the quantity of heat generated in the adsorption by one layer on the surface of adsorbent. This heat can decrease linearly with coverage, and that referred to adsorbent-adsorbate interaction. The linear form of Temkin model is given by:

$$\ln q_e = \frac{RT}{b_T} \ln K_T + \frac{RT}{b_T} \ln C_e \qquad (5.12)$$

Where $b_T$ is the Temkin constant and is related to the heat of sorption (kJ/mol), $k_T$ is the equilibrium binding constant, which is equal to the maximum binding energy (L/g), R is universal gas constant ($8.314x10^{-3}$ ), and T is the absolute temperature (degrees Kelvin) (M. Idrisa 2011 ). The plot of $q_e$ versus $\ln C_e$ is illustrated in fig (5.13), and the isotherm constants were calculated from the slope and intercept table (5.3).

Table 5. 3 Langmuir, Freundlich, and Temkin isotherm constants for chlorinated hydrocarbon adsorption on ZnO–NP/AC.

| Compound | | Langmuir isotherm constants | | | | Freundlich isotherm constants | | | | Temkin isotherm constants | | |
|---|---|---|---|---|---|---|---|---|---|---|---|---|
| | T (k) | $q_m$ (mg/g) | $K_L$ (L/mg) | $R_L$ | $R^2$ | 1/n | n | $K_F$ | $R^2$ | $K_T$ (L/gm) | $b_T$ (KJ/mol) | $R^2$ |
| $CH_2Cl_2$ | 298.16 | 39.22 | 0.145 | 0.408 | 0.9971 | 0.44 | 2.26 | 10.14 | 0.9114 | 29.37 | 0.87 | 0.955 |
| $CHCl_3$ | 298.16 | 86.28 | 4.46 | 0.022 | 0.9983 | 0.03 | 31.65 | 8.96 | 0.7955 | $1.48x10^{13}$ | 8.38 | 0.806 |
| $CCl_4$ | 298.16 | 81.63 | 1.28 | 0.072 | 0.9991 | 0.09 | 10.60 | 8.92 | 0.9776 | $3.32x10^{4}$ | 2.89 | 0.9815 |

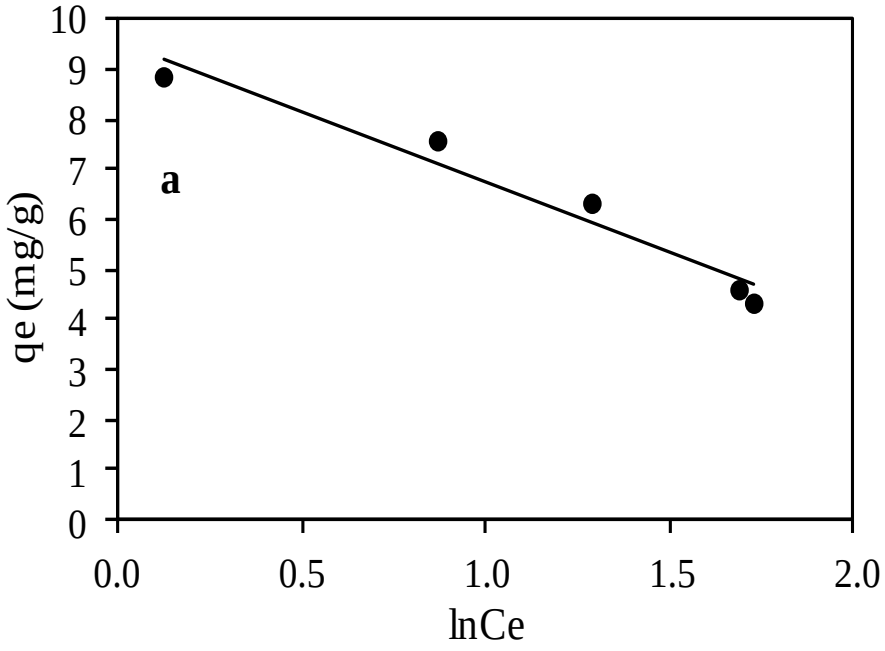
10
9
8
7
6
5
4
3
2
1
0
qe (mg/g)
a
0.0
0.5
1.0
1.5
2.0
lnCe

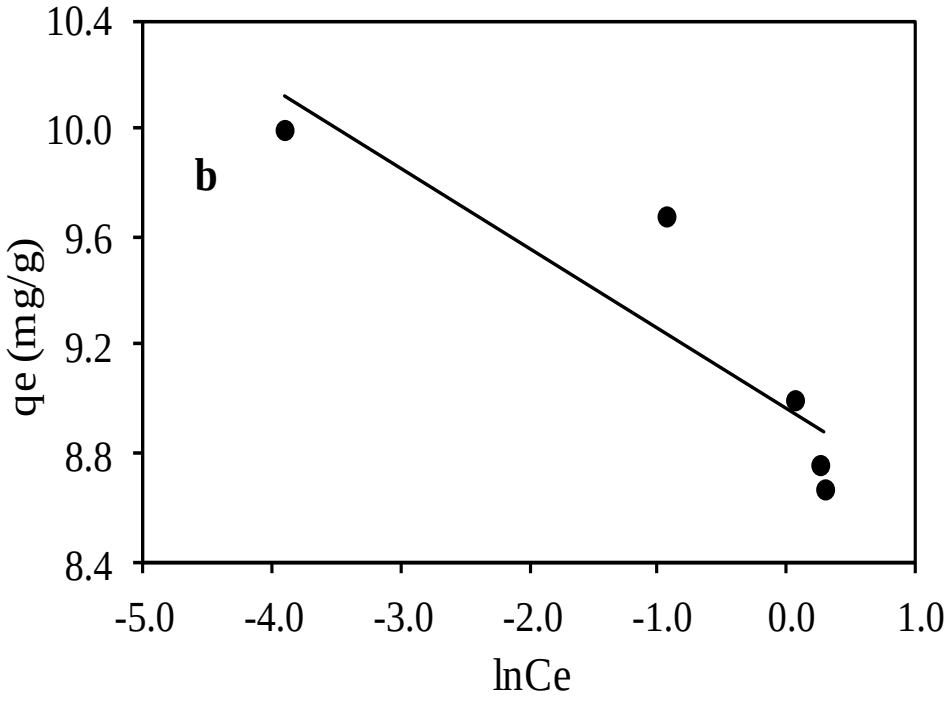
10.4
10.0
9.6
9.2
8.8
8.4
qe (mg/g)
b
-5.0
-4.0
-3.0
-2.0
-1.0
0.0
1.0
lnCe

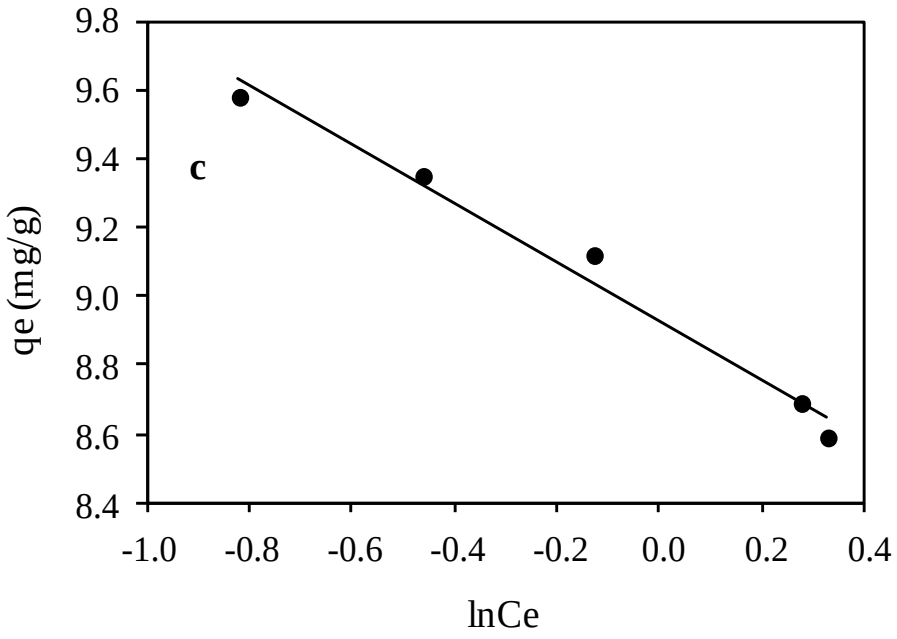


**Figure 5. 13 Temkin model for adsorption of (a) dichloromethane (b) chloroform (c) carbon tetrachloride at different concentrations, and temperature 25˚C.**

## 5.6 Regeneration of the adsorbent

Adsorbent has limited capacity for adsorbate molecules, and at the equilibrium in the adsorption process, the rates of adsorption and desorption are equal, where the net uptaking of the adsorbate on the adsorbent cannot increase further. Thus, it is necessary either to dispose or regenerate the adsorbent. In the present study, the feasibility of adsorbent regeneration was examined with a chemical and thermal treatment. The chemical treatment was tested using solvent, and the thermal treatment was conducting by heating the adsorbent/adsorbate up to 120˚C. The material was tested for three cycles, and the results showed excellent re-generability with almost the same percentage of removal. The results presented in fig (5.14), indicate that the prepared adsorbent is of excellent desorption and regeneration nature within acceptable experimental errors.

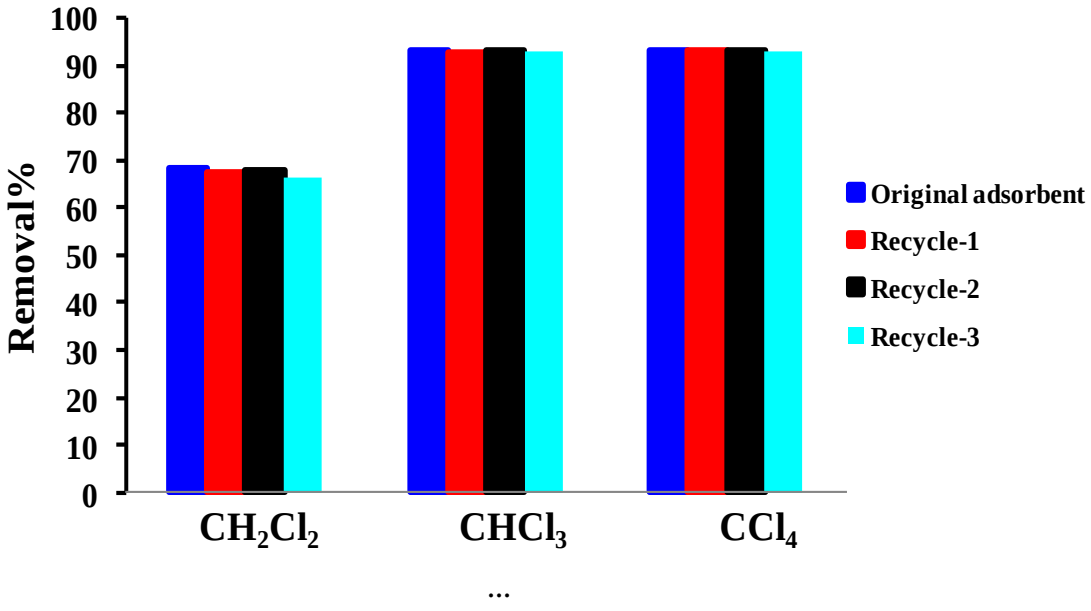


**Figure 5. 14 Regenatration adsorption of (a) dichloromethane (b) chloroform (c) carbon tetrachloride at ZnO-NP/AC dosage 0.1 g/L, contact time 60 min, and temperature 25˚C**

# CHAPTER 6

# Sorption by $SiO_2$-NP/AC

## 6.1 Characterization of $SiO_2$-NP/AC

The morphology of $SiO_2$–NP/AC composite is presented in fig (6.3). As shown, the surface of the composite is rough and has large amount of nanoparticles, which represents additional active sites for surface adsorption on the activated carbon surface. Using the scale of the SEM image, one may estimate the average diameter of the silica particles as approximately 50 nm. This value has been confirmed by taking more images and by taking the average of the nanoparticles on each image. The EDX spectrum presented in fig (6.4) indicates the elements presented in the composite, i.e. carbon, oxygen, silicon and sodium. Thermal stability of $SiO_2$–NP/AC composite was also evaluated. Thermogravimetric analysis of the prepared composites is very important for identification of the thermal stability and optimal conditions of calcination. In fig (6.2) example of TGA curve collected for the sample in flowing nitrogen is presented. As it is shown, $SiO_2$–NP/AC has better thermal stability than pristine activated carbon (AC). The FT-IR spectrum of $SiO_2$–NP/AC composite is depicted in fig (6.1). The spectra of pristine AC and pristine silica were obtained for comparison. The characteristic adsorption bands of silicon dioxide, such as the Si–O–Si asymmetric and symmetric stretching vibration at 1080 and almost 800 $cm^{-1}$, respectively, and the O–Si–O symmetric bending vibration at

470 $cm^{-1}$. Also, the band at 1720 $cm^{-1}$ corresponds to stretching vibration of C=O in carboxyl group on the activated carbon surface. Through comparing the FT-IR spectra of $SiO_2$–NP/AC composite and that of AC and silica, it can be observed that some functional groups have been introduced into the surface of the prepared composite. This may help explain the enhanced absorption character of the $SiO_2$–NP/AC composite. The XRD patterns of $SiO_2$–NP/AC composite is depicted in fig (6.5). At low diffraction angles, the typical broad diffraction band of amorphous silicon dioxide can be observed. The XRD pattern of the carbon exhibits a weak diffraction peak that is attributed to the aromatic carbon sheets oriented in a considerably random fashion.

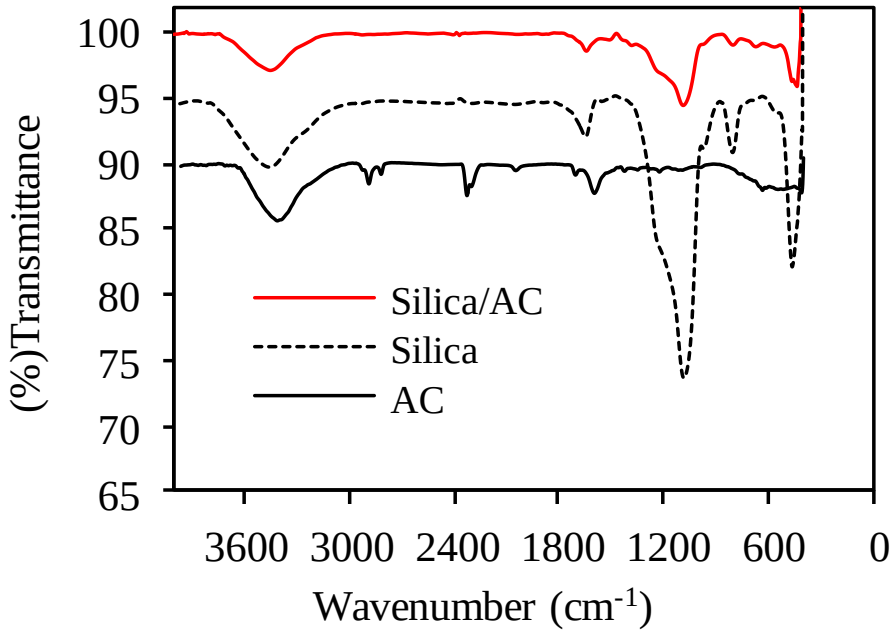


**Figure 6. 1 FT-IR spectrum of the $SiO_2$–NP/AC**

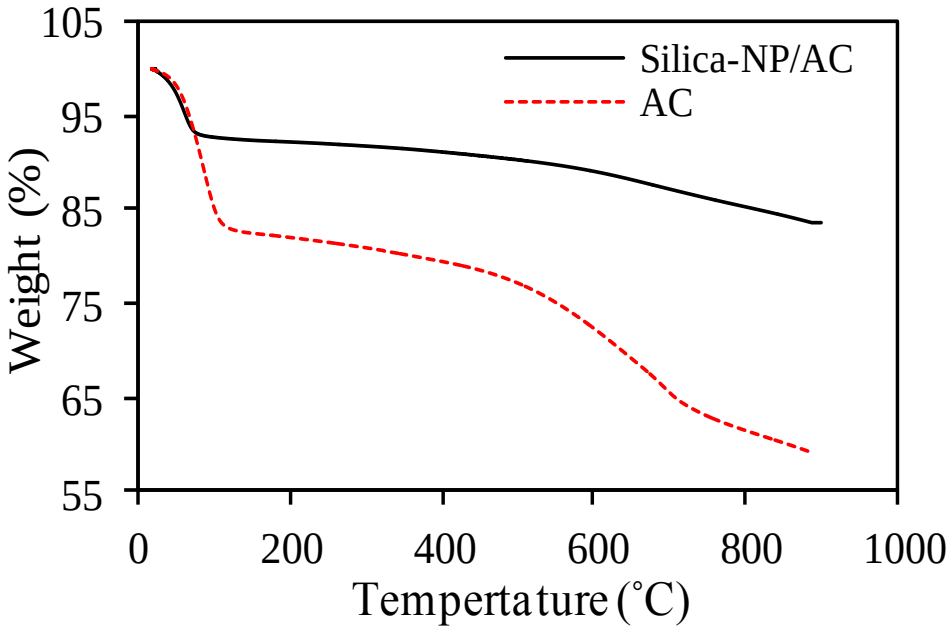


**Figure 6. 2 TGA analysis of $SiO_2$–NP/AC.**

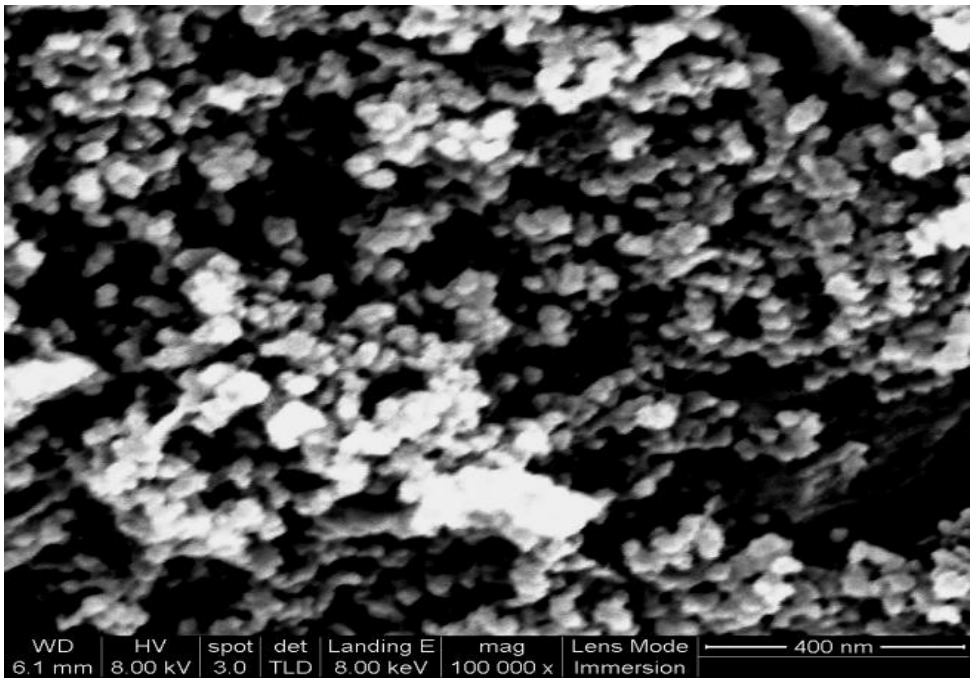


**Figure 6. 3 SEM image of $SiO_2$–NP/AC.**

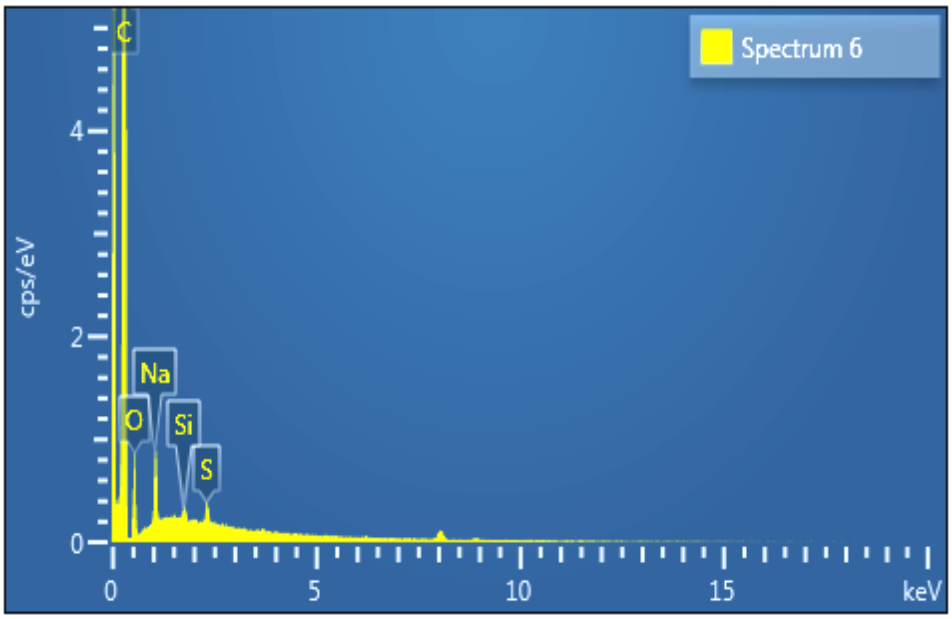


**Figure 6. 4 EDX analysis of $SiO_2$–NP/AC.**

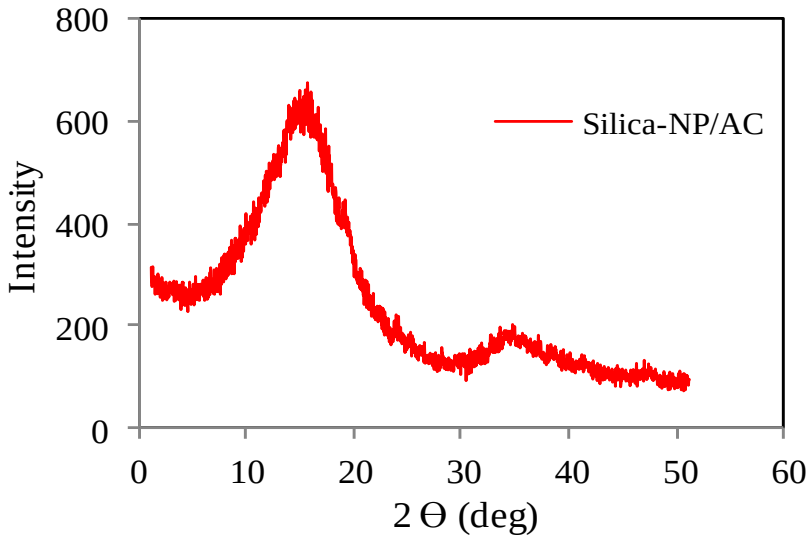


**Figure 6. 5 XRD pattern of $SiO_2$–NP/AC.**

## 6.2 Effect of contact time and initial concentration

The effect of contact time on the removal capacity of chlorinated hydrocarbons by using $SiO_2$–NP/AC (derived from rubber tires waste) composite at different three initial concentrations and constant dosage is shown in fig (6.6). It illustrates the adsorption profile of chlorinated hydrocarbons increased sharply with a contact time and then progressed by slower rate until it reaches the equilibrium step. This result is attributed to the large vacant active sites, for this reason the initial step of the adsorption it was very fast followed by slower internal diffusion process (Gialamouidis D. 2010). However, the quantity of chlorinated hydrocarbons adsorbed per unit of $SiO_2$–NP/AC mass increased as initial chlorinated hydrocarbons concentration increased due to the increase of mass transfer between the solution and the adsorbent by action of the concentration factor which is considered as the driving force in the adsorption process. The amount adsorbed of chlorinated hydrocarbons per gram of $SiO_2$–NP/AC after 10 min increased from 1.47 to 8.80 mg/g for dichloromethane, 3.40 to 15.99 mg/g for chloroform and from 4.58 to 18.61 mg/g for carbon tetrachloride as the initial chlorinated hydrocarbons concentration was increased from 5 to 20 mg/L. Therefore the adsorption was fast in the first 10 min and then decrease to be constant at the equilibrium point. The time of saturation is almost reached in 30 min.

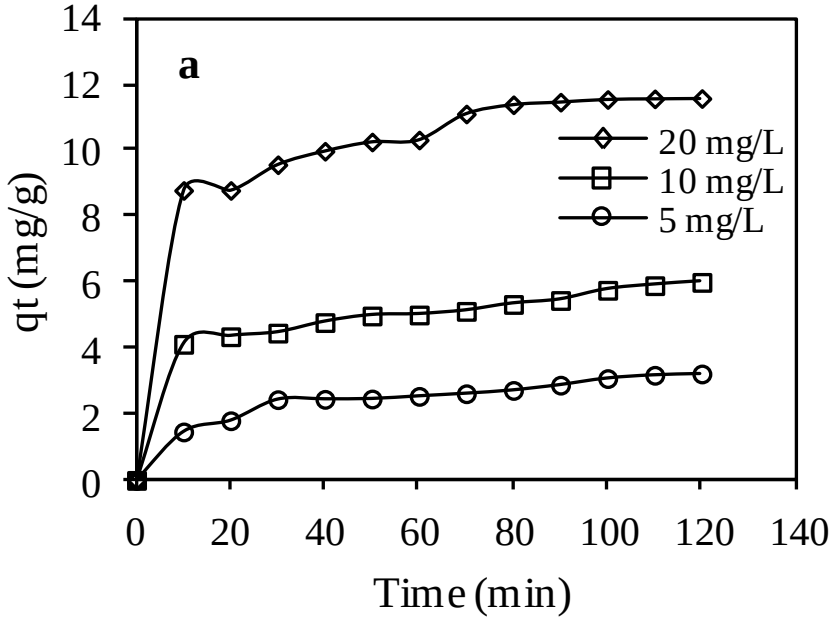
a
20 mg/L
10 mg/L
5 mg/L
qt (mg/g)
Time (min)
0
2
4
6
8
10
12
14
0
20
40
60
80
100
120
140

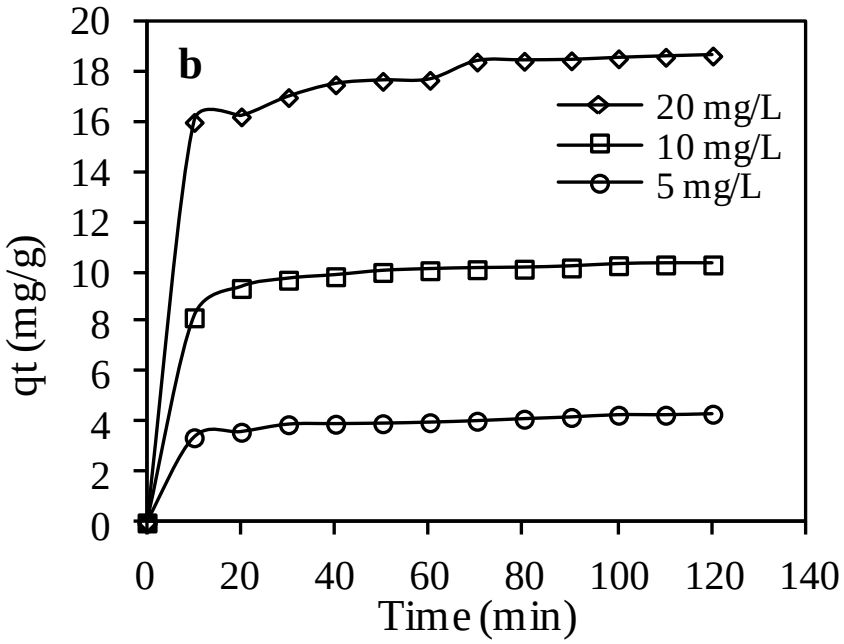
b
20 mg/L
10 mg/L
5 mg/L
qt (mg/g)
Time (min)
0
2
4
6
8
10
12
14
16
18
20
0
20
40
60
80
100
120
140

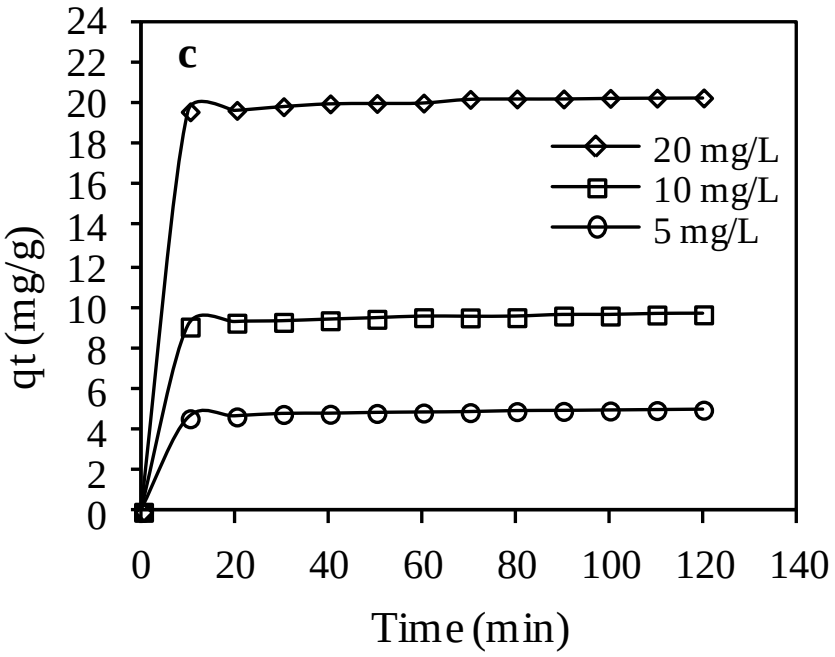


**Figure 6.6 Effect of contact time on adsorption of (a) dichloromethane, (b) chloroform, (c) carbon tetrachloride at different concentrations, and temperature 25˚C.**

## 6.3 Effect of adsorbent dosage

The amount of the adsorbent is an essential factor because it can identify the capacity of the adsorption at certain initial concentration of the adsorbate (Ouazene N 2010), fig (6.7) shows the effect of $SiO_2$–NP/AC dosage on the removal of chlorinated hydrocarbons. Different adsorbent dosages were applied for dichloromethane, chloroform and carbon tetrachloride at initial concentration 10 mg/L temperature, 25˚C and shaking time 60 min. The results illustrated that when the adsorbent dosage increased, the percent removal of chlorinated hydrocarbons was increased from 39.96 % to 91.00 % for dichloromethane, from 77.03% to 97.18 % for chloroform and from 93.71% to 99.91 % for carbon tetrachloride, with an increase of adsorbent dosage from 0.25 to 5.00 g/L. This may be

attributed to the large surface area and vacant pore volume as a result of increase the adsorbent mass in addition to the high number of adsorption active sites and more functional groups for a constant concentration of chlorinated hydrocarbons (Y.H. Li 2003, A. R. V.K. Gupta 2008). However, when the adsorbent dose exceeded 3 g/L, the increase of percent removal of chlorinated hydrocarbons was insignificantly increased (Mittal A 2005, VK 2011). The removal percentage of chlorinated hydrocarbons in solution was calculated by Eq. (6.1) as follow:

$$\% \text{ Removal} = \frac{C_\circ - C_e}{C_\circ} \times 100 \qquad (6.1)$$

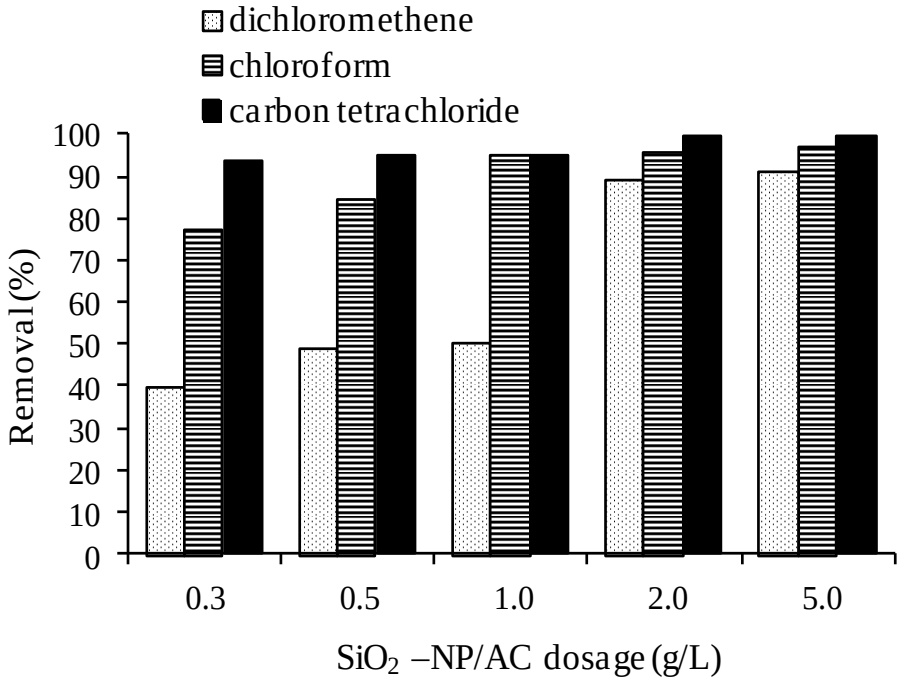


**Figure 6. 7 Effect of adsorbent dosage on the adsorption of dichloromethane, chloroform and carbon tetrachloride at different concentrations, and temperature 25˚C.**

## 6.4 Adsorption kinetics

The kinetic studies explain the rate control step and the equilibrium of the adsorption process. Also, the adsorption kinetic describes the interaction between adsorbent and solution interface and it can identify the mechanism of the adsorption processes, which might be described by the pseudo first-order (A. Sharma 2004), pseudo second-order rate equation (HoYS 2001) and intraparticle diffusion models (Wang S B 2008). The agreement between experimental results and the kinetic model expected values was indicated by the correlation coefficient ($R^2$) values. However, the relatively high ($R^2$) value it gives evidence for the successfully obeying a certain kinetic model of chlorinated hydrocarbons adsorption.

### 6.4.1 The pseudo-first order model

The pseudo-first order equation was used to interpret the adsorption data collected at three different initial concentrations of chlorinated hydrocarbons for investigating the controlling mechanism of the adsorption steps (A. Sari 2008 ). This model can be described by the following Lagergren rate equation (Lagergren 1898):

$$\log(q_e - q_t) = \frac{k_1}{2.303}\, t \qquad (6.2)$$

Where $k_1$ is the Lagergren rate constant (1/min), $q_e$ and $q_t$ are the quantity of chlorinated hydrocarbons (mg/g) at contact time t and at equilibrium, respectively. The plots of log ($q_e$-$q_t$) versus t represented in fig (6.8), the values of the rate constant $k_1$ and adsorption quantity $q_e$ at equilibrium were calculated from the slopes and intercepts table (6.1). The value of the correlation coefficient ($R^2$) of the plots was low for the three concentrations, which indicate the lack of linearity. The correspondence between the calculated $q_e$ from

the equation (6.2) and observed $q_e$ was very poor. This indicated that the adsorption of chlorinated hydrocarbons did not obey the pseudo-first-order kinetic model and the mechanism of the adsorption on the surface of the $SiO_2$–NP/AC may not fit the pseudo-first-order model well.

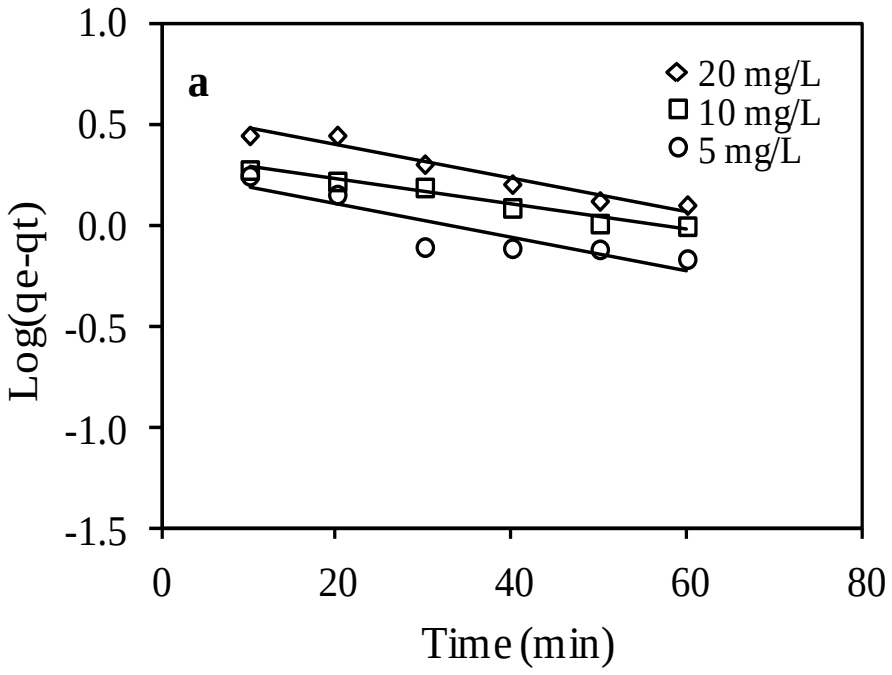

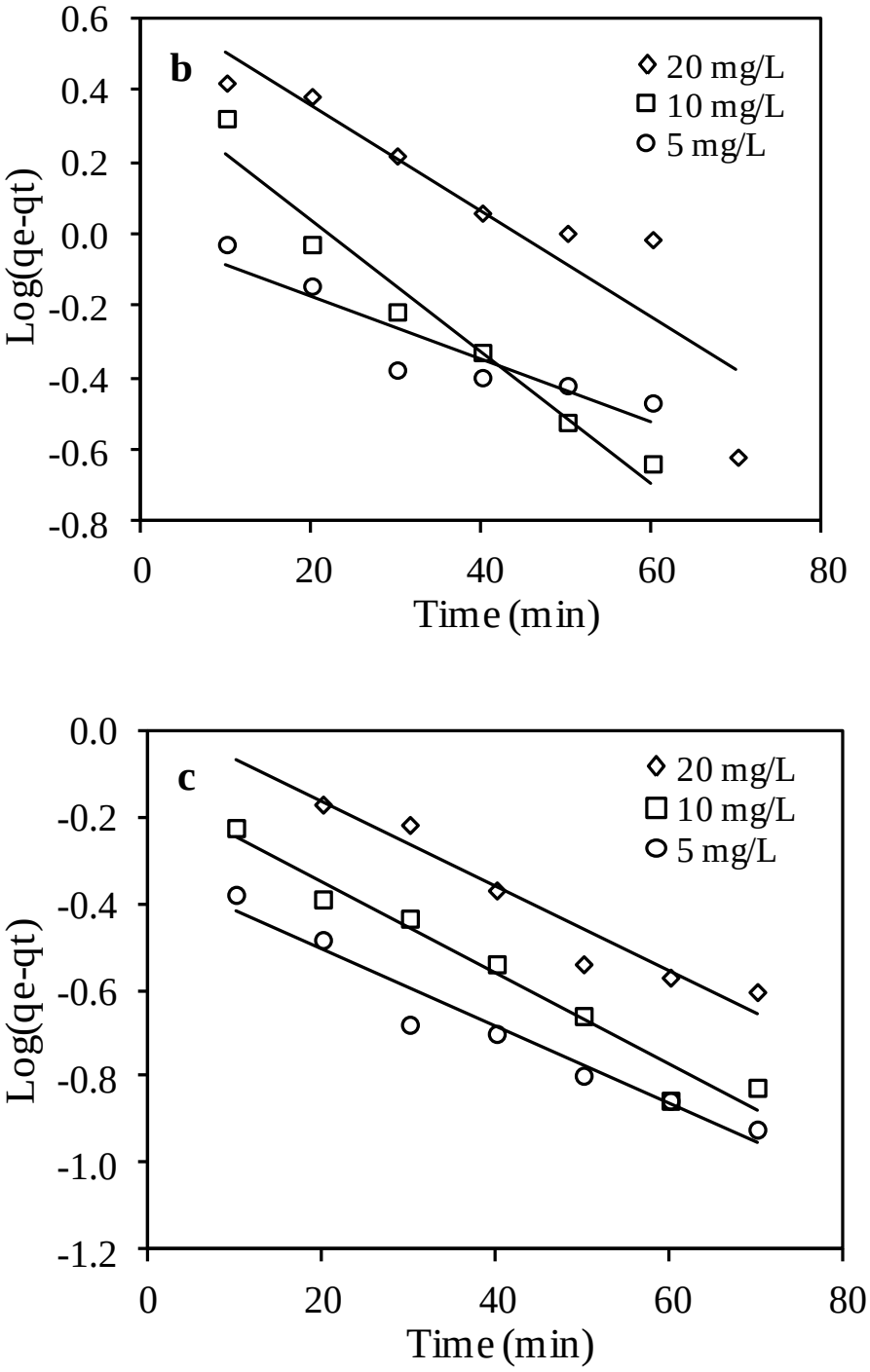


**Figure 6. 8 Lagergren first order plot for adsorption of (a) dichloromethane (b) chloroform (c) Carbon tetrachloride at different concentrations and temperature 25˚C.**

### 6.4.2 The pseudo-second order model

The pseudo second-order rate equation for the adsorption kinetic was explained by the following equation (HoYS 2000):

$$\frac{dq_t}{dt} = k_2(q_e - q_t)^2 \quad (6.3)$$

Where $k_2$ is the rate constant (g/mg.min), $q_e$ and $q_t$ are the adsorbed amount of the chlorinated hydrocarbons at equilibrium and time t, respectively. When the boundary conditions are applied from t=0 to t=t and $q_t$=0 to $q_t$=$q_e$, the equation (6.4) after the integration becomes:

$$\frac{1}{q_e - q_t} = \frac{1}{q_e} + k_2 t \quad (6.4)$$

Equation (6.5) can be expressed in the linear form as below:

$$\frac{t}{q_t} = \frac{1}{k_2 q_e^2} + \frac{t}{q_e} \quad (6.5)$$

Where h is the initial adsorption rate at t = 0 , h (mg/g.min) can be described as :

$$h = k_2 q_e^2 \quad (6.6)$$

Therefore equation (6.6) can be written in a form as:

$$\frac{t}{q_t} = \frac{1}{h} + \frac{t}{q_e} \quad (6.7)$$

The plots of $t/q_t$ against t of equation (6.7) at different initial concentrations (5,10 and 20 ppm) of the chlorinated hydrocarbons are shown in fig (6.9). The adsorption parameters were calculated and listed in table (6.1). From the plots, it was observed that the correlation coefficient values ($R^2$) ($R^2$>0.99) for all the data at different concentrations means high linearity and the adsorption kinetics between $SiO_2$–NP/AC composite and the chlorinated hydrocarbons follow the pseudo-second order. Moreover, the agreement

between the $q_e$, cal and $q_e$, (Rodrigues LA 2010) prove the fitting is best represented by the pseudo-second order model. It can be suggested that the overall rate of chlorinated hydrocarbons adsorption appears to be controlled by a chemisorption mechanism through the participation of electrons or by covalent bonds between the surface of $SiO_2$–NP/AC and adsorbate.

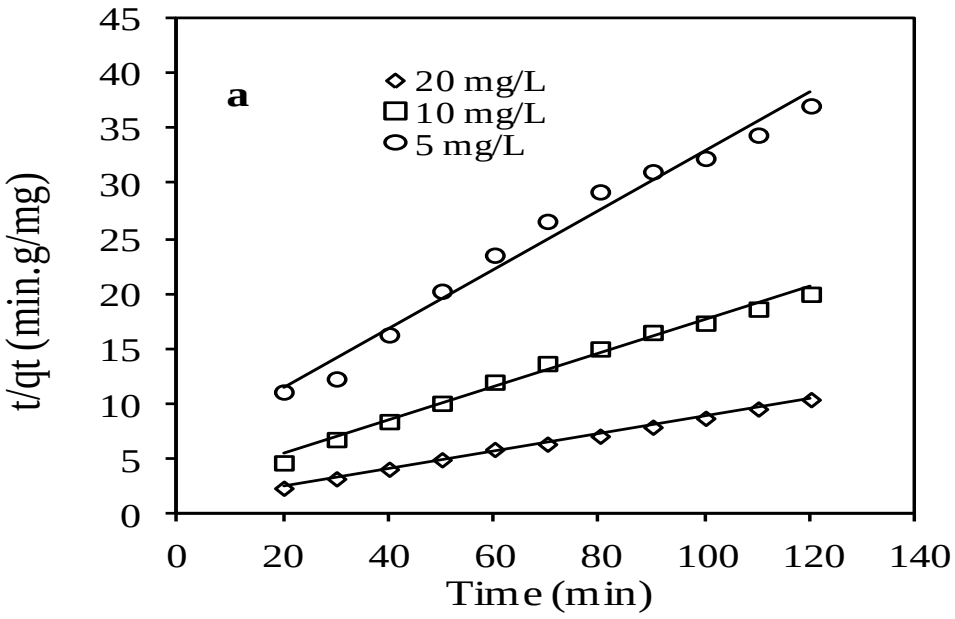

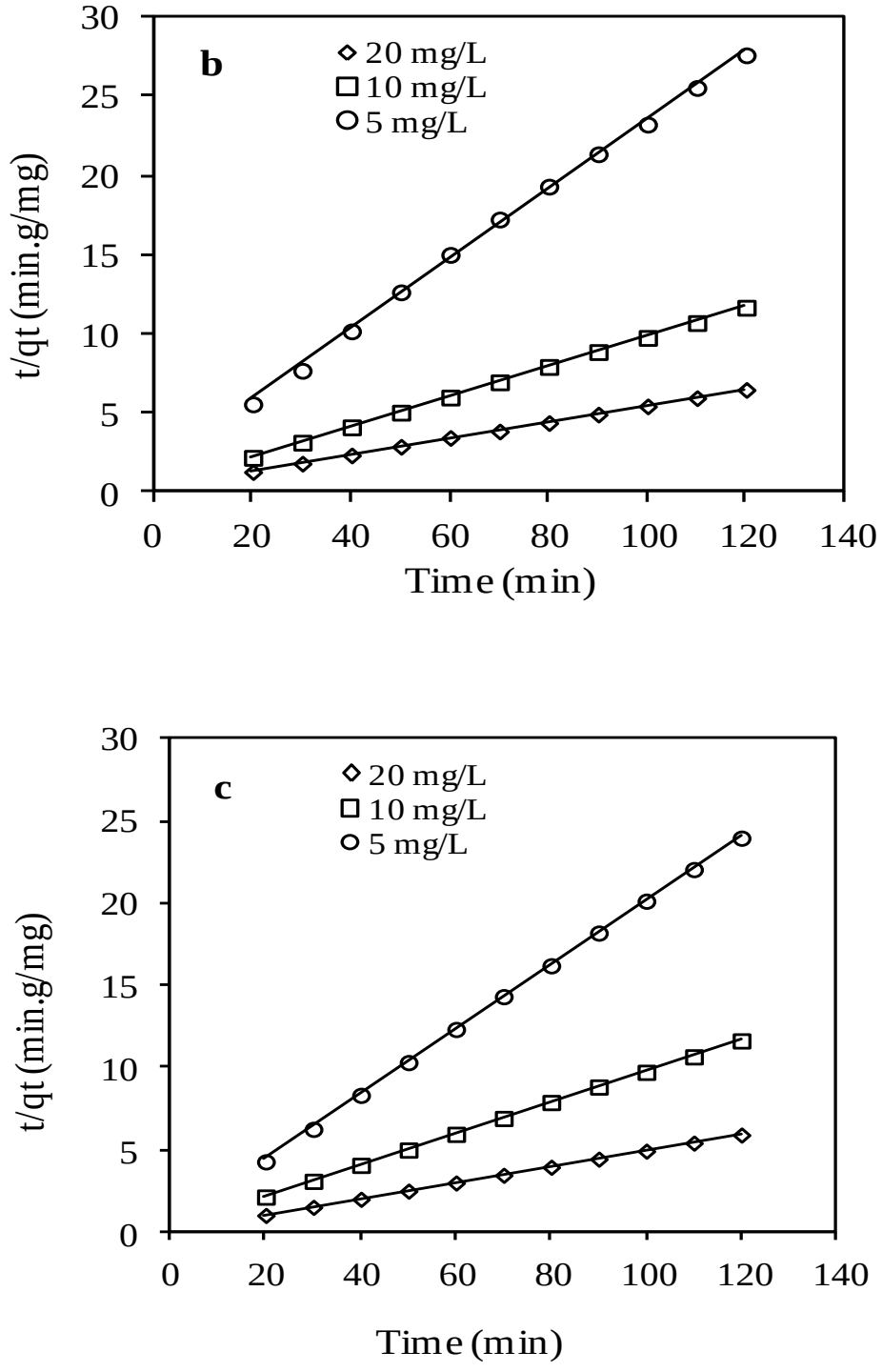


**Figure 6. 9 Linear regression of kinetics Plot: pseudo second order for (a) dichloromethane (b) Chloroform (c) Carbon tetrachloride at different concentrations and temperature 25˚C.**

### 6.4.3 The intraparticle diffusion model

The investigation of the possibility of intraparticle diffusion and prediction of the rate determining step were carried out by using Weber and Morris model (W.J. Weber 1963, Wu 2007). The rate constants ($k_{id}$) can be determined by using the following equation:

$$q_t = k_{id} t^{\frac{1}{2}} + C \qquad (6.8)$$

The plots of $q_t$ versus $t^{1/2}$ are illustrated in fig (6.10). The lines of the different concentration does not go through the point of origin, which means the mechanism cannot determine the rate of the overall process, and the adsorption mechanism is likely to be very complex (G. Cunha 2010).

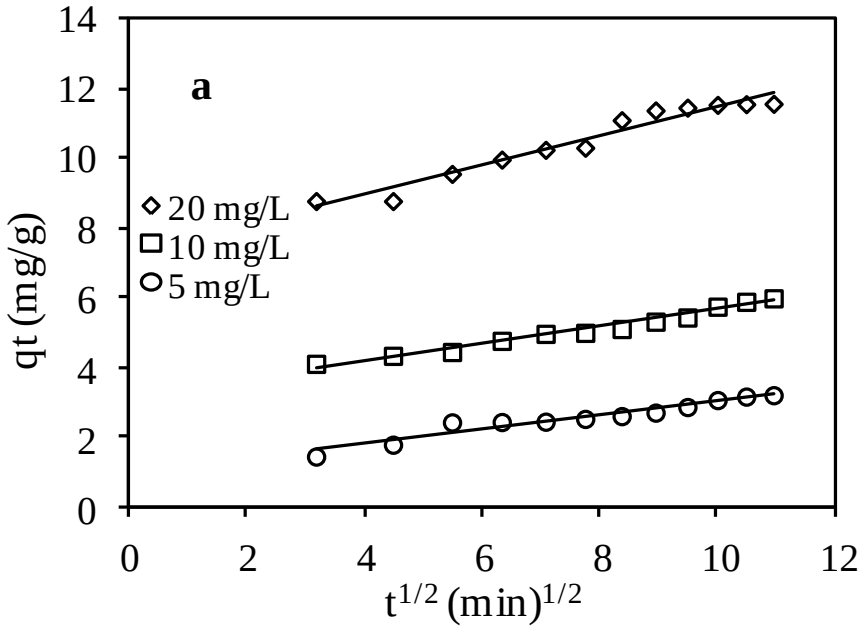

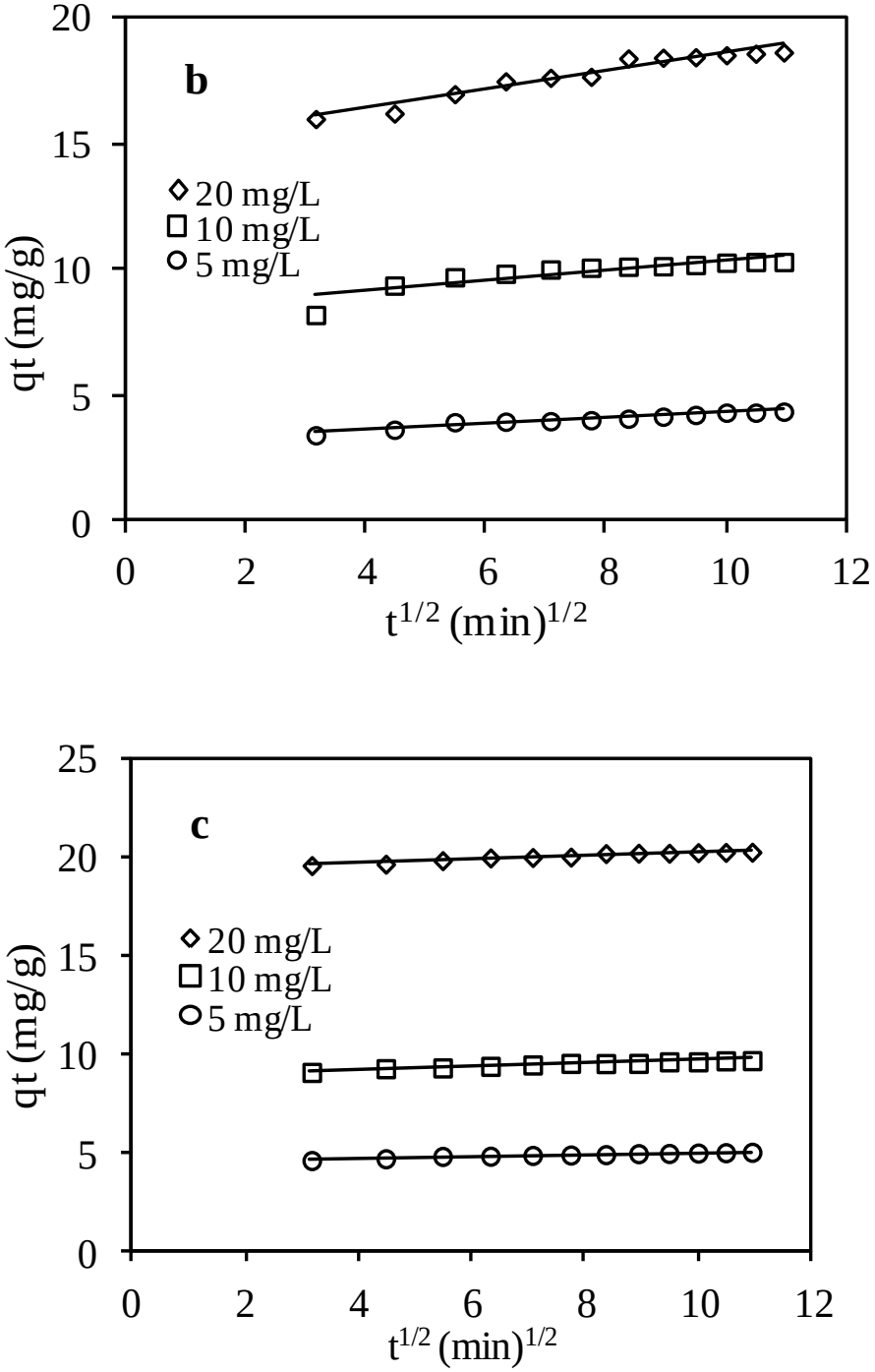


**Figure 6. 10 Intraparticle diffusion kinetic plot for (a) dichloromethane (b) chloroform (c) carbon tetrachloride at different concentrations and temperature 25˚C.**

Table 6. 1 Kinetic constant parameters obtained from chlorinated hydrocarbons adsorption on $SiO_2$–NP/AC

| Compound | Pseudo-first order | | | | | Pseudo-second order | | | Intraparticle diffusion model | | |
|---|---|---|---|---|---|---|---|---|---|---|---|
| | $C_i$ (mg/L) | $q_e$exp (mg/g) | $k_1(10^3)$ ($min^{-1}$) | $q_e$cal (mg/g) | $R^2$ | $k_2(10^{-3})$ (g/mg min) | $q_e$cal (mg/g) | $R^2$ | $k_{id}$ (mg/g min) | C (mg/g) | $R^2$ |
| | 20 | 11.590 | 18.424 | 18.468 | 0.948 | 7.765 | 12.642 | 0.998 | 0.423 | 7.283 | 0.953 |
| $CH_2Cl_2$ | 10 | 6.010 | 14.048 | 6.077 | 0.967 | 10.008 | 6.570 | 0.991 | 0.245 | 3.230 | 0.974 |
| | 5 | 3.230 | 18.885 | 4.188 | 0.802 | 11.725 | 3.724 | 0.990 | 0.206 | 0.994 | 0.933 |
| | 20 | 18.640 | 34.084 | 32.693 | 0.835 | 12.252 | 19.305 | 0.999 | 0.368 | 14.917 | 0.941 |
| $CHCl_3$ | 10 | 10.300 | 42.145 | 8.656 | 0.962 | 35.201 | 10.526 | 1.000 | 0.212 | 8.237 | 0.767 |
| | 5 | 3.230 | 20.036 | 1.004 | 0.850 | 36.022 | 4.519 | 0.998 | 0.111 | 3.159 | 0.946 |
| | 20 | 20.290 | 22.339 | 1.162 | 0.935 | 53.614 | 20.450 | 1.000 | 0.094 | 19.337 | 0.947 |
| $CCl_4$ | 10 | 9.670 | 24.412 | 2.051 | 0.961 | 35.201 | 10.526 | 1.000 | 0.073 | 8.906 | 0.966 |
| | 5 | 5.000 | 20.497 | 5.757 | 0.954 | 91.630 | 5.068 | 0.999 | 0.051 | 4.462 | 0.965 |

## 6.5 Adsorption isotherms

The adsorption isotherm describes the interactions between the adsorbate molecules in the liquid phase and the solid phase adsorbent (Hameed 2006). The maximum adsorption capacity can be determined from the isotherms. Various isotherm models were used for investigation of adsorption capacity in adsorption of chlorinated hydrocarbon from aqueous solution; three models were introduced in this study (Langmuir, Freundlich, and Temkin isotherms).

### 6.5.1 Langmuirm isotherms model

The Langmuir explains that the monolayer adsorption process occurs between the adsorbate and homogeneous surface of the adsorbent which has a specific active sites and energies (Langmuir 1916, Deng H 2009). The linear equation is given by:

$$\frac{C_e}{q_e} = \frac{1}{k_L q_m} + \frac{C_e}{q_m} \qquad (6.9)$$

Where $k_L$ is Langmuir equilibrium constant (L/mg), and $q_m$ (mg/g) is the quantity of the adsorbate in the adsorbent by monolayer adsorption. Both values were calculated from the plot $C_e/q_e$ versus $C_e$ fig (6.11). The characteristic parameter of Langmuir isotherm can be illustrated in terms of dimensionless equilibrium factor, $R_{L,}$ also known as separation factor and is defined by Weber and Chakkravorti:

$$R_L = \frac{1}{1 + K_L C_o} \qquad (6.10)$$

The plots of $C_e/q_e$ versus $C_e$ shows high linearity and is confirmed by the values of the correlation coefficient $R^2$ , which indicated that the isotherm data fit this model well. The Langmuir parameter constants were calculated and listed in table (6.2).

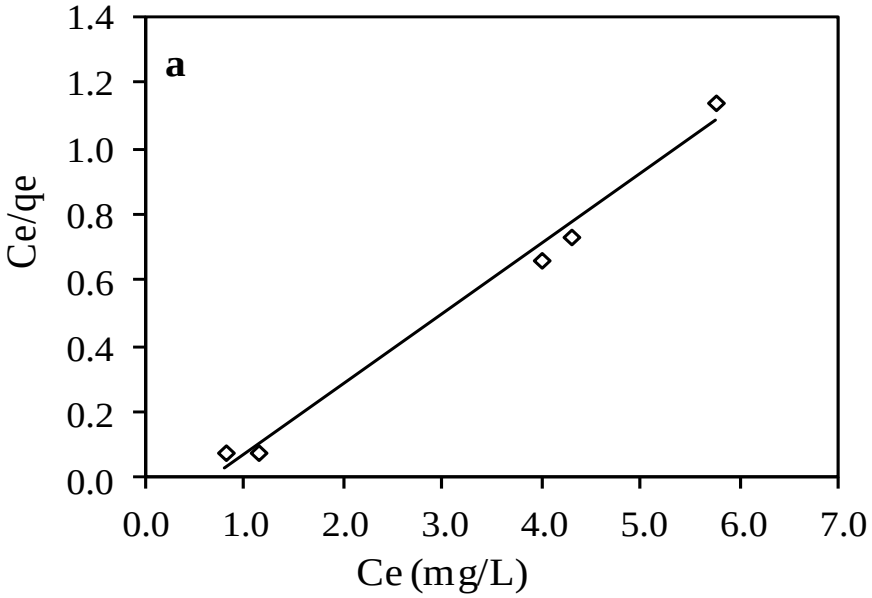
a
Ce/qe
1.4
1.2
1.0
0.8
0.6
0.4
0.2
0.0
0.0
1.0
2.0
3.0
4.0
5.0
6.0
7.0
Ce (mg/L)

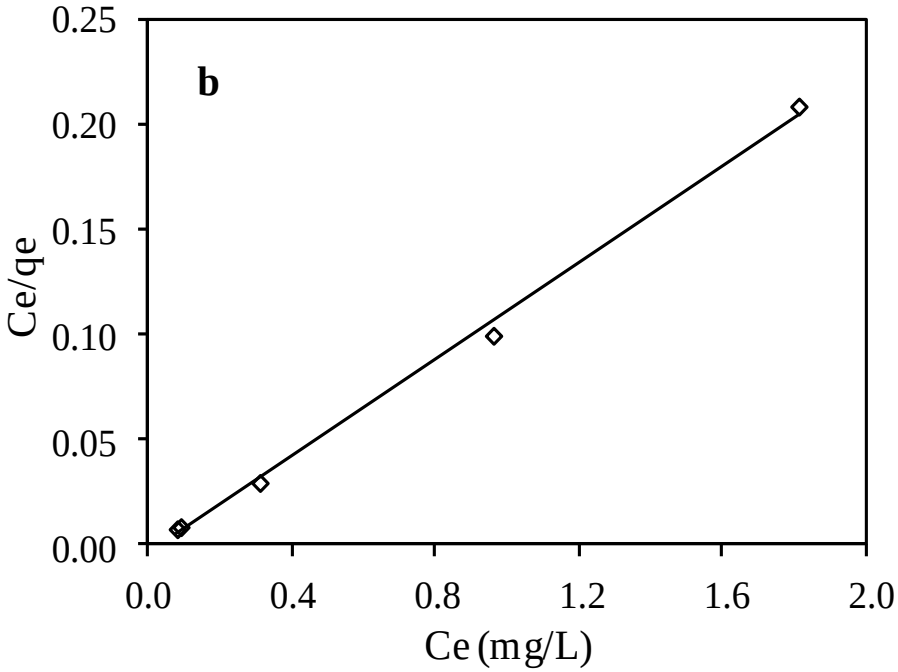
b
Ce/qe
0.25
0.20
0.15
0.10
0.05
0.00
0.0
0.4
0.8
1.2
1.6
2.0
Ce (mg/L)

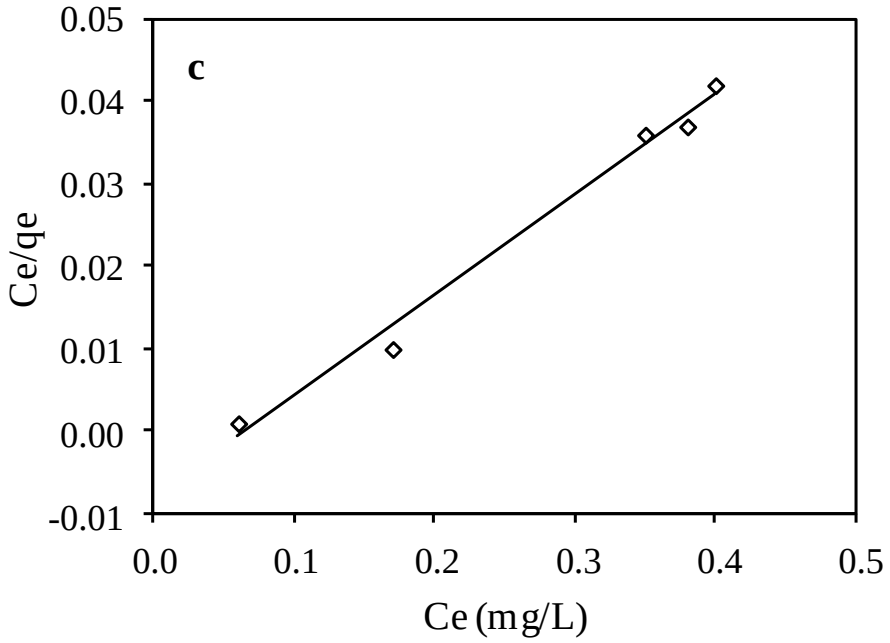


**Figure 6. 11 Langmuir model for adsorption of (a) dichloromethane (b) chloroform (c) carbon tetrachloride at different concentrations, and temperature 25°C.**

### 6.5.2 Freundlich isotherms model

Freundlich model is usually used to express adsorption on a heterogeneous surface of an adsorbent (Freundlich 1906). The Freundlich is defined by the following logarithmic equation:

$$\ln q_e = \ln K_f + \frac{1}{n} \ln C_e \qquad (6.11)$$

Where $k_F$ (L/g) and n are the adsorption capacity and adsorption intensity, respectively, and can be obtained from the linear plot by plotting $\ln q_e$ versus $\ln C_e$ fig (6.12). The Freundlich isotherm constants, $K_F$ and n, were calculated table (6.2). The n value is characteristic for the favorability of the adsorption process. The values of n > 1 demonstrate favorable adsorption conditions (Treybal 1968, V.J.P. Poots 1978, Y.S. Ho 1998). The correlation coefficient values indicate that the linearity is poor, but Freundlich

isotherm could be used to evaluate the chlorinated hydrocarbons adsorption capacity and adsorption intensity.

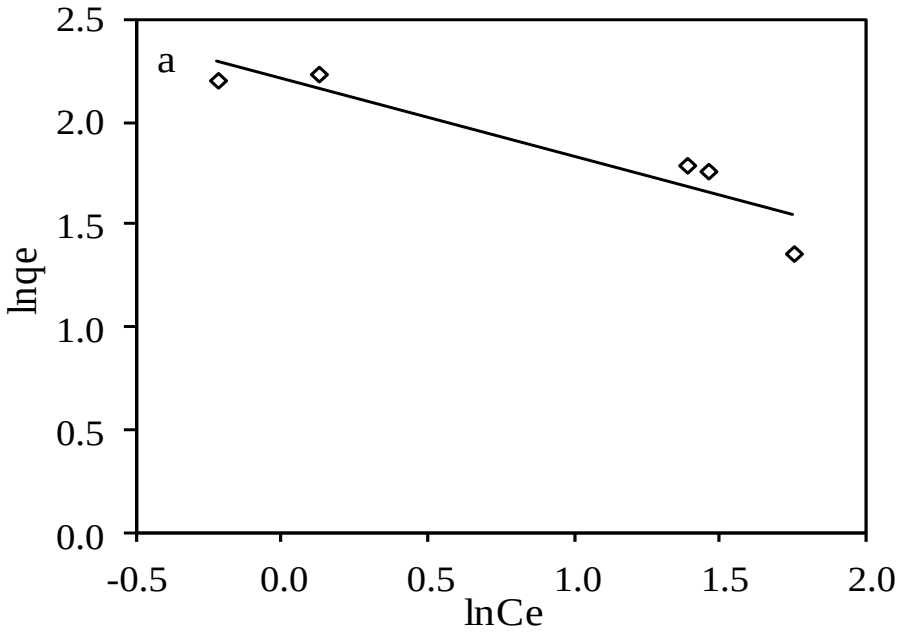


3

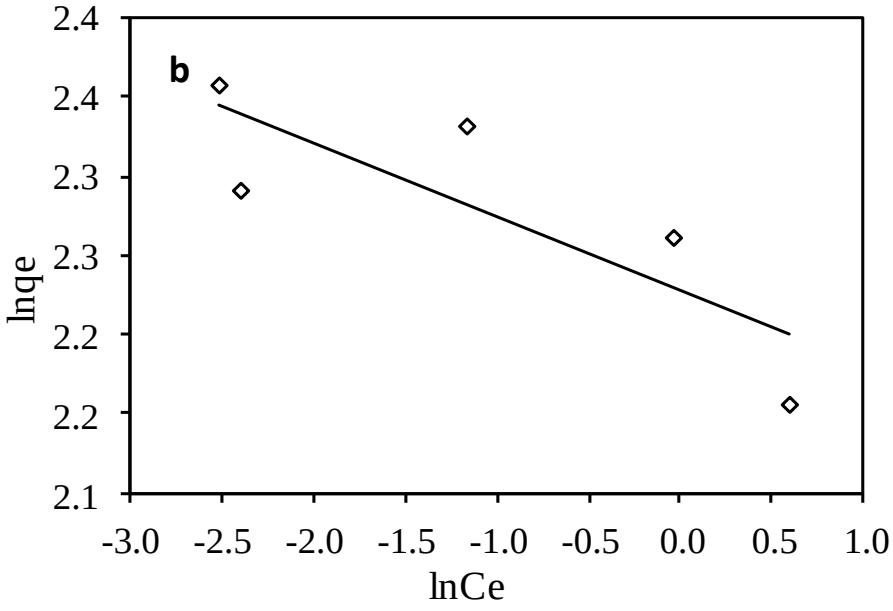

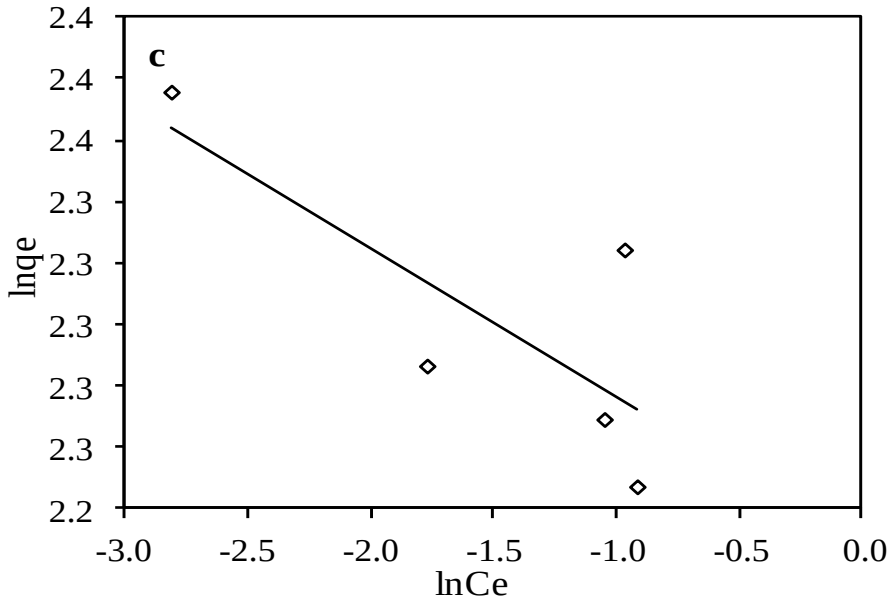


**Figure 6. 12 Freundlich model for adsorption of (a) dichloromethane (b) Chloroform (c) Carbon tetrachloride at different concentrations, and temperature 25˚C.**

### 6.5.3 Temkin isotherm model

Temkin adsorption isotherm represents the amount of the energy needed for the adsorption by one layer on the surface of adsorbent. The linear form of Temkin model is given by:

$$\ln q_e = \frac{RT}{b_T} \ln K_T + \frac{RT}{b_T} \ln C_e \qquad (6.12)$$

Where $b_T$ is the temkin constant related to the heat of sorption (kJ/mol), $k_T$ is the binding energy constant at equilibrium which is equal to the maximum binding energy (L/g), R is universal gas constant ($8.314x10^{-3}$ ), and T is the absolute temperature (degrees Kelvin) (M. Idrisa 2011 ). The plot of $q_e$ versus $\ln(C_e)$ is illustrated in fig (6.13), and the isotherm data were calculated from the slope and intercept table (6.2).

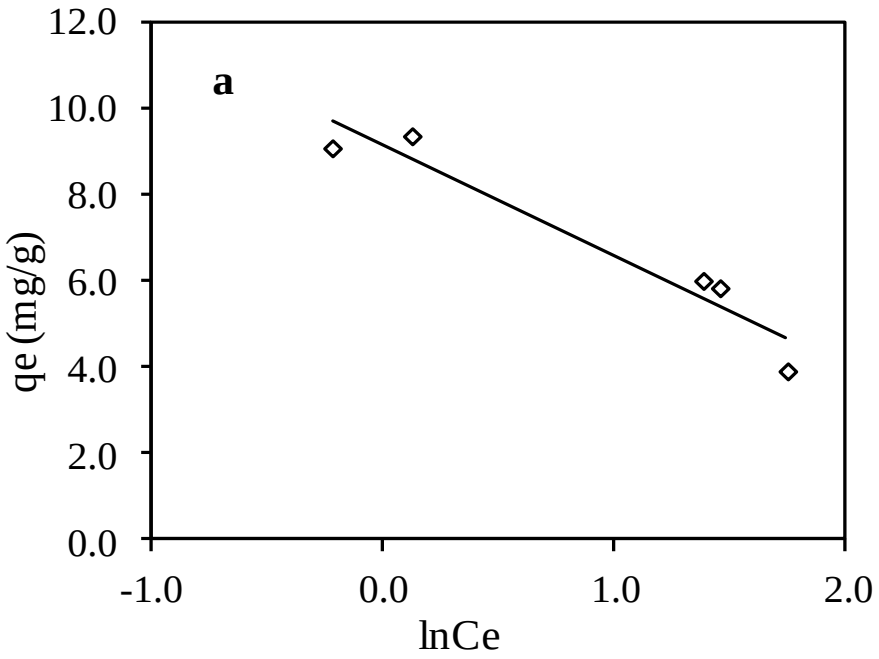
a
12.0
10.0
8.0
6.0
4.0
2.0
0.0
qe (mg/g)
-1.0
0.0
1.0
2.0
lnCe

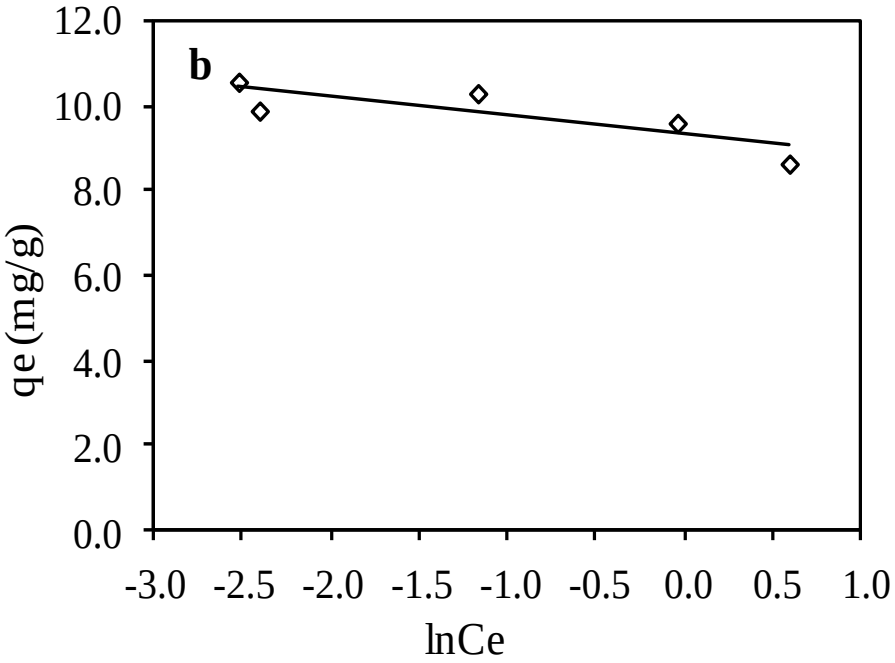
b
12.0
10.0
8.0
6.0
4.0
2.0
0.0
qe (mg/g)
-3.0
-2.5
-2.0
-1.5
-1.0
-0.5
0.0
0.5
1.0
lnCe

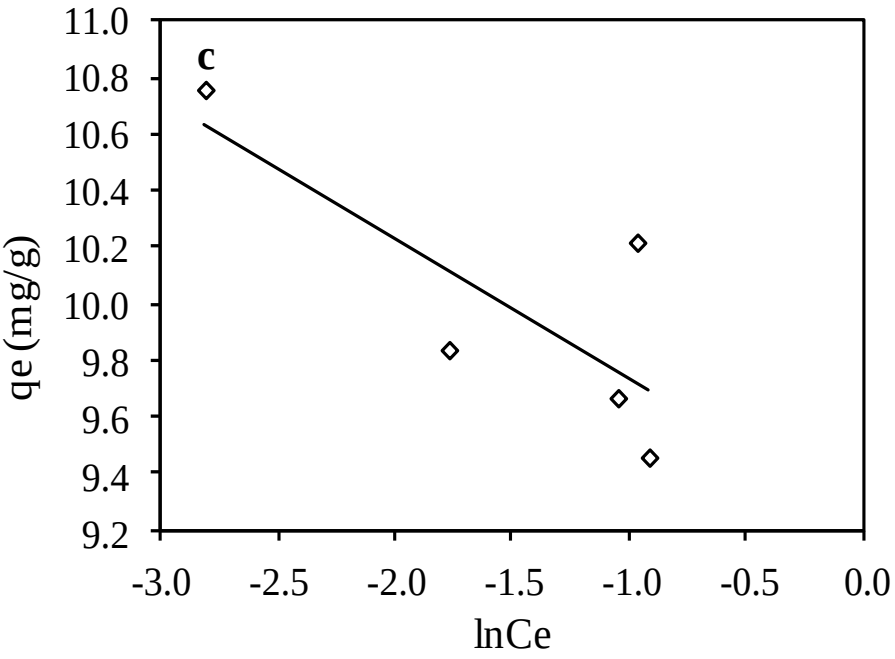


**Figure 6. 13 Temkin model for adsorption of (a) dichloromethane (b) Chloroform (c) Carbon tetrachloride at different concentrations, and temperature 25°C.**

Table 6. 2 Langmuir, Freundlich, and Temkin isotherm constants for chlorinated hydrocarbon adsorption on $SiO_2$–NP/AC

| Compound | | Langmuir isotherm constants | | | | Freundlich isotherm constants | | | | Temkin isotherm constants | | |
|---|---|---|---|---|---|---|---|---|---|---|---|---|
| | T (K) | $q_m$ (mg/g) | $k_L$ (L/mg) | $R_L$ | $R^2$ | 1/n | n | $K_F$ | $R^2$ | $k_T$ (L/gm) | $b_T$ (KJ/mol) | $R^2$ |
| $CH_2Cl_2$ | 298.16 | 4.697 | 1.525 | 0.062 | 0.988 | 0.380 | 2.632 | 9.157 | 0.981 | 36.40 | 0.977 | 0.927 |
| $CHCl_3$ | 298.16 | 8.658 | 29.615 | 0.003 | 0.997 | 0.046 | 21.739 | 9.286 | 0.999 | $13.35x10^8$ | 5.596 | 0.679 |
| $CCl_4$ | 298.16 | 8.170 | 15.111 | 0.007 | 0.988 | 0.049 | 20.408 | 9.276 | 0.605 | $12.58x10^7$ | 5.001 | 0.614 |

## 6.6 Regeneration of the adsorbent

Regarding to the applications, the disposal of adsorbent as by products in the adsorption process is not economically feasible or recommended, therefore regeneration should be attempted (H. M. K. Yogesh Kumar 2013). The possibility of regenerating the adsorbent with a chemical and thermal treatment was tested. The chemical treatment was examined using solvent and thermal treatment was conducting by heating the adsorbent/sorbent up to 100˚C. The material was tested for three cycles and the results showed excellent re-generality with almost the same percentage of removal fig (6.14).

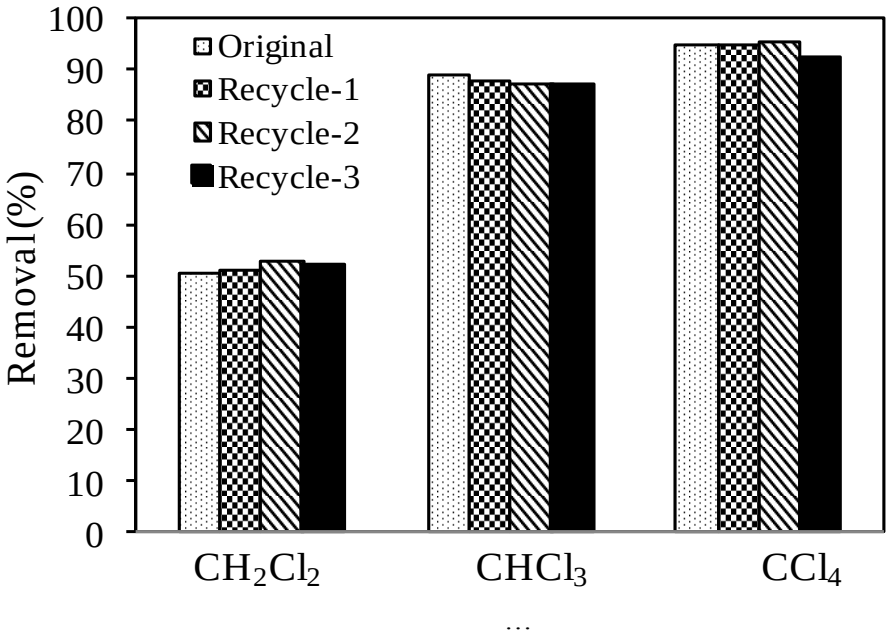


**Figure 6. 14 regenatration adsorption of (a) dichloromethane (b) Chloroform (c) Carbon tetrachloride at $SiO_2$–NP/AC dosage 0.1 g/L, contact time 60 min, and temperature 25˚C.**

# CHAPTER 7

# Sorption by $CeO_2$-NP/AC

## 7.1 Characterization of $CeO_2$-NP/AC

The morphology of $CeO_2$–NP/AC composite is presented in fig (7.2). As shown, the surface of the composite has a large number of nanoparticles, which represents additional active sites for surface adsorption on the activated carbon surface. Using the scale of the SEM image, one may estimate the average diameter of the silica particles as approximately 60 nm. This value has been confirmed by taking the average of the nanoparticles on several images. The EDX spectrum presented in fig (7.3), indicates which elements are represented in the composite, i.e. carbon, oxygen and cerium. Thermal stability of $CeO_2$–NP/AC composite was also investigated. Thermal analysis of the prepared composites is very important to determine their thermal stability and optimal conditions of calcination. In fig (7.5) example of TGA curve collected for the sample in flowing nitrogen is presented. As it is shown, $CeO_2$–NP/AC has better thermal stability than pristine activated carbon. The FT-IR spectrum of $CeO_2$–NP/AC composite is illustrated in fig (7.1). The band laying around 1640 $cm^{-1}$ represents the enhancement in the aromatic C=C groups (carbonization). The strong and broad band at 3400 $cm^{-1}$ represent O–H mode, and the band at 2900 $cm^{-1}$ is C–H aliphatic mode. The band at 1054 $cm^{-1}$ can be attributed to C-O stretching vibration. The FTIR spectrum of the cerium oxide nanoparticles exhibits strong broad peak below 700 $cm^{-1}$, which is due to the (Ce–O)

vibration mode. The XRD patterns of $CeO_2$–NP/AC composite is illustrated in fig (7.4). At low diffraction angles, the typical broad diffraction band of ceria nanoparticles can be observed. The XRD pattern of the carbon exhibits a weak diffraction peak that is attributable to the aromatic carbon sheets oriented in a considerably random fashion.

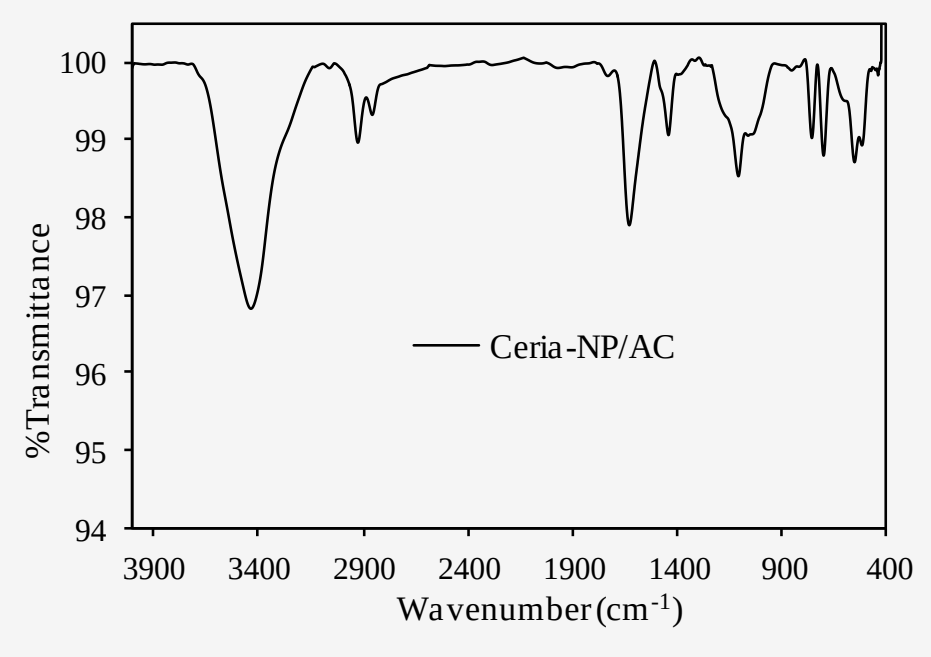


**Figure 7. 1 IR spectrum of the $CeO_2$-NP/AC.**

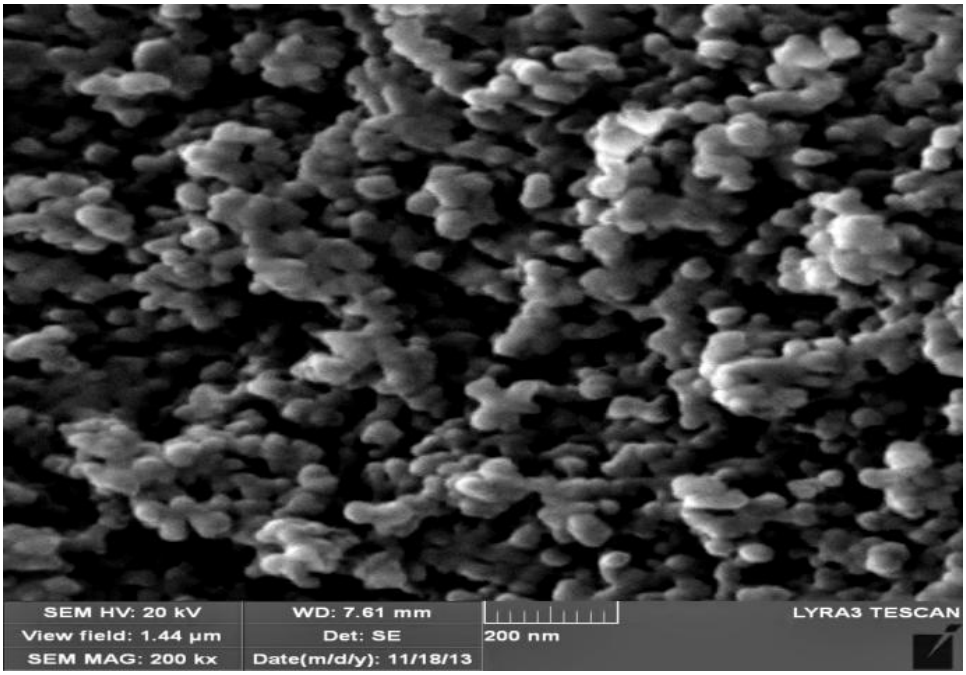


**Figure 7. 2 SEM images of the surface structure of the $CeO_2$-NP/AC.**

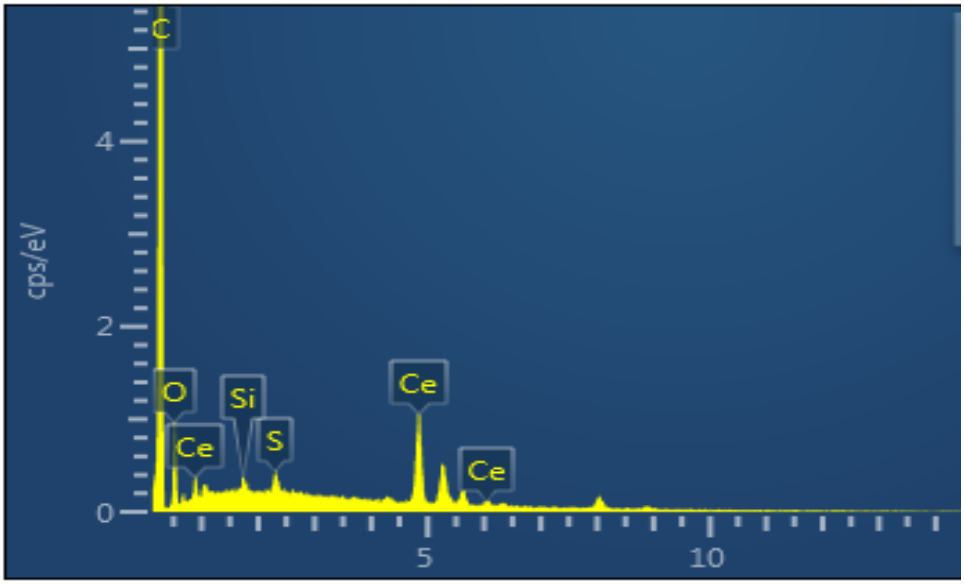


**Figure 7. 3 EDX analysis of $CeO_2$–NP/AC.**

**Table 7. 1 Chemical composition of $CeO_2$–NP/AC adsorbent.**

| Elements | Weight(%) | Atomic(%) |
|---|---|---|
| C | 52.28 | 87.96 |
| O | 4.61 | 5.82 |
| Ce | 43.11 | 6.22 |
| Total | 100 | |

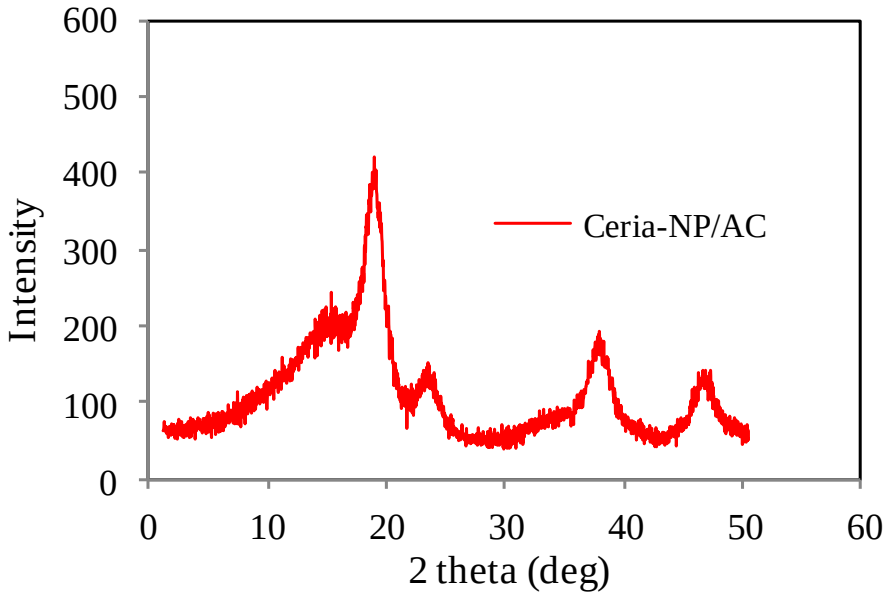


**Figure 7. 4 XRD pattern of $CeO_2$–NP/AC.**

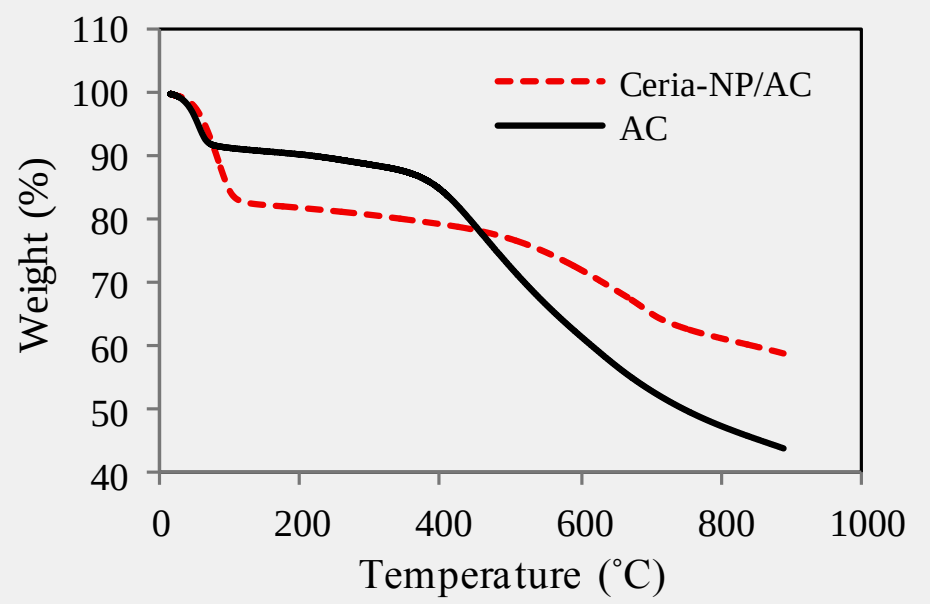


**Figure 7. 5 TGA analysis of $CeO_2$–NP/AC.**

## 7.2 Effect of contact time and initial concentration

The effect of contact time on the removal capacity of chlorinated hydrocarbons by using $CeO_2$–NP/AC (derived from rubber tires waste) composite is illustrated in fig (7.6), and it shows that the removal of chlorinated hydrocarbons increased quickly with a contact time and then progressed by slower rate until it reach the saturation step. This result is due to the large number of active sites on the external surface of the adsorbent. Consequently the initial step of the adsorption was initially very fast but was then followed by internal diffusion process that is a slow step. Moreover, the large number of vacant active sites observed after a certain time indicate that it is difficult to uptake the solute molecules, due to the repulsion force between the solute molecules on the $CeO_2$–NP/AC and bulk phases (Y. Wu 2008, M.K. Aroua 2008). However, the quantity of chlorinated hydrocarbons adsorbed per unit of $CeO_2$–NP/AC mass increased as the initial concentration of

chlorinated hydrocarbons increased due to the increase of mass transfer between the solution and the adsorbent by action of the concentration factor, which is considered as the driving force in the adsorption process (Garg 2003, Selvi 2001) . The amount adsorbed of chlorinated hydrocarbons per gram of $CeO_2$–NP/AC after 10 min increased from 1.47 to 8.80 mg/g for dichloromethane, 3.40 to 15.99 mg/g for chloroform and from 4.58 to 18.61 mg/g for carbon tetrachloride as the initial chlorinated hydrocarbons concentration was increased from 5 to 20 mg/L. Therefore the adsorption was very rapid in the first 10 min and then decrease to be constant at the equilibrium point. The time of saturation is almost reached in 30 min.

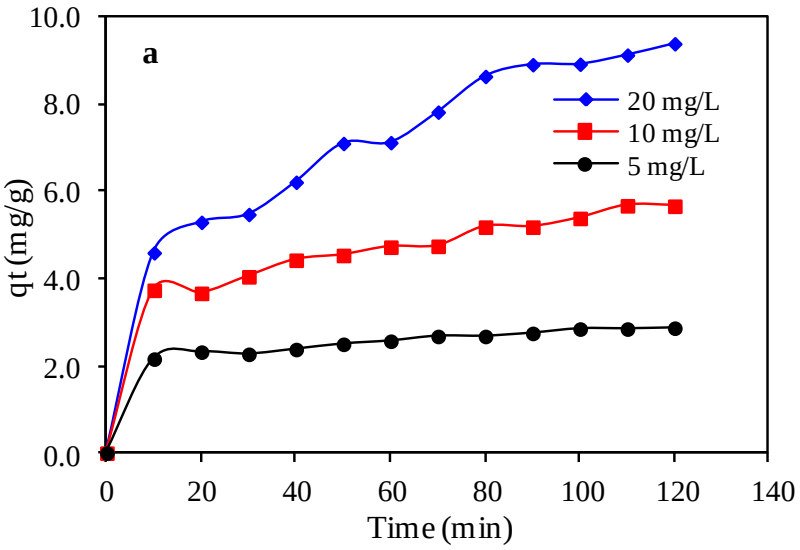

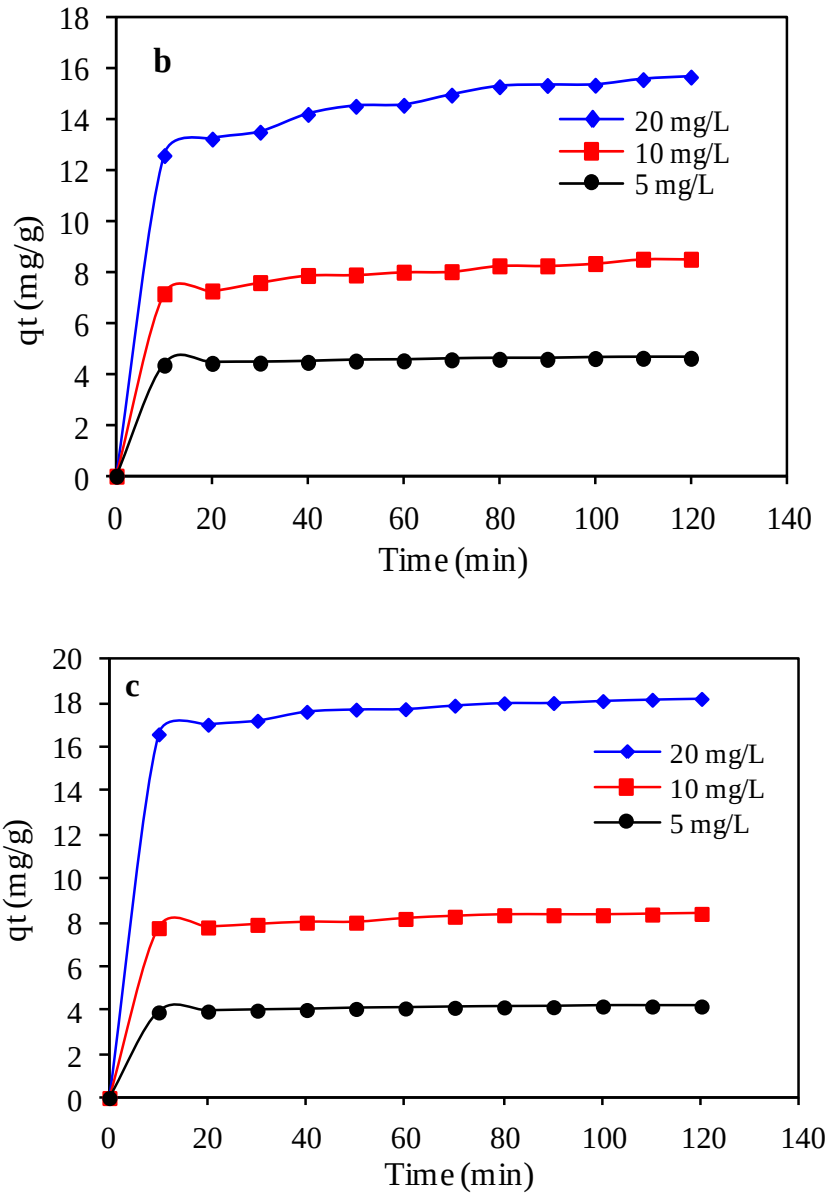


**Figure 7. 6 Effect of contact time on adsorption of (a) dichloromethane, (b) chloroform, (c) carbon tetrachloride at different concentrations, and temperature 25˚C.**

## 7.3 Effect of adsorbent dosage

The amount of the adsorbent is a significant factor because it can identify the capacity of the adsorption for a given initial concentration of the adsorbate (Ouazene N 2010). fig

(7.7) shows the effect of $CeO_2$–NP/AC dosage on the removal of chlorinated hydrocarbons. Different adsorbent dosage were applied for dichloromethane, chloroform, and carbon tetrachloride at initial concentration 10 mg/L temperature, 25˚C , and a shaking time 60 min. The results illustrated that when the adsorbent dosage increased, the percent removal of chlorinated hydrocarbons was increased from 32.04 % to 82.72 % for dichloromethane, from 57.14% to 99.40 % for chloroform and from 71.74% to 89.42 % for carbon tetrachloride, with an increase of adsorbent dosage from 0.25 to 5.00 g/L. This may be attributed to the large vacant active sites as a result of increase the adsorbent mass in addition to high number of adsorption active sites more functional groups for a constant concentration of chlorinated hydrocarbons (Y.H. Li 2003, A. R. V.K. Gupta 2008). However, when the adsorbent dose exceeded 3 g/L, the increase of percent removal of chlorinated hydrocarbons was insignificantly increased (Mittal A 2005, VK 2011). The removal percentage of chlorinated hydrocarbons in solution was calculated by Eq. (7.1) as follow:

$$\% \text{ Removal} = \frac{C_\circ - C_e}{C_\circ} \times 100 \qquad (7.1)$$

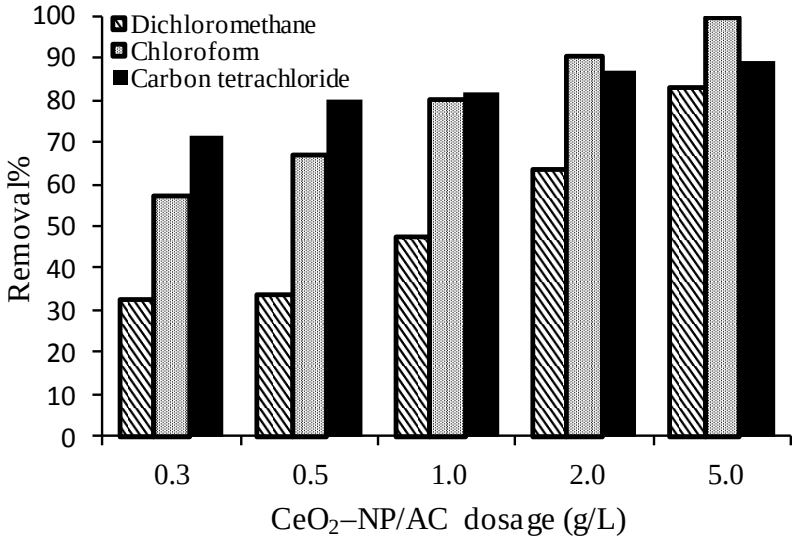


**Figure 7. 7 Effect of adsorbent dosage on the adsorption of dichloromethane, chloroform and carbon tetrachloride at different concentrations, and temperature 25°C.**

## 7.4 Adsorption kinetics

The kinetic studies explain the rate control step and the equilibrium of the adsorption process. Also, the adsorption kinetic describes the interaction between adsorbent and solution interface and can determine the mechanism of the adsorption processes. Such a mechanism might be explained by the pseudo first-order (A. Sharma 2004), pseudo second-order rate equation (HoYS 2001) and intraparticle diffusion models (Wang S B 2008). The agreement between the adsorption experimental data and the kinetic model expected values could be explained by the correlation coefficient ($R^2$) values.

### 7.4.1 The pseudo-first order model

The pseudo-first order equation was used to examine the kinetic adsorption data collected at three different initial concentrations of chlorinated hydrocarbons for investigation the rate controlling mechanism of the adsorption process (A. Sari 2008 ). The pseudo-first order equation can be described by the following Lagergren model (Lagergren 1898):

$$\log(q_e - q_t) = \frac{k_1}{2.303}\, t \qquad (7.2)$$

Where $k_1$ is the Lagergren rate constant (1/min), $q_e$ and $q_t$ are the quantities of chlorinated hydrocarbons (mg/g) at contact time t and at equilibrium, respectively. The plots of log ($q_e$-$q_t$) versus t represented in fig (7.8), the values of the rate constant $k_1$ and adsorption quantity $q_e$ at equilibrium were calculated from the plots illustrated in table (7.2). The value of the correlation coefficient ($R^2$) of the plots was low for the three concentrations, which indicate the lack of linearity for pseudo-first-order kinetic model. The correspondence between the calculated $q_e$ from the equation (7.2) and observed $q_e$ was very poor. This indicated that the adsorption of chlorinated hydrocarbons did not obey the pseudo-first-order kinetic model, and the mechanism of the adsorption on the surface of the $CeO_2$–NP/AC may not follow the pseudo-first-order model well.

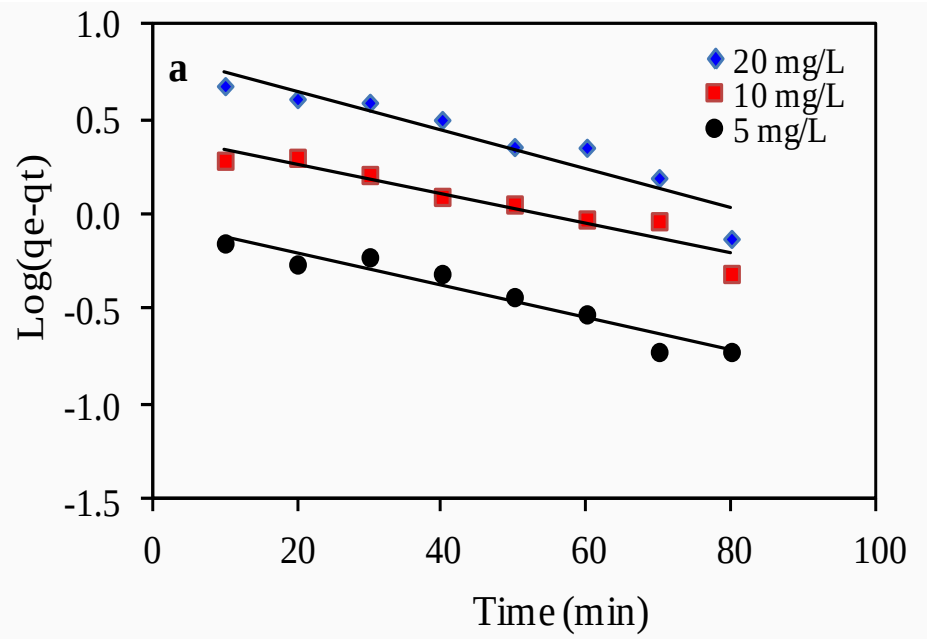
a
20 mg/L
10 mg/L
5 mg/L
Log(qe-qt)
Time (min)
1.0
0.5
0.0
-0.5
-1.0
-1.5
0
20
40
60
80
100

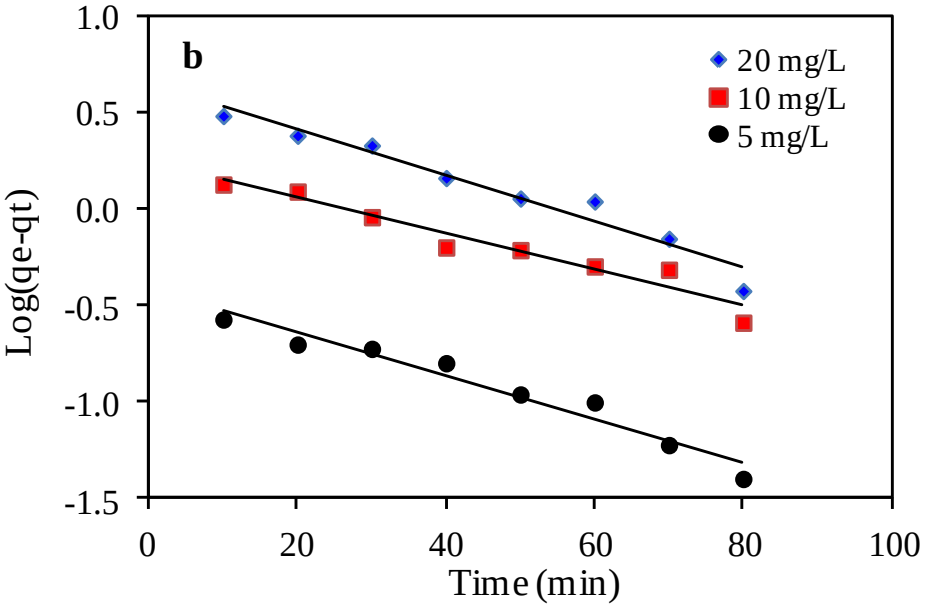
b
20 mg/L
10 mg/L
5 mg/L
Log(qe-qt)
Time (min)
1.0
0.5
0.0
-0.5
-1.0
-1.5
0
20
40
60
80
100

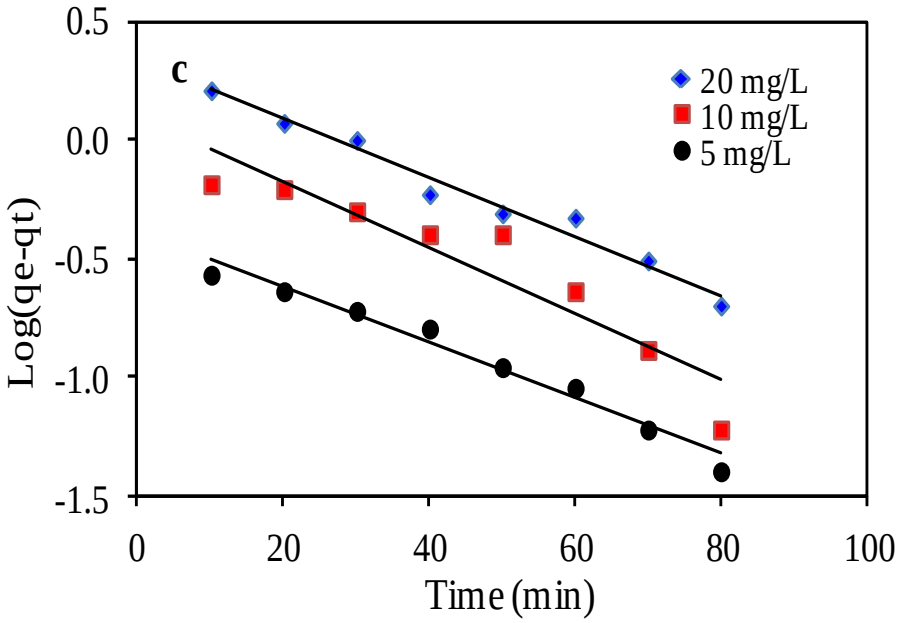


**Figure 7. 8 Lagergren first order plot for adsorption of (a) dichloromethane (b) chloroform (c) Carbon tetrachloride at different concentrations and temperature 25˚C.**

### 7.4.2 The pseudo-second order model

The pseudo second-order model of the adsorption kinetic was explained by the following equation (Ho YS 2000):

$$\frac{dq_t}{dt} = k_2(q_e - q_t)^2 \qquad (7.3)$$

Where $k_2$ the rate constant (g/mg.min), $q_e$ and $q_t$ are the adsorbed amount of the chlorinated hydrocarbons at equilibrium and time t, respectively. When the boundary conditions are applied from t=0 to t=t and $q_t$=0 to $q_t$=$q_e$, the equation (7.4) after the integration becomes:

$$\frac{1}{q_e - q_t} = \frac{1}{q_e} + k_2 t \qquad (7.4)$$

Equation (7.5) represents the integrated form of pseudo-second-order model it can be expressed in the linear form as below:

$$\frac{t}{q_t} = \frac{1}{k_2 q_e^2} + \frac{t}{q_e} \quad (7.5)$$

Where h is the initial adsorption rate at t = 0 , h (mg/g.min) can be described as :

$$h = k_2 q_e^2 \quad (7.6)$$

Therefore equation (7.6) can be written in a form as:

$$\frac{t}{q_t} = \frac{1}{h} + \frac{t}{q_e} \quad (7.7)$$

The plots of $t/q_t$ against $t$ of equation (7.7) at different initial concentrations (5,10 and 20 ppm) of the chlorinated hydrocarbons are shown in fig (7.9). The adsorption parameter $q_e$, cal and $k_2$ were calculated from the plots and listed in table (7.2). From the plots it was observed that the correlation coefficient values ($R^2$) more than ($R^2$>0.99) from all the data at different concentrations, which means high linearity and the adsorption kinetics between $SiO_2$–NP/AC composite and the chlorinated hydrocarbons follow the pseudo-second order. Moreover the correspondence between the $q_e$, cal and $q_e$, (Rodrigues LA 2010) illustrate the fitting of this model. It can be suggested that the rate of the adsorption seems to be controlled by a chemisorption mechanism through the participation of electrons or by covalent bonds between the surface of $CeO_2$–NP/AC and adsorbate.

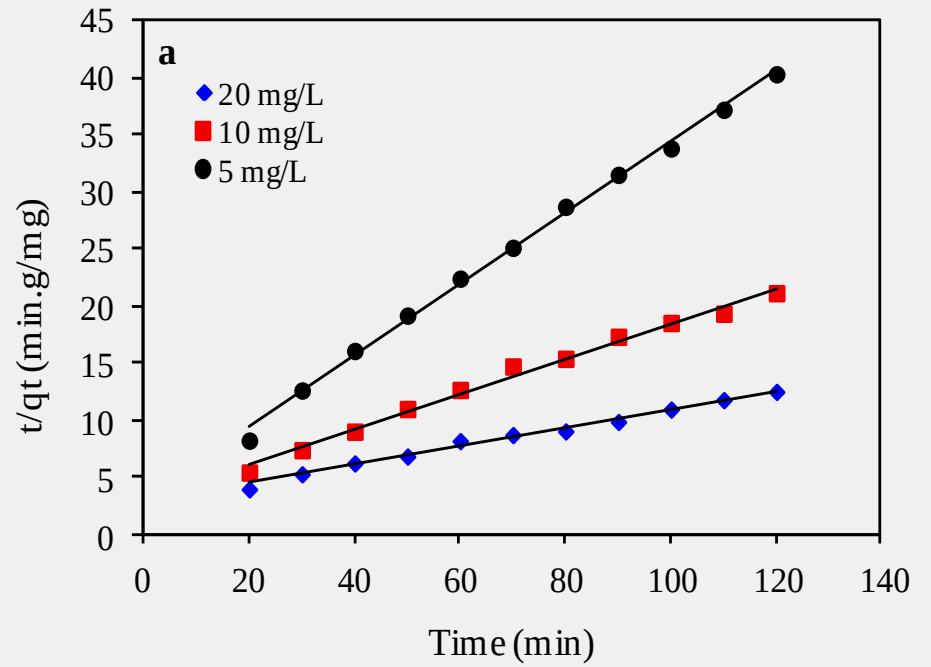
a
20 mg/L
10 mg/L
5 mg/L
t/qt (min.g/mg)
Time (min)
0
5
10
15
20
25
30
35
40
45
0
20
40
60
80
100
120
140

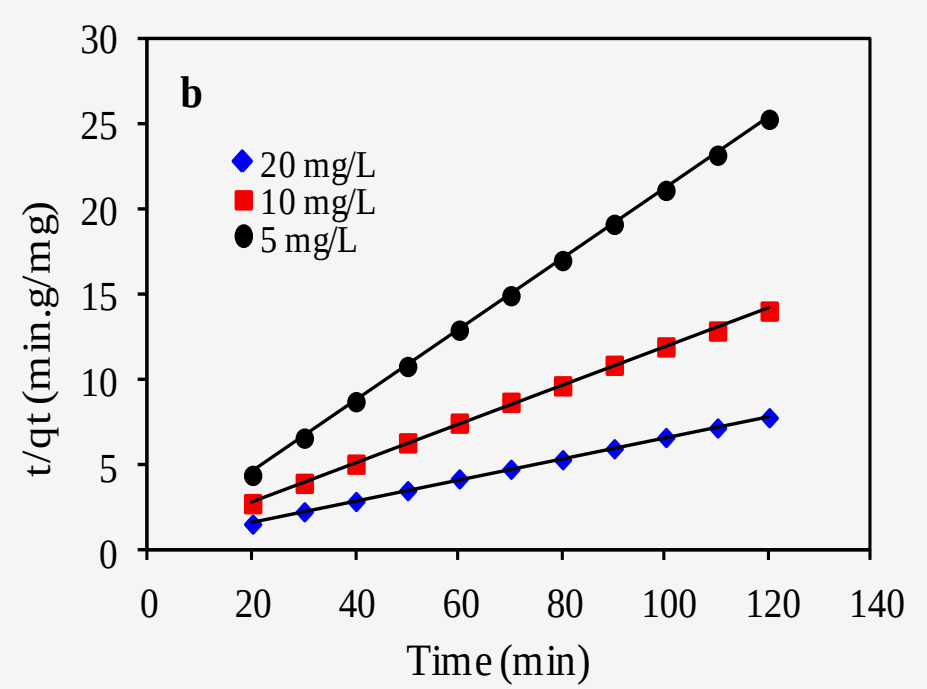
b
20 mg/L
10 mg/L
5 mg/L
t/qt (min.g/mg)
Time (min)
0
5
10
15
20
25
30
0
20
40
60
80
100
120
140

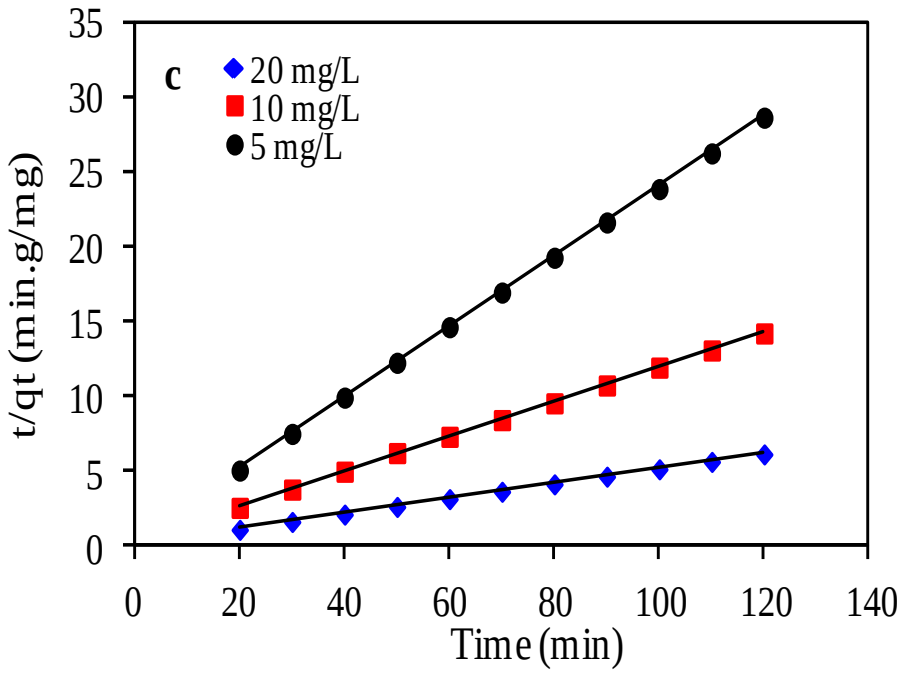


**Figure 7. 9 Linear regression of kinetics Plot: pseudo second order for (a) dichloromethane (b) chloroform (c) carbon tetrachloride at different concentrations and temperature 25˚C.**

### 7.4.3 The intraparticle diffusion model

The investigation for the possibility of intraparticle diffusion and prediction of the rate controlling step in the adsorption process were carried out by using Weber and Morris model (W.J. Weber 1963, Wu 2007). The rate constants of intra-particle diffusion ($k_{id}$) can be identified by using the following equation:

$$q_t = k_{id} t^{\frac{1}{2}} + C \qquad (7.8)$$

Where $q_t$ is the adsorbed quantity of chlorinated hydrocarbons at time t. The plots of $q_t$ versus $t^{1/2}$ are illustrated in fig (7.10) The lines of the different concentration does not pas through the origin, which means the mechanism cannot determine the rate of the overall

adsorption process, and the adsorption mechanism suppose to be very complex (G. Cunha 2010).

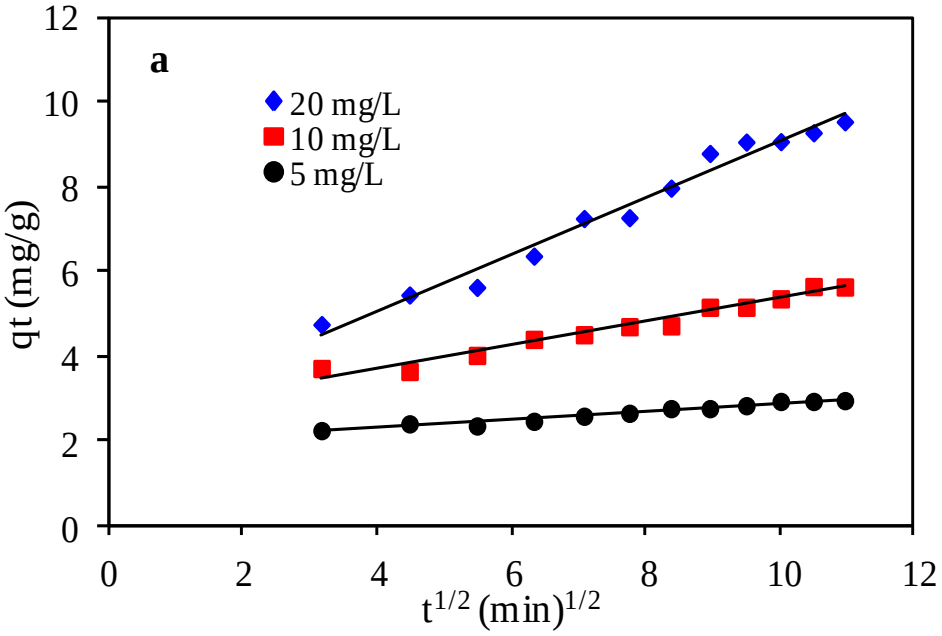


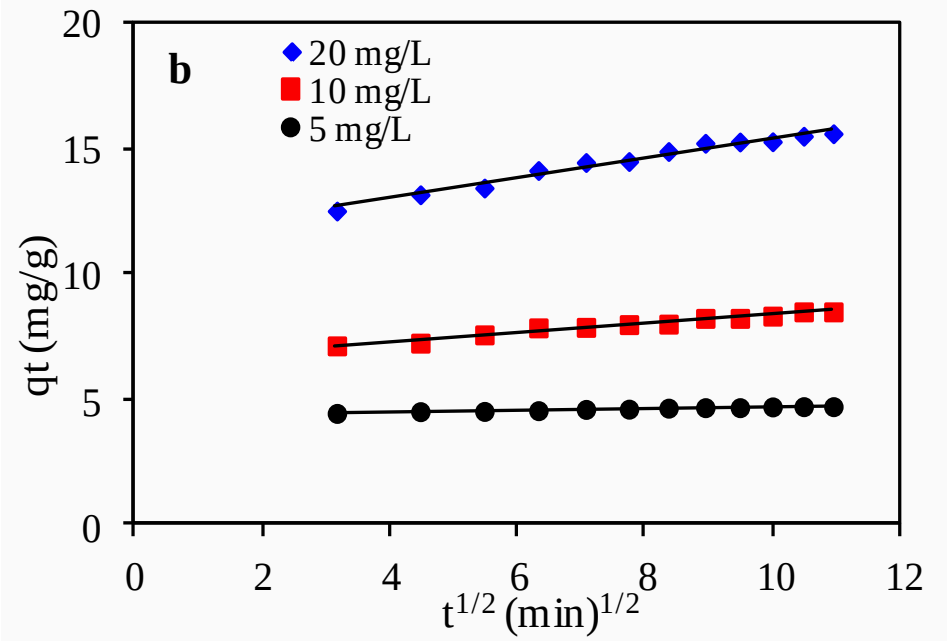

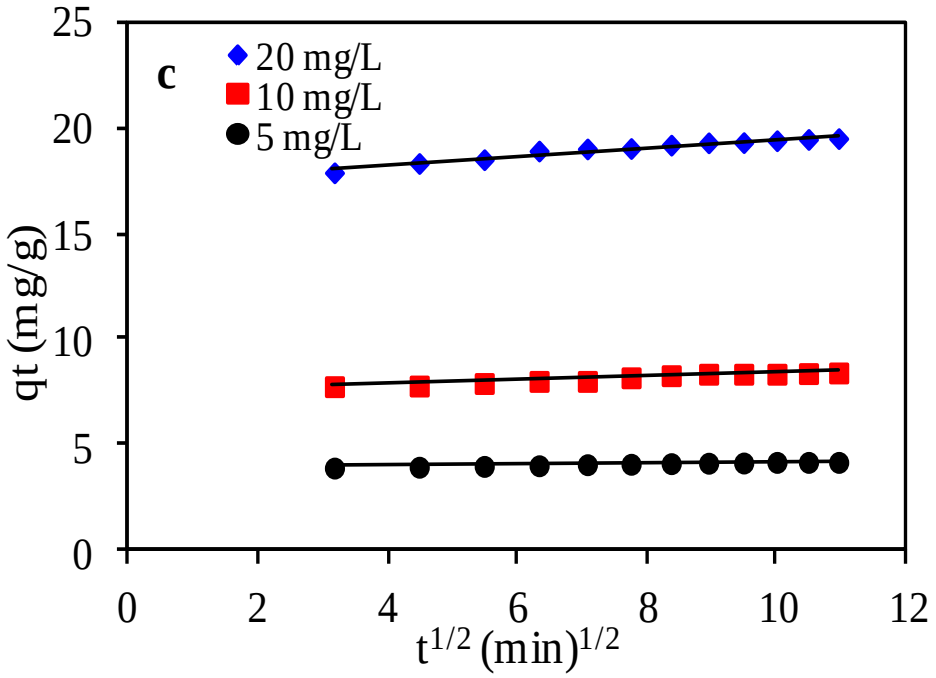


**Figure 7. 10 Intraparticle diffusion kinetic plot for (a) dichloromethane (b) chloroform (c) carbon tetrachloride at different concentrations and temperature 25˚C.**

## 7.5 Adsorption isotherm

The adsorption isotherm describes the interactions between the molecules of the adsorbate in the liquid phase and the solid phase adsorbent (Hameed 2006). Also, the maximum adsorption capacity can be determined from the isotherms. Various isotherm models were used for investigation of adsorption capacity in adsorption of chlorinated hydrocarbon from aqueous solution. The three models introduced in this study are Langmuir, Freundlich, and Temkin isotherms.

Table 7. 2 Kinetic constant parameters obtained from chlorinated hydrocarbons adsorption on $CeO_2$–NP/AC.

| Compound | Pseudo-first order | | | | | Pseudo-second order | | | Intraparticle diffusion model | | |
|---|---|---|---|---|---|---|---|---|---|---|---|
| | $C_i$ (mg/L) | $q_e$exp (mg/g) | $k_1(10^3)$ ($min^{-1}$) | $q_e$cal (mg/g) | $R^2$ | $k_2(10^{-3})$ (g/mg min) | $q_e$cal (mg/g) | $R^2$ | $k_{id}$ (mg/g min) | C (mg/g) | $R^2$ |
| | 20 | 9.57 | 23.491 | 172.139 | 0.889 | 0.234 | 12.24 | 0.990 | 0.670 | 2.394 | 0.975 |
| $CH_2Cl_2$ | 10 | 5.67 | 18.194 | 85.949 | 0.907 | 0.800 | 6.45 | 0.991 | 0.277 | 2.606 | 0.966 |
| | 5 | 2.97 | 20.004 | 4.802 | 0.935 | 3.033 | 3.20 | 0.997 | 0.098 | 1.918 | 0.968 |
| | 20 | 15.64 | 27.406 | 131.033 | 0.950 | 0.989 | 16.08 | 0.999 | 0.402 | 11.435 | 0.974 |
| $CHCl_3$ | 10 | 8.52 | 21.418 | 49.424 | 0.939 | 2.112 | 8.83 | 0.999 | 0.179 | 6.596 | 0.974 |
| | 5 | 4.73 | 25.794 | 83.538 | 0.952 | 0.121 | 4.79 | 1.000 | 0.035 | 4.355 | 0.982 |
| | 20 | 19.53 | 28.327 | 66.119 | 0.975 | 2.551 | 19.81 | 1.000 | 0.199 | 17.47 | 0.949 |
| $CCl_4$ | 10 | 8.42 | 32.012 | 18.926 | 0.872 | 4.344 | 8.59 | 0.999 | 0.095 | 7.424 | 0.955 |
| | 5 | 4.18 | 26.945 | 78.415 | 0.973 | 11.527 | 4.25 | 1.000 | 0.038 | 3.789 | 0.984 |

### 7.5.1 Langmuir isotherm model

The Langmuir explains that the adsorption process occurs on homogeneous surface of the adsorbent by monolayer of the adsorbate, which has a specific active sites and energies (Langmuir 1916, Deng H 2009). The linear equation is given by:

$$\frac{C_e}{q_e} = \frac{1}{k_L q_m} + \frac{C_e}{q_m} \qquad (7.9)$$

Where $k_L$ is Langmuir equilibrium constant (L/mg), and $q_m$ (mg/g) is the maximum amount by monolayer adsorption, they were calculated from a plot $C_e/q_e$ versus $C_e$ fig (7.11). The characteristic dimensionless equilibrium parameter for this model is the separation factor, defined by Weber and Chakkravorti:

$$R_L = \frac{1}{1 + K_L C_o} \qquad (7.10)$$

The plots of $C_e/q_e$ versus $C_e$ shows high linearity confirmed by the values of the correlation coefficient $R^2$ , which indicated that the isotherm data fit the this model well. The Langmuir parameters constants were calculated and listed in table (7.3).

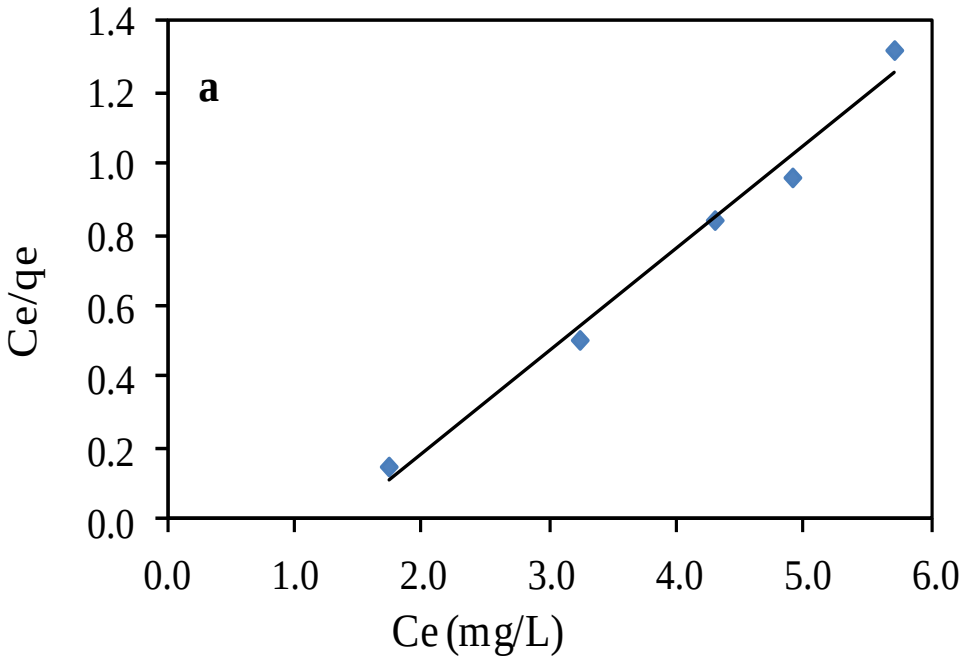
a
1.4
1.2
1.0
0.8
0.6
0.4
0.2
0.0
Ce/qe
0.0
1.0
2.0
3.0
4.0
5.0
6.0
Ce (mg/L)

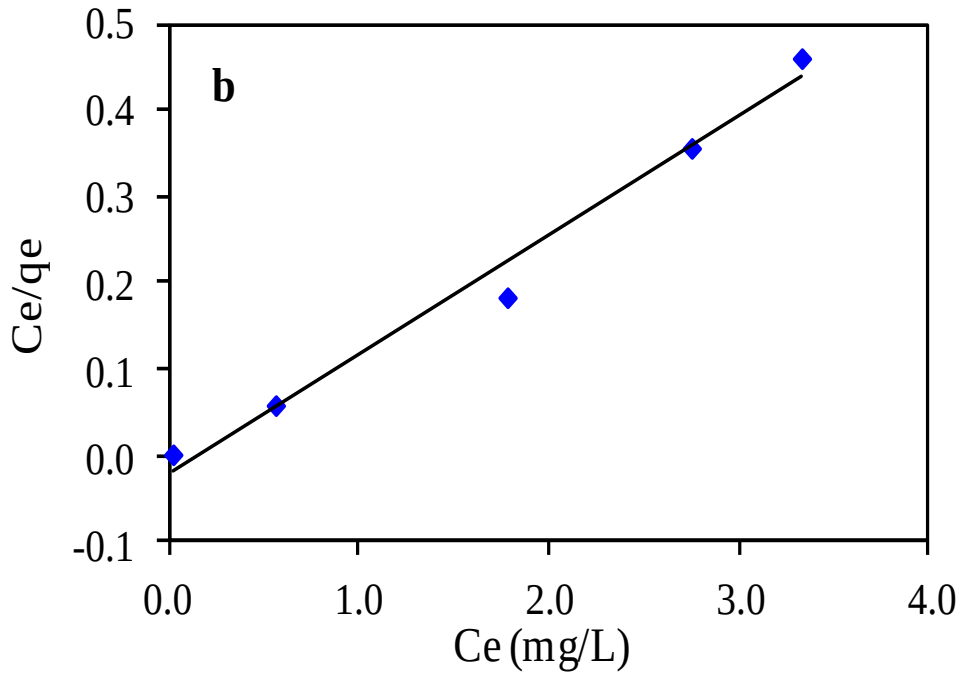
b
0.5
0.4
0.3
0.2
0.1
0.0
-0.1
Ce/qe
0.0
1.0
2.0
3.0
4.0
Ce (mg/L)

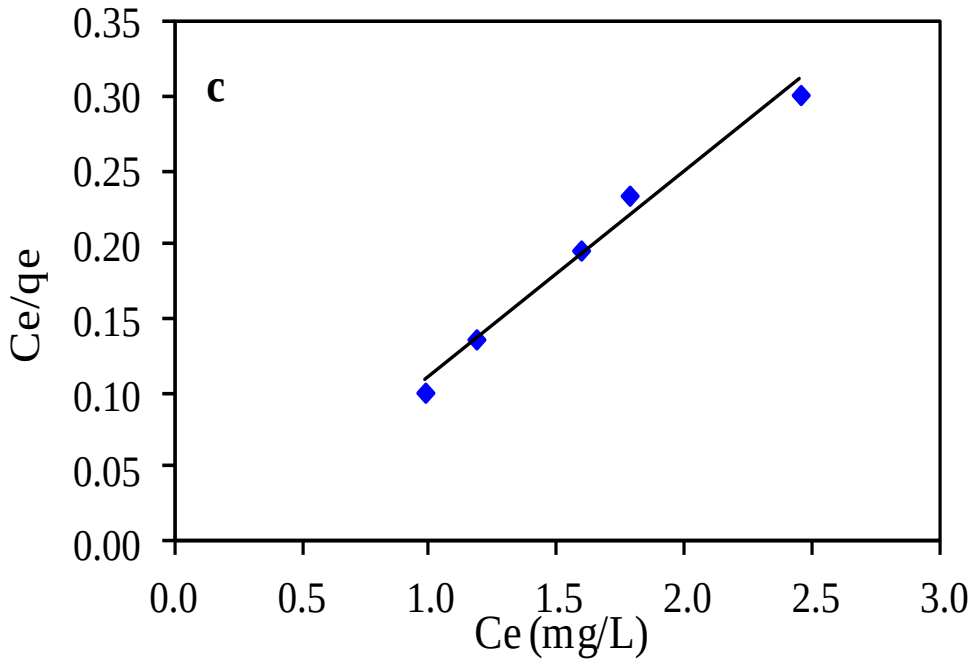


**Figure 7. 11 Langmuir model for adsorption of (a) dichloromethane (b) chloroform (c) carbon tetrachloride at different concentrations, and temperature 25˚C.**

### 7.5.2 Freundlich isotherm model

Freundlich model is usually used to explain the adsorption by a heterogeneous surface of an adsorbent (Freundlich 1906). The well-known form of Freundlich equation is defined as following:

$$\ln q_e = \ln K_f + \frac{1}{n} \ln C_e \qquad (7.11)$$

Where $k_F$ (L/g) and n are the adsorption capacity and adsorption intensity, respectively. The Freundlich constants can be obtained by plotting $Lnq_e$ versus $LnC_e$ fig (7.12). The Freundlich isotherm constants, $K_F$ and n, were calculated table(7. 2). The values of n > 1 represent favorable adsorption condition (Treybal 1968, V.J.P. Poots 1978, Y.S. Ho 1998). The values of the correlation coefficient gives an indication for the poor linearity,

but Freundlich isotherm could be used to investigate the chlorinated hydrocarbons adsorption capacity and adsorption intensity.

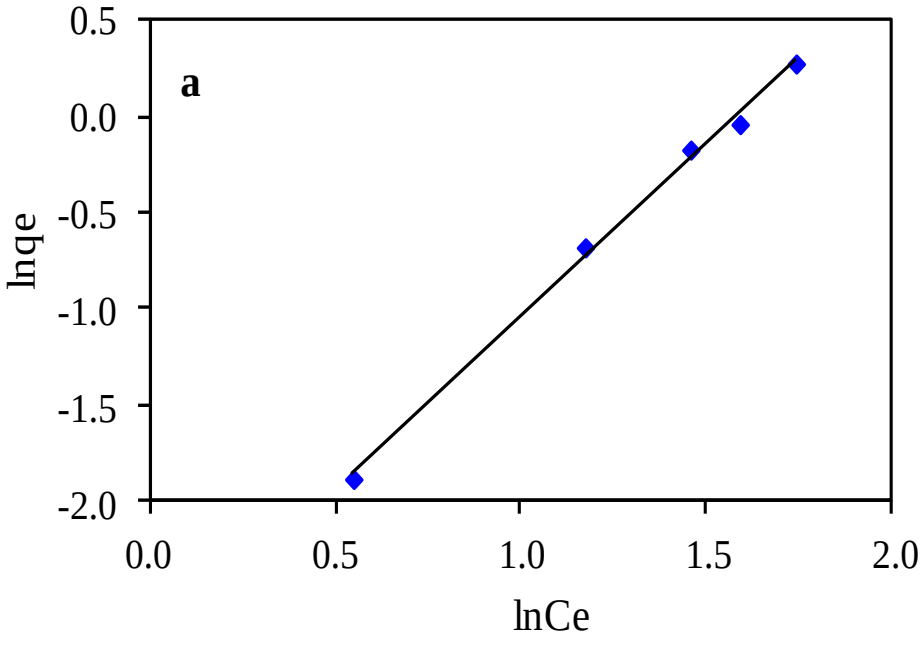


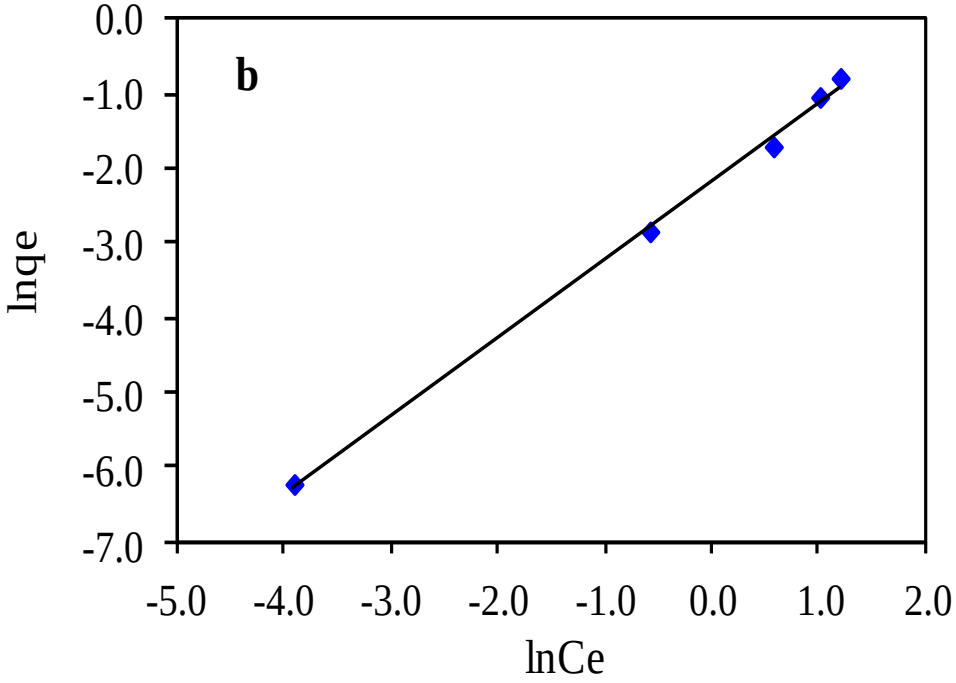

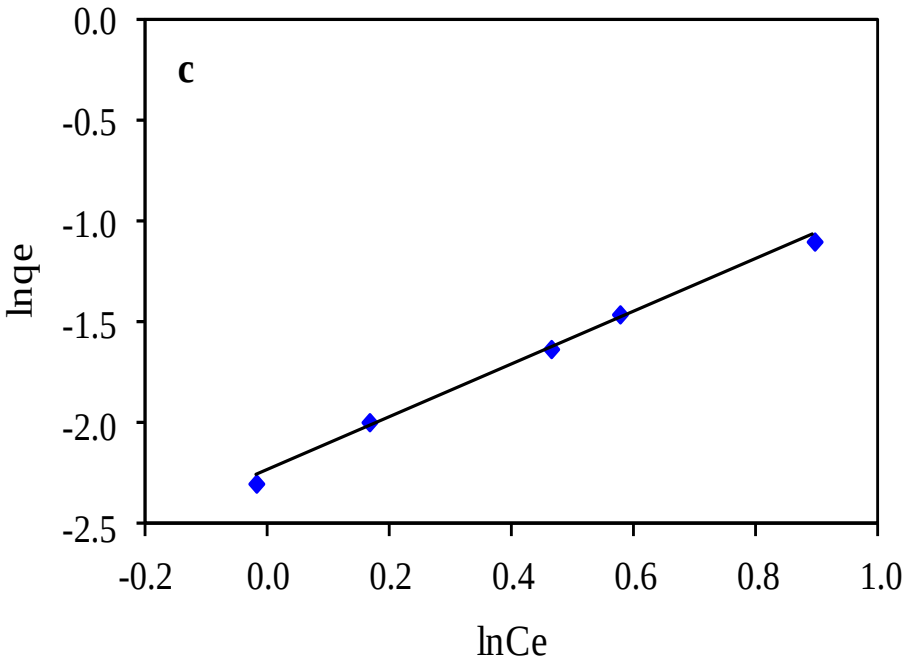


**Figure 7. 12 Freundlich model for adsorption of (a) dichloromethane (b) Chloroform (c) Carbon tetrachloride at different concentrations, and temperature 25˚C.**

### 7.5.3 Temkin isotherm model

The Temkin isotherm represents the quantity of heat needed for the adsorption by one layer of adsorbate on the surface of adsorbent. The linear form of Temkin model is given by:

$$\ln q_e = \frac{RT}{b_T} \ln K_T + \frac{RT}{b_T} \ln C_e \qquad (7.12)$$

Where $b_T$ is the temkin constant related to the heat of sorption (kJ/mol), $k_T$ is the equilibrium binding constant and is equal to the maximum binding energy (L/g), R is universal gas constant ($8.314 \times 10^{-3}$ ), and T is the absolute temperature (degrees Kelvin)

(M. Idrisa 2011). The plot of $q_e$ versus ln($C_e$) is illustrated in fig (7.13) and the isotherm constants were determined from the slope and intercept table (7.3).

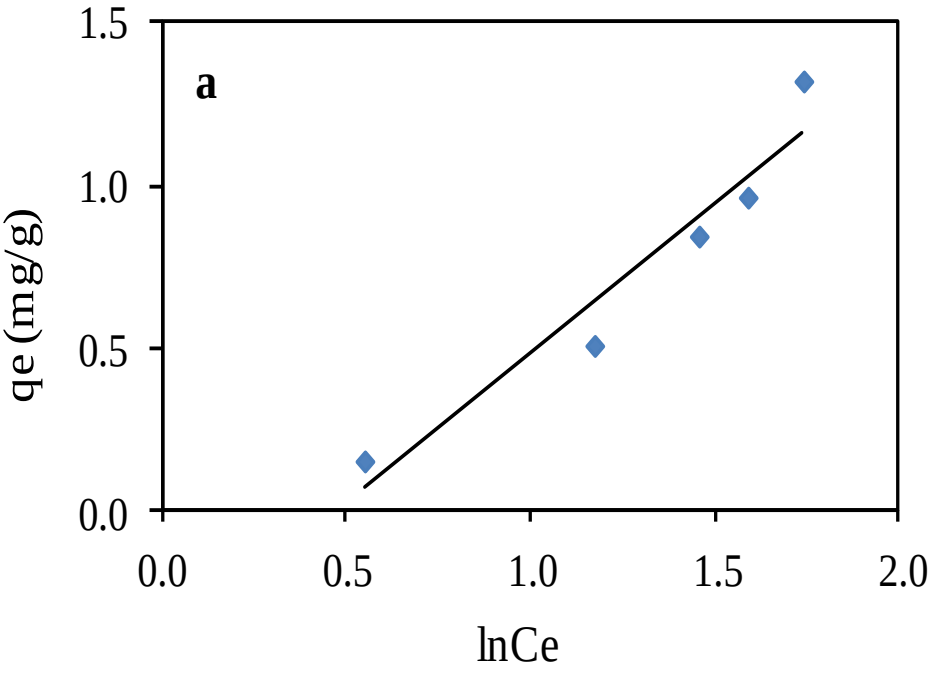


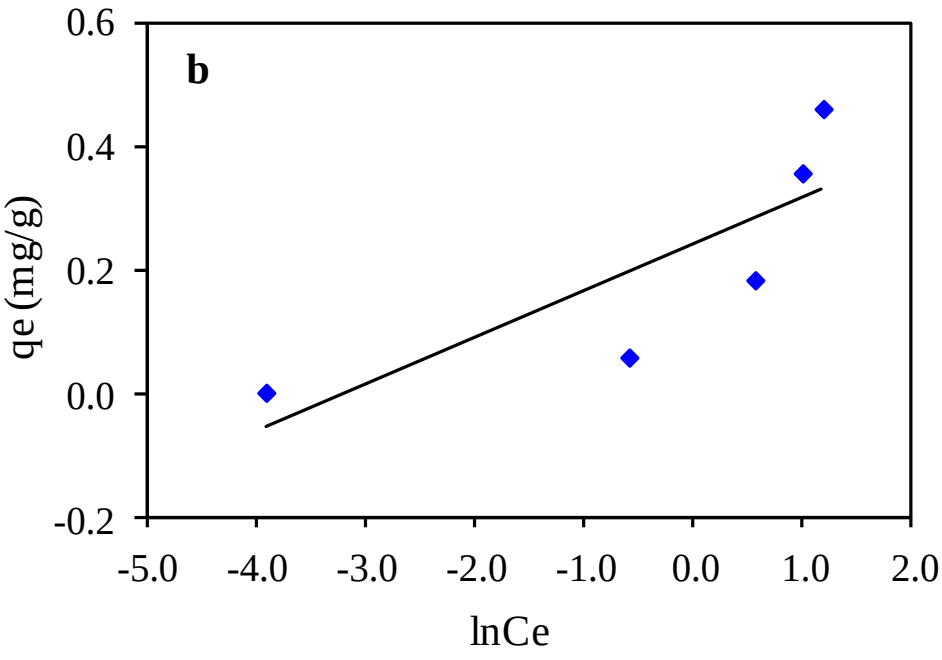

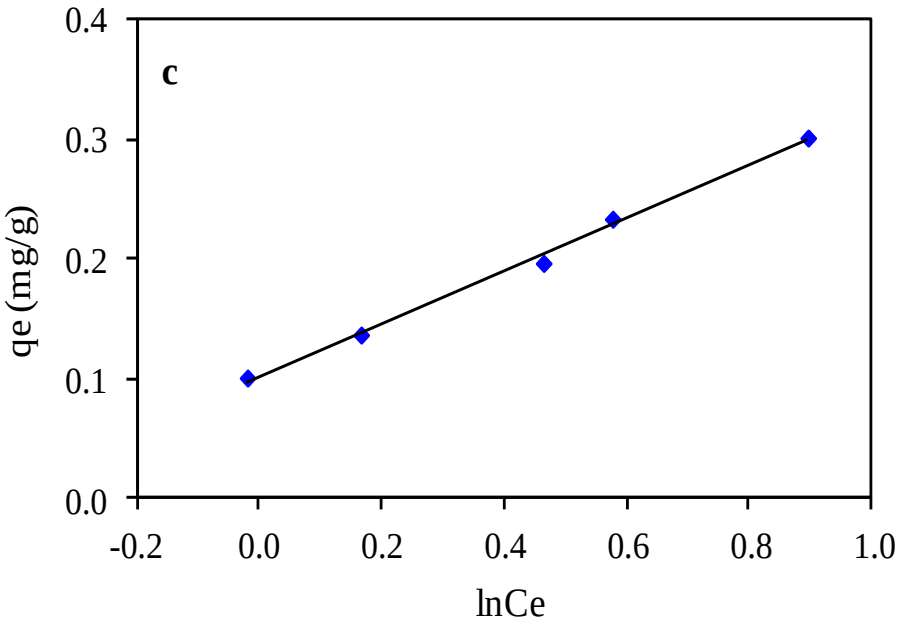


**Figure 7. 13 Temkin model for adsorption of (a) dichloromethane (b) Chloroform (c) Carbon tetrachloride at different concentrations, and temperature 25˚C.**

Table 7. 3 Langmuir, Freundlich, and Temkin isotherm constants for chlorinated hydrocarbon adsorption on CeO2–NP/AC.

| Compound | | Langmuir isotherm constants | | | | Freundlich isotherm constants | | | | Temkin isotherm constants | | |
|---|---|---|---|---|---|---|---|---|---|---|---|---|
| | T (K) | $q_m$ (mg/g) | $k_L$ (L/mg) | $R_L$ | $R^2$ | 1/n | n | $K_F$ | $R^2$ | $k_T$ (L/gm) | $b_T$ (KJ/mol) | $R^2$ |
| $CH_2Cl_2$ | 298.16 | 3.476 | 0.750 | 0.118 | 0.986 | 1.802 | 0.555 | 17.167 | 0.997 | 0.474 | 2.705 | 0.929 |
| $CH_3Cl$ | 298.16 | 7.283 | 7.151 | 0.014 | 0.983 | 1.049 | 0.954 | 8.602 | 0.998 | 3.170 | 33.008 | 0.666 |
| $CCl_4$ | 298.16 | 7.289 | 5.532 | 0.018 | 0.985 | 1.303 | 0.768 | 9.319 | 0.996 | 0.461 | 11.197 | 0.996 |

## 7.6 Regeneration of adsorbent

Regarding to the applications, the disposal of adsorbent as byproducts in the adsorption process is not economical; therefore, regeneration should be carried out (H. M. K. Yogesh Kumar 2013). The possibility of regenerating the adsorbent with a chemical and thermal treatment was tested. The chemical treatment was examined using solvent, and thermal treatment was conducting by heating the adsorbent/sorbent up to 100˚C. The material was tested for three cycles, and the results showed excellent re-generality with almost the same percentage of removal fig (7.14).

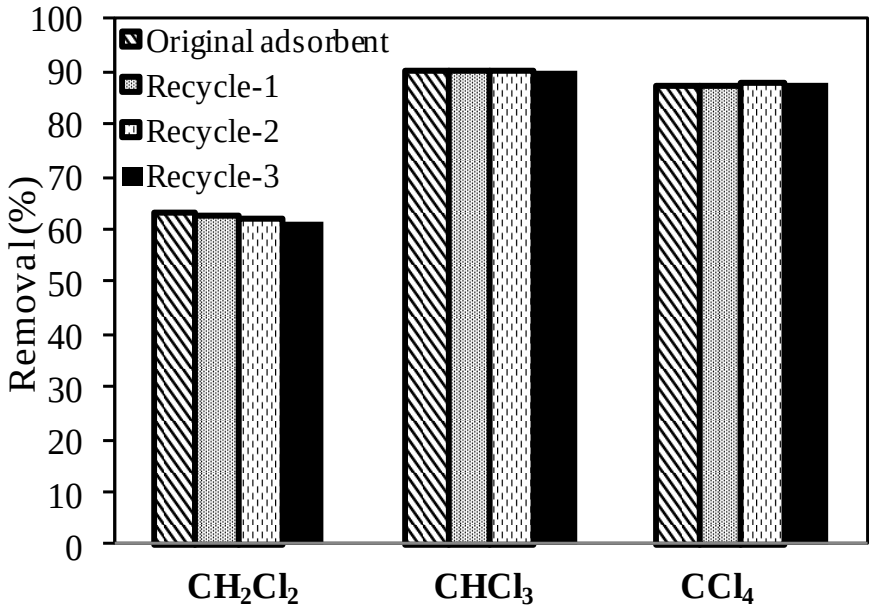


**Figure 7. 14 regenatration adsorption of (a) dichloromethane (b) Chloroform (c) Carbon tetrachloride at $SiO_2$–NP/AC dosage 0.1 g/L, contact time 60 min, and temperature 25˚C.**

# Conclusion

In this work, four adsorbents were synthesized: activated carbon derived from the rubber waste tires, ZnO-NP/AC, $SiO_2$-NP/AC and $CeO_2$-NP/AC composites. These materials were characterized by the means of SEM, EDX, FTIR, XRD, TGA. The prepared materials were tested for the adsorptive removal of dichloromethane, trichloromethane and carbon tetrachloride from aqueous media at ambient conditions, in batch adsorption mode. Waste rubber tires are cost-effective and are a readily available precursor material that can act as a better replacement source for commercial AC. The results indicate that the activated carbon loaded with nanopartciles exhibited better sorption activity than the pristine activated carbon. Also, the presence of the metal oxide nanoparticles enhances the thermal stability of the composites materials. The order of the sorption efficiency is as following: $SiO_2$-NP/AC > ZnO-NP/AC > $CeO_2$-NP/AC > AC. The experimental data were found to better obey the pseudo-second-order kinetic model, and the isotherms could be well described by the Langmiur isotherm equation for $SiO_2$-NP/AC and ZnO-NP/AC, but the AC and $CeO_2$-NP/AC were found to follow the Freundlich isotherm equation. All the materials were reused for several times after being thermally regenerated, and the obtained removal capacities were approximately the same for three cycles.

# References

(ATSDR), Agency for Toxic Substances and Disease Registry. *Toxicological profile for trichloroethylene (TCE).* Department of Health and Human Services, Atlanta, GA: U.S. Public Health Service, U.S., 1997.

A. Anfruns, M.J. Martin, M.A. Montes-Moran. " Removal of odourous VOCs using sludge-based adsorbents." *Chem. Eng. J* 166 (2011): 1022–1031.

A. Buekens, H. Huang. "Comparative evaluation of techniques for controlling the formation and emission of chlorinated dioxins/furans in municipal waste incineration." *J. Hazard. Mater* 62 (1998): 1–33.

A. Buekens, H. Huang. "Comparative evaluation of techniques for controlling the formation and emission of chlorinated dioxins/furans in municipal waste incineration." *J. Hazard. Mater* 62 (1998): 1–33.

A. Corma, P. Atienzar, H. Garcia, J.Y. Chane-Ching. "Hierarchically mesostructured doped CeO2 with potential for solar-cell use." *Nat. Mater* 3 (2004 ): 394–397.

A. Sari, M. Tuzen. "Biosorption of cadmium(II) from aqueous solution by red algae (Ceramium virgatum): equilibrium, kinetic and thermodynamic studies." *J. Hazard. Mater* 157 (2008 ): 448–454.

A. Sharma, K.G. Bhattacharyya. "Adsorption of chromium(VI) on Azadirachta indica (Neem) leaf powder." *Adsorption* 10 ( 2004): 327–338.

A.L. Willis, N.J. Turro, S. O'Brien. " Spectroscopic characterization of the surface of iron oxide nanocrystals." *Chem. Mater* 17 (2005): 5970–5975.

A.R. Cestari, E.F.S. Vieira, G.S. Vieira, L.E. Almeida. "The removal of anionic dyes from aqueous solutions in the presence of anionic surfactant using aminopro- pylsilica—a kinetic study." *J. Hazard. Mater.* 138 (2006 ): 133–141.

Adam, Farook, Jimmy Nelson Appaturi, and Anwar Iqbal. "The utilization of rice husk silica as a catalyst: Review and recent progress." *Catalysis Today* 190 (2012): 2-14.

Ali, Zeid A. ALOthman. Mu Naushad. Rahmat. "Kinetic, equilibrium isotherm and thermodynamic studies of Cr(VI) adsorption onto low-cost adsorbent developed from peanut shell activated with phosphoric acid." *Environ Sci Pollut Res* 20 (2013): 3351–3365.

Ariyadejwanich, P., Tanthapanichakoon, W., Nakagawa, K., Mukai, S. R., & Tamon, H. "Preparation and characterization of mesoporous activated carbon from waste tires." *Carbon* 41 (2003): 157-164.

Arjan Giaya, Robert W. Thompson, Raymond Denkewicz Jr. "Liquid and vapor phase adsorption of chlorinated volatile organic compounds on hydrophobic molecular sieves." *Microporous and Mesoporous Materials* 40 (2000): 1-3.

B. de Rivas, C. Sampedro, R.López-Fonseca et al. "Low-temperature combustion of chlorinated hydrocarbons over $CeO_2$/H-ZSM5 catalysts." (Applied Catalysis A: General) 417-418 (2012): 417-418.

B. Illy, B.A. Shollock, J.L. MacManus-Driscoll, M.P. Ryan, "Electrochemical growth of ZnO nanoplates." *Nanotechnology* 16 (2005): 320–324.

B. Pavoni, D. Drusian, a Giacometti, and M. Zanette."Assessment of organic chlorinated compound removal from aqueous matrices by adsorption on activated carbon." *Water research* 40 (2006): 3571-3579.

B.H. Hameed, A.L. Ahmad, K.N.A. Latiff,. "Adsorption of basic dye (methylene blue) onto activated carbon prepared fromrattan sawdust." *Dyes Pigm.* 75 (2007): 143–149.

B.L. Cushing, V.L. Kolesnichenko, C.J. O'Connor. " Recent advances in the liquid-phase syntheses of inorganic nanoparticles." *Chem. Rev* 104 (2004): 3893–3946.

B.Q. Cao, X.M. Teng, S.H. Heo, Y. Li, S.O. Cho, G.H. Li, W.P. Cai. " Different ZnO nanostructures fabricated by a seed-layer assisted electrochemical route and their photoluminescence and field emission properties." *J. Phys. Ch* 111 (2007 ): 2470–2476.

Bansode, R. R., Losso, J. N., Marshall, W. E., Rao, R. M., & Portier, R. J. "Adsorption of metal ions by pecan shell-based granular activated carbons." *Bioresource technology* 89 (2003): 115-119.

C. Xu, D. Kim, J. Chun, K. Rho, B. Chon, S. Hong, T. Joo. "Temperature controlled growth of ZnO nanowires and nanoplates in the temperature range 250–300 degrees C." *J. Phys. Chem* 110 (2006 ): 21741–21746.

C.V. Taty-Costodes, H. Fauduet, C. Porte, A. Delacroix. "Removal of Cd(II) and Pb(II) ions, from aqueous solutions, by adsorption onto sawdust of Pinus sylvestris." *J. Haz. Mat.* B105 (2003): 121–142.

Chiou, M. S., and Li, H. Y. "Equilibrium and kinetic modelling of adsorption of reactive dyes on cross-linked chitosan beads." *J. Hazard. Mater* 93 (2002): 233-248.

Chungsiriporn, Juntima, Charun Bunyakan, and Roumporn Nikom. "Toluene removal by oxidation reaction in spray wet scrubber: experimental, modeling and optimization." Songklanakarin." *J. Sci. Technol* 28 (2006): 1265-1274.

D. Verhulst, A. Buekens, P. Spencer, G. Eriksson. "Thermodynamic behavior of metal chlorides and sulfates under the conditions of incineration furnaces." *Environ. Sci. Technol* 30 (1996): 50–56.

Deng H, Yang L, Tao G, Dai J. " Preparation and characterization of activated carbon from cotton stalk by microwave assisted chemical activation—application in methylene blue adsorption from aqueous solution." *J Hazard Mater* 166 (2009): 1514–1521.

E. Dobrzynska, M. Posniak, M. Szewczynska, B. Buszewski. " Chlorinated volatile organic compounds-old, however, actual analytical and toxicological problem." *Crit. Rev. Anal. Chem* 40 (2010): 41–57.

E. Ramos-Ferna´ndez, J. Serrano-Ruiz, J. Silvestre-Albero, A. Sepu´ lveda-Escribano, F. Rodrı´guez-Reinoso. "The effect of the cerium precursor and the carbon surface chemistry on the dispersion of ceria on activated carbon." *J. Mater. Sci.* 43 (2008): 1525–1.

E.L. Brosha, R. Mukundan, D.R. Brown, F.H. Garzon, J.H. Visser. "Development of ceramic mixed potential sensors for automotive applications." *Solid State Ionics* 148 (2002): 61–69.

F. Calisir, F.R. Roman,L. Alamo,O. Perales,M.A. Arocha,S. Akman. "Removal of Cu(II) from aqueous solutions by recycled tire rubber." *Desalination* 249 (2009): 515–518.

F. Xu, Z.Y. Yuan, G.H. Du, T.Z. Ren, C. Bouvy, M. Halasa, B.L. Su. " Simple approach to highly oriented ZnO nanowire arrays: large-scale growth, photoluminescence and photocatalytic properties." *Nanotechnology* 17 (2006 ): 588–594.

F. Zhang, Q. Jin, S.W. Chan. "Ceria nanoparticles: size, size distribution, and shape Jpn." *J. Appl. Phys.* 95 (2004): 4319–4326.

Freundlich, H. "Uber die adsorption in l¨ osungen (adsorption in solution)." (Z. Phys. Chem) 57 (1906): 384–470.

G. Bereket, A.Z. Aroguz, M.Z. Ozel. " Removal of Pb(II), Cd(II), Cu(II), and Zn(II) from aqueous solutions by adsorption on bentonite." *J. Coll. Interf. Sci.* 187 (1997): 338–343.

G. Cunha, L. Romão, M. Santos, B. Araújo, S. Navickiene, V. Pádua. "Adsorption of trihalomethanes by humin: Batch and fixed bed column studies." *Bioresour. Technol* 101 ( 2010): 3345–3354.

G. Cunha, L. Romão, M. Santos, B. Araújo, S. Navickiene, V. Pádua. "Adsorption of trihalomethanes by humin: Batch and fixed bed column studies." (Bioresour. Technol) 101 (2010): 3345–3354.

G.H Chen, B.S. Fu, C.J. Cai, M.Q. Lu, Y. Yang, S.H. Yi, C. Xu, H. Li, G.S. Wang,T. Zhang. " A single-center experience of retransplantation for liver transplant recipients with a failing graft." *Transplant. Proc.* 40 (2008): 1485–1487.

Garg, V. K., Renuka Gupta, Anu Bala Yadav, and Rakesh Kumar. "Dye removal from aqueous solution by adsorption on treated sawdust." *Bioresource Technology* 89 (2003): 121-124.

Gialamouidis D., Mitrakas M., Liakopoulou-Kyriakides M. "Equilibrium, thermodynamic and kinetic studies sp.,Staphylococcus xylosus and Blakeslea trispora cells." *Journal of hazardous materials* 182 (2010): 672-680.

GM, Pajonk. "Some applications of silica aerogels." *Colloid and Polymer Science* 281 (2003): 637–651.

Gonzalez-Serrano, E., Cordero, T., Rodriguez-Mirasol, J., Cotoruelo, L., Rodriguez, J.J. "Removal of water pollutants with activated carbons prepared from H3PO4 activation of lignin from Kraft black liquors." *Water Res* 38 (2004): 3043–3050.

Gupta, Vinod K., Alok Mittal, Lisha Kurup, and Jyoti Mittal. "Adsorption of a hazardous dye, erythrosine, over hen feathers." *Journal of Colloid and Interface Science* 304 (2006): 52-57.

Gupta, Vinod K., Rajendra Prasad, and Azad Kumar. "Preparation of ethambutol–copper (II) complex and fabrication of PVC based membrane potentiometric sensor for copper." *Talanta* 60 (2003): 149-160.

Gupta, Vineet K., and Nishith Verma. " Removal of volatile organic compounds by cryogenic condensation followed by adsorption." *Chemical Engineering Science* 57 (2002): 2679-2696.

Senturk, Hasan Basri, Duygu Ozdes, Ali Gundogdu, Celal Duran, and Mustafa Soylak. "Removal of phenol from aqueous solutions by adsorption onto organomodified Tirebolu bentonite: equilibrium, kinetic and thermodynamic study." *Journal of Hazardous Materials* 172 (2009): 353-362.

H.B. Zeng, W.P. Cai, P.S. Liu, X.X. Xu, H.J. Zhou, C. Klingshirn, H. Kalt. "ZnO-based hollow nanoparticles by selective etching: Elimination and reconstruction of metal–semiconductor interface, improvement of blue emission and photo-catalysis." *ACS Nano* 2 (2008): 1661–1670.

Hamadi, Nadhem K., Sri Swaminathan, and Xiao Dong Chen. "Adsorption of paraquat dichloride from aqueous solution by activated carbon derived from used tires." *Journal of hazardous materials* 112 (2004): 133-141.

Hameed, B. H., Din, A. T. M., & Ahmad, A. L. "Adsorption of methylene blue onto bamboo-based activated carbon: kinetics and equilibrium studies." *Journal of Haz. Mat* 49 (2006): 1-7.

Ho YS, Mckay G, Wase DAJ, Foster CF. "Study of the sorption of divalent metal ions on to peat." *Adsorpt Sci Technol* 18 (2000): 639– 650.

Ho, Y. S., and Chiang, C. "Sorption studies of acid dyes by mixed sorbents." *Adsorption* 7 (2001): 139-147.

Hui KS, Chao CYH, Kot SC. "Removal of mixed heavy metal ions in wastewater by zeolite 4A and residual products from recycled coal fly ash.." *J. Hazard. Mater* 127,(2004): 89-101.

Hung, Chinte, Hsunling Bai, and Mani Karthik. ""Ordered mesoporous silica particles and Si-MCM-41 for the adsorption of acetone: A comparative study." *Separation and Purification technology* 64 (2009): 265-272.

J. L. Gurav, I. K. Jung, H. H. Park, E. S. Kang, and D. Y. Nadargi. "Silica aerogel: synthesis and applications." *Journal of Nanomaterials* 2010 (2010): 23.

J. Lemus, J. Palomar, L. Gomez-sainero, M. A. Gilarranz, and J. J. Rodriguez, ,". *Removal of chlorinated organic volatile compounds by gas phase adsorption with activated carbon. Chemical Engineering Journal* 211 (2012): 246-254.

J. Park, K.J. An, Y.S. Hwang, J.G. Park, H.J. Noh, J.Y. Kim, J.H. Park, N.M. Hwang, T.Hyeon. " Ultra-large-scale syntheses of monodisperse nanocrystals." *Nat. Mater* 3 (2004): 891–895.

J. Pires, A. Carvalho, M.B. de Carvalho. "Adsorption of volatile organic compounds in Y zeolites and pillared clays." *Microporous Mesoporous Mater* 43 (2001 ): 277–287.

J. Wang, S. Zheng, J. Liu, Z. Xu. "Tannic acid adsorption on amino-functionalized magnetic mesoporous silica." *Chem. Eng. J* 165 (2010 ): 10–16.

J.C. Serrano-Ruiz, E.V. Ramos-Ferna´ndez, J. Silvestre-Albero, A. Sepu´ lveda-Escribano, F. Rodrı´guez-Reinoso. "Preparation and characterization of CeO2 highly dispersed on activated carbon." *Mater. Res. Bull* 43 (2008): 1850–1857.

J.H. Lee, B.S. Kim, J.C. Lee, S. Park. "Removal of $Cu^{2+}$ ions from aqueous Cu-EDTA solution using ZnO nanopowder." In *Materials Science Forum* 486 (2005): 510-513.

J.R. Xiao, T.Y. Peng, R. Li, Z.H. Peng, C.H. Yan. "Preparation, phase transformation and photocatalytic activities of cerium-doped mesoporous titania nanoparticles." *J. Solid State Chem* 179 (2006): 1161–1170.

J.W. Lee, H.J. Jung, D.H. Kwak, P.G. Chung. "Adsorption of dichloromethane from water onto a hydrophobic polymer resin XAD-1600." *Water Res* 39 (2005 ): 617–629.

Jankowska, H., Swiatkowski, A., Choma, J. "Active Carbon." ( Ellis Horwood, Chichester, UK) 1991.

Jesus Lemus, M. Martin-Martinez, Jose Palomar, Luisa Gomez-Sainero, Miguel Angel Gilarranz, Juan J. Rodriguez. "Removal of chlorinated organic volatile compounds by gas phase adsorption with activated carbon." *Chemical Engineering Journal* 211-212 (2012): 246-254.

Jin Chul Joo, Chang Hyuk Ahn, Dae Gyu Jang, Young Han Yoon, Jong Kyu Kim, Luiz Campos, Hosang Ahn. *Photocatalytic degradation of trichloroethylene in aqueous phase using nano-ZNO/Laponite composites. Journal of hazardous materials* 263 (2013): 569-574.

K. P. Ramaiah, D. Satyasri, S. Sridhar, and a Krishnaiah. *Removal of hazardous chlorinated VOCs from aqueous solutions using novel ZSM-5 loaded PDMS/PVDF composite membrane consisting of three hydrophobic layers. Journal of hazardous materials* 261 (2013): 362-371.

K. Yogesh Kumar, H.B. Muralidhara, Y. Arthoba Nayaka, J. Balasubramanyam, H. Hanumanthapp. "Low-cost synthesis of metal oxide nanoparticles and their application in adsorption of commercial dye and heavy metal ion in aqueous solution." *Powder Technology* 246 (2013): 125-136.

Karthikeyan, S., P. Sivakumar, and P. N. Palanisamy. "Novel activated carbons from agricultural wastes and their characterization." *Journal of Chemistry* 5 (2008): 409-426.

L. Gomez-Sainero, X. Seoane, A. Arcoya. "Hydrodechlorination of carbon tetrachloride in the liquid phase on a Pd/carbon catalyst: kinetic and mechanistic studies." *Appl. Catal. B-Environ* 53 (2004): 101–110.

L. Li, M.H. Fan, R.C. Brown, J.H. Van Leeuwen, J.J. Wang, W.H. Wang, Y.H.Song, P.Y. Zhang. "Synthesis, properties, and environmental applications of nanoscale iron-based materials: a review." *Crit. Rev. Environ. Sci. Technol* 36 (2006 ): 405–431.

L. Wang, J. Zhang, R. Zhao, Y. Li, C. Li, C. Zhang. "Adsorption of Pb(II) on activated carbon prepared from Polygonum orientale Linn.: kinetics, isotherms, pH, and ionic strength studies." *Bioresour. Technol* 101 (2010): 5808–5814.

L. Yang, S. Zhou, G. Gu, L. Wu. " "Film-forming behavior and mechanical properties of colloidal silica/polymer latex blends with high silica load." *Journal of Applied Polymer Science* 129 (2013): 1434-1445.

L.Y. Wang, K.L. Zhang, Z.T. Song, S.L. Feng. " Ceria concentration effect on chemical mechanical polishing of optical glass." *Appl. Surf. Sci.* 253 (2007): 4951–4954.

Lagergren, Svenska. "About the theory of so-called adsorption of solution substances." *kunglia srenska vertens Ka psakademiens Handlingar* 24 (1898): 1-39.

Langmuir, I. "The constitution and fundamental properties of solids and liquids." *J. Am. Chem. Soc* 38 (1916): 2221–2295.

Lillo-Ródenas, M. A., D. Cazorla-Amorós, and A Linares-Solano. "Behaviour of activated carbons with different pore size distributions and surface oxygen groups for benzene and toluene adsorption at low concentrations." *Carbon* 43 ( 2005): 1758−1767.

Lillo-Ródenas, M. A., D. Cazorla-Amorós, and A. Linares-Solano. " Behaviour of activated carbons with different pore size distributions and surface oxygen groups for benzene and toluene adsorption at low concentrations." *Carbon* 43 ( 2005): 1758−1767.

López-Cortés, C., G. Osorio-Revilla, T. Gallardo-Velázquez, and S. Arellano-Cárdenas. "Adsorption of vapor-phase VOCs (benzene and toluene) on modified clays and its relation with surface properties." *Canadian Journal of Chemistry* 86 (2008): 305-311.

M. Ballikaya, S. Atalay, H. Alpay, F. Atalay. "Catalytic combustion of methylenechloride." *Combust. Sci. Technol* 120 (1996 ): 169–184.

M. Idrisa, Z. Ahmada, M. Ahmad. "Adsorption equilibrium of malachite green dye onto rubber seed coat based activated carbon." (International Journal of Basic & Applied Sciences IJBAS-IJENS) 11 (2011): 38-43.

M.A. Alvarez-Montero, L.M. Gomez-Sainero, J. Juan-Juan, A. Linares-Solano, J.J. Rodriguez. "Gas-phase hydrodechlorination of dichloromethane with activated carbon-supported metallic catalysts." *Chem. Eng. J* 162 (2010): 599–608.

M.A. Hassanien, K.S. Abou-El-Sherbini. " Synthesis and characterization of morin-functionalized silica gel for the enrichment of some precious metal ions." *Talanta* 68 (2006): 1550–1559.

M.K. Aroua, S.P.P. Leong, L.Y. Teo, C.Y. Yin, W.M.A.W. Daud. " Real-time determination of kinetics of adsorption of lead(II) onto palm shell-based activated carbon using ion selective electrode." *Bioresour. Technol.* 99 (2008): 5786– 5792.

McKay, G. "The adsorption of basic dye onto silica from aqueous–solution solid diffusion-model." *Chem. Eng. Sci* 39 (1984): 129-138.

Miguel, Guillermo San Fowler, Geoffrey D Dall'Orso, Marco Sollars, Christopher J. "Porosity and surface characteristics of activated carbons produced from waste tyre rubber." *Journal of Chemical Technology and Biotechnology* 77 (2002): 1-8.

Mittal A, Kurup L, Gupta VK. "Use of waste materials bottom ash and deoiled soya, as potential adsorbents for the removal of amaranth from aqueous solutions." *J Hazard Mater* 117 (2005): 171–178.

Mohd Nazri Idrisa, Zainal Arifin Ahmada, Mohd Azmier Ahmad. "Adsorption equilibrium of malachite green dye onto rubber seed coat based activated carbon." *International Journal of Basic & Applied Sciences IJBAS-IJENS* 11 (2011): 38-43.

Mui, E. L., Cheung, W. H., & McKay, G. "Tyre char preparation from waste tyre rubber for dye removal from effluents. Journal of hazardous materials,." 175 (2010): 151-158.

N. Zhang, R. Yi, R.R. Shi, G.H. Gao, G. Chen, X.H. Liu. "Novel rose-like ZnO nanoflowers synthesized by chemical vapor deposition." *Mater. Lett* 63 (2009): 496–499.

N.M. Mahmoodi, S. Khorramfar, F. Najafi. "Amine-functionalized silica nanoparticle: preparation, characterization and anionic dye removal ability." *Desalination* 279 (2011): 61–68.

Ouazene N, Sahmoune MN. "Equilibrium and kinetic modeling of astrazon yellow adsorption by sawdust: effect of important parameters." *International Journal of Chemical Reactor Engineering* 8 (2010).

P. Navarri, D. Marchal, A. Ginestet."Activated carbon fibre materials for VOC removal". *Filtration & separation* 38 (2001): 33-40.

Palacio, Luz A., Juliana Velásquez, Adriana Echavarría, Arnaldo Faro, F. Ramôa Ribeiro, and M. Filipa Ribeiro. "Total oxidation of toluene over calcined trimetallic hydrotalcites type catalysts." *Journal of hazardous materials* 177 (2010): 407-413.

Pan, H., Tian, M., Zhang, H., Zhang, Y., & Lin, Q. "Adsorption and Desorption Performance of Dichloromethane over Activated Carbons Modified by Metal Ions". *Journal of Chemical & Engineering Data* 58 (2013): 2449-2454.

Panda L, Das B, Rao DS, Mishra BK. "Application of dolochar in the removal of cadmium and hexavalent chromium ions from aqueous solutions". *Journal of hazardous materials* 192 (2011): 822-831.

Parker, W.J. " A multi-parameter sensitivity analysis of a model describing the fate of volatile organic compounds in trickling filters." *Journal of the Air and Waste Management Association* 47 (1997): 871–880.

Pires, J., Carvalho, A., Carvalho de, M.B. " Adsorption of volatile organic compounds in Y zeolites and pillared clays." *Microporous Mesoporous Mater* 43 ( 2001): 277–287.

Pires, João, Ana Carvalho, Patrícia Veloso, and M. Brotas de Carvalho. "Preparation of dealuminated faujasites for adsorption of volatile organic compounds." *Journal of Materials Chemistry* 12 (2002): 3100-3104.

R. Iranpour, H. Coxa, M. Deshusses, E. Schroeder. "Literature review of air pollution control biofilters and biotrickling filters for odor and volatile organic compound removal." *Environ. Prog.* 24 (2005): 254–267.

R. Murillo, E. Aylón, M.V. Navarro, M.S. Callén, A. Aranda, A.M. Mastral. "The application of thermal processes to valorise waste tyre." *Fuel Process. Technol* 87 (2006): 143–147.

R. Serna-Guerrero, Y. Belmabkhout, A. Sayari. " Modeling $CO_2$ adsorption onamine-functionalized mesoporous silica. 1. A semi-empirical equilibrium model." *Chem. Eng. J* 161 (2010): 173–181.

R.A. Meyers, D. Kender Dittrick. *The Wiley encyclopedia of environmental pollution and cleanup (2 volumes)*. John Wiley and Sons, 1999.

R.E. Wing, W.H. Doanc, C.R. Russell. " Insoluble starch xanthate: use in heavy metal removal." *J. Appl. Polymer Sci.* 19 (1975): 847.

R.F. Dunn, M.M. El-Halwagi. " Optimal design of multicomponent VOCs conden- sation systems." *Journal of Hazardous Materials* 38 (1994): 187–206.

Rafał Janus, Piotr Kus´trowski, Barbara Dudek, Zofia Piwowarska, Andrzej Kochanowski. "Removal of methyl–ethyl ketone vapour on polyacrylonitrile-derived carbon/mesoporous silica nanocomposite adsorbents." *Microporous and Mesoporous Materials* 145 (2011): 65-73.

Rajmohan T, Palanikumar K, Arumugam S. " Synthesis and characterization of sintered hybrid aluminium matrix composites reinforced with nanocopper oxide particles and microsilicon carbide particles". *Composites Part B: Engineering* 59 (2014): 43-49.

Rexwinkel, G., Heesink, B.B.M., van Swaaij, P.M. "Adsorption of halogenated hydrocarbons from aqueous solutions by wetted and nonwetted hydrophobic and hydrophilic sorbents: equilibria." *J. Chem. Eng. Data* 44 ( 1999): 1139–1145.

RM Laine, KY Blohowiak, TR Robinson, ML Hoppe, P Nardi, J Kampf, J Uhm. "Synthesis of pentacoordinate silicon complexes from $SiO_2$." *Nature* 353 (1991): 642–644.

Robert Pełech, EugeniuszMilchert,Marcin Bartkowiak. "Fixed-bed adsorption of chlorinated hydrocarbons from multicomponent aqueous solution onto activated carbon: Equilibrium column model." *Journal of colloid and interface science* 296 (2006): 458-64.

Rodrigues LA, Maschio LJ, da Silva RE, da Silva MLCP. " Adsorption of Cr(VI) from aqueous solution by hydrous zirconi- um oxide." *J Hazard Mater* 173 (2010): 630–636.

Rösch, Lutz, Peter John, and Rudolf Reitmeier. *Silicon compounds, organic. Ullmann's Encyclopedia of Industrial Chemistry* (2000).

S. Atalay, H. Alpay, F. Atalay. "Catalyst preparation and testing for catalytic combustion of chloromethanes, Principles and methods for accelerated catalyst design and testing." *Nato Sci. Ser* 69 (2002): 355–364.

S. Carrettin, P. Concepcion, A. Corma, J.M.L. Nieto, V.F. Puntes. " Nanocrystalline CeO2increases the activity of an for CO oxidation by two orders of magnitude." *Angew. Chem. Int. Ed* 43 (2004 ): 2538–2540.

S. Karagoz, T. Tay, S. Ucar, M. Erdem. "Activated carbons from waste biomass by sulfuric acid activation and their use on methylene blue adsorption." *Bioresour. Technol* 99 (2008): 6214–6222.

S. Tsunekawa, K. Ishikawa, Z.Q. Li, Y. Kawazoe, A. Kasuya. " Origin of anomalous lattice expansion in oxide nanoparticles." *Phys. Rev. Lett.* 85 (2000): 3440–3443.

S. Tsunekawa, T. Fukuda, A. Kasuya. "Blue shift in ultraviolet absorption spectra of monodisperse $CeO_{2-x}$ nanoparticles." *Jpn. J. Appl. Phys* 87 (2000): 1318–1321.

S. Yabe, T. Sato. " Cerium oxide for sunscreen cosmetics." *J. Solid State Chem* 171 (2003): 7–11.

Salvador, S., J-M. Commandré, and Y. Kara. "Thermal recuperative incineration of VOCs: CFD modelling and experimental validation." *Applied thermal engineering* 26 (2006): 2355-2366.

Selvi, K., S. Pattabhi, and K. Kadirvelu. "Removal of Cr (VI) from aqueous solution by adsorption onto activated carbon." *Bioresource Technology* 80 (2001): 87-89.

Shawwa, A.R., Smith, D.W., Sego, D.C. "Color and chlorinated organics removal from pulp mills wastewater using activated petroleum coke. ." *Water Res.* 35 ( 2001): 745–749.

Singh VK, Tiwari PN. "Removal and recovery of chromium(VI) from industrial waste water." *Journal of Chemical Technology and Biotechnology* 69, no. 3 (1997): 376-382.

Soleimani Dorcheh, A., and M. H. Abbasi."Silica aerogel; synthesis, properties and characterization." *Journal of materials processing technology* 199 (2008): 10-26.

Sonoyama, N., Ezaki, K., Sakata, T. " Continuous electrochemical decomposition of dichloromethane in aqu- eous solution using various column electrodes." *Advances in Environmental Research* 6 (2001): 1–8.

Sotelo, J.L., Ovejero, G., Delgado, J.A., Martı ´nez, I. "Comparison of adsorption equilibrium and kinetics of four chlorinated organics from water onto GAC." *Water Res* 36 (2002): 599–608.

Srivastava SK, Gupta VK, Dwivedi MK, Jain S. Vol. 32. Anal Proc Incl Anal Commun, 1995.

Srivastava, V.C., Swamy, M.M., Mall, I.D., Prasad, B., Mishara, I.M. " Adsorptive removal of phenol by bagasse fly ash and activated carbon: Equilibrium, kinetics and thermodynamic" *Colloids and Surfaces A: Physicochemical and Engineering Aspects* 272 (2006): 89-104.

Stenzel, M.H., Gupta, S.U.,. "Air pollution control with granular activated carbon and air stripping." *Journal of Hazardous Waste Management* 35 (1995): 1304–1309.

T. Ghoshal, S. Kar, S. Chaudhuri. " ZnO doughnuts: controlled synthesis, growth mechanism, and optical properties." *Cryst. Growth Des.* 7 (2007): 136–141.

T.M. Shang, J.H. Sun, Q.F. Zhou, M.Y. Guan. "Controlled synthesis of various morphologies of nanostructured zinc oxide: flower, nanoplate, and urchin." *Cryst. Res. Technol* 42 (2007): 1002–1006.

T.P. Chou, Q.F. Zhang, G.E. Fryxell, G.Z. Cao. "Hierarchically structured ZnO film for dye-sensitized solar cells with enhanced energy conversion efficiency ." *Adv. Mater* 19 (2007 ): 2588–2592.

Treybal, R.E. *Mass Transfer Operations.* 2nd ed. McGraw Hill, New York, 1968.

Uhrlandt, S. "Kirk-Othmer Encyclopedia of Chemical Technology." Hoboken: Wiley, 2006.

V. Hecht, D. Brebbermann, P. Bremer, W.D. Deckwer. "Cometabolic degradation of trichloroethylene in a bubble column bioscrubber." *Biotechnology and Bioengineering* 47 ( 1995): 461–469.

V. Janda, P. Vasek, J. Bizova, and Z. Belohlav."Kinetic models for volatile chlorinated hydrocarbons removal by zero-valent iron". *Chemosphere* 54 (2004): 917-925.

V.J.P. Poots, G. McKay, J.J. Healy."Removal of basic dye from effluent using wood as an adsorbent". *Journal (Water Pollution Control Federation)* (1978): 926-935.

V.K. Gupta, A. Rastogi. "Biosorption of lead from aqueous solutions by green algae Spirogyra species: kinetics and equilibrium studies,." *J. Hazard. Mater* 152 (2008): 407–414.

V.K. Gupta, Bina Gupta,Arshi Rastogi,Shilpi Agarwal,Arunima Nayak. "A comparative investigation on adsorption performances of mesoporous activated carbon prepared from waste rubber tire and activated carbon for a hazardous azo dye—Acid Blue 113." *Journal of Hazardous Materials* 186 (2011 ): 891–901.

V.K. Gupta, C.K. Jain, A. Imran, M. Sharma, V.K. Saini. "Removal of cadmium and nickel from wastewater using bagassefly ash a sugar industry waste." *Water Res.* 37 (2003): 4038–4044.

V.K. Gupta, Suhas. " Application of low-cost adsorbents for dye removal – a review." *Journal of Environment Management* 90 (2009 ): 2313–2342.

Vinod Kumar Gupta, Imran Ali, Tawfik A. Saleh, M. N. Siddiqui and Shilpi Agarwal. "Chromium removal from water by activated carbon developed from waste rubber tires." *Environ Sci Pollut Res* 20 (2013 ): 1261–1268.

Vivero-Escoto, Juan L., Brian G. Trewyn, and Victor S-Y. Lin. "Mesoporous silica nanoparticles: synthesis and applications." *Annu. Rev. Nano Res* 3 (2010): 191-231.

W.G. Shim, J.W. Lee, H. Moon. "Heterogeneous adsorption characteristics of volatile organic compounds (VOCs) on MCM-48." *Sep. Sci. Tech.* 41 (2006): 3693–3719.

W.J. Weber, J.C. Morriss. "Kinetics of adsorption on carbon from solution." *J. Sanit. Eng. Div. Am. Soc. Civil Eng* 89 (1963): 31–60.

W.P. Cunningham, M.A. Cunningham, B. Saigo. *Environmental Science, a Global Concern.* New York, USA: Mc Graw-Hill Education, 2005.

W.S. Wan Ngah, S. Ab Ghani, A. Kamari. " Adsorption behavior of Fe(II) and Fe(III) ions in aqueous solution on chitosan and cross-linked chitosan beads." *Bioresour Technol.* 96 (2005): 443–450.

Wang S B, Ma Q, Zhu Z H. "Characteristics of coal fly ash and adsorption application." *Fuel* 87 (2008): 3469–3473.

Wang, Shaobin, and Z. H. Zhu. "Effects of acidic treatment of activated carbons on dye adsorption." *Dyes and Pigments* 75 (2007): 306-314.

Weber T.W., Chakkravorti R.K. "Pore and solid diffusion models for fixed-bed absorbers." *AlChE. J* 20 (1974): 228-238.

Wu, Chung-Hsin. "Adsorption of reactive dye onto carbon nanotubes: equilibrium, kinetics and thermodynamics." *Journal of hazardous materials* 144 (2007): 93-100.

X. Ren, C. Chen, M. Nagatsu, X. Wang. "Carbon nanotubes as adsorbents in environmental pollution management: a review." *Chem. Eng. J* 170 (2011 ): 395–410.

X. Wang, J. Zhuang, Q. Peng, Y.D. Li. " A general strategy for nanocrystal synthesis." *Nature* 437 (2005 ): 121–124.

X. Zhang, X. Zhao, J. Hu, C. Wei, H.T. Bi. " Adsorption dynamics of trichlorofluoromethane in activated carbon fiber beds." *Journal of hazardous materials* 186 (2011): 1816-1822.

X.B. Wang, W.P. Cai et al. "Mass production of micro/nanostructured porous ZnO plates and their strong structurally enhanced and selective adsorption performance for environmental remediation." *J. Mater. Chem* 20 (2010): 8582–8590.

X.F. Ma, Y.Q. Wang, M.J. Gao, H.Z. Xu, G.A. Li. " A novel strategy to prepare ZnO/PbS heterostructured functional nanocomposite utilizing the surface adsorption property of ZnO nanosheets." *Catal. Today* 158 (2010): 459–463.

X.L Cao, H.B. Zeng, M. Wang, X.J. Xu, M. Fang, S.L. Ji, L.D. Zhang. "Large scale fabrication of quasi-aligned ZnO stacking nanoplates." *J. Phys. Chem* 112 (2008):5267–5270.

Xie, B., S. B. Liang, Y. Tang, W. X. Mi, and Y. Xu. "Petrochemical wastewater odor treatment by biofiltration." *Bioresource technology* 100 (2009): 2204-2209.

Xifei Yang, Zhiguo Shen, Bing Zhang, Jianping Yang, Wen-Xu Hong, Zhixiong Zhuang. "Silica nanoparticles capture atmospheric lead: implications in the treatment of environmental heavy metal pollution." *Chemosphere* 90 (2013): 653-6.

Y. Ju-Nam, J.R. Lead. "Manufactured nanoparticles: an overview of their chemistry, interactions and potential environmental implications." *Sci. Total Environ* 400 (2008): 396–414.

Y. Nuhoglu, E. Malkoc. "Thermodynamic and kinetic studies for environmentaly friendly Ni(II) biosorption using waste pomace of olive oil factory." *Bioresour. Technol* 100 ( 2009): 2375–2380.

Y. Wu, S. Zhang, X. Guo, H. Huang. "Adsorption of chromium(III) on lignin." *Biore-sour. Technol* 99 (2008): 7709–7715.

Y.H. Li, Z. Luan, X. Xiao, C. Xu, D. Wu, B.Wei. "Removal of Cu2+ ions from aqueous solutions by carbon nanotubes." *Adsorpt. Sci. Technol.* 21 ( 2003): 475–485.

Y.H. Xu, H.R. Chen, Z.X. Zeng, B. Lei. "Investigation on mechanism of photocatalytic activity enhancement of nanometer cerium-doped titania." *Appl. Surf. Sci.* 252 (2006): 8565–8570.

Y.S. Ho, G. McKay. " Sorption of dye from aqueous solution by peat." *Chemical Engineering Journal* 70 (1998): 115-124.

Yu, J.-J., Chou, S.-Y. "Contaminated site remedial investiga- tion and feasibility removal of chlorinated volatile organic compounds from groundwater by activated carbon fiber adsorption." *Chemosphere* 41 (2000): 371–378.

Yun, J.-H., Choi, D.-K., Kim, S.-H. " Adsorption equilibria of chlorinated organic solvents onto activated carbon." *Ind. Eng. Chem. Res* 37 (1998): 1422–1427.

Z.H. Jing, J.H. Zhan. " Fabrication Gas-sensing properties of porous ZnO nanoplates." *Adv. Mater.* 20 (2008): 4547–4551.

Z.M. de Pedro, L.M. Gomez-Sainero, E. Gonzalez-Serrano, J.J. Rodriguez. "Gas phase hydrodechlorination of dichloromethane at low concentrations with palladium/carbon catalysts." *Ind. Eng. Chem. Res* 45 (2006): 7760–7766.

Zhang H, Tang Y, Cai D, Liu X, Wang X, Huang Q, Yu Z. "Hexavalent chromium removal from aqueous solution by algal bloom residue derived activated carbon: equilibrium and kinetic studies." *Journal of hazardous materials* 181 (2010): 801-808.

Zhang Q, Zhang K, Xu D, et al. "CuO nanostructures. Synthesis, characterization, growth mechanisms, fundamental properties, and applications." *Progress in Materials Science* 60 (2014): 208-337.

# Vitae


| | |
|---|---|
| Name | : MOHAMMED SALAH AHMED ABDELBASSIT |
| Nationality | : Sudanese |
| Date of Birth | : 05/04/1988 |
| Email | : mohammed.bassit@live.com |
| Address | : Khartoum, Sudan |
| Academic Background | : B.Sc. in Chemistry from Sudan University of Science and Technology |


## Career history:

| | |
|---|---|
| January 2012-May 2014 | : Research assistant at KFUPM, Saudi Arabia |
| May 2011 - January 2012 | : Quality control chemist in Emarati Foodstuff & plastic packing company in (Sudan) |
| October 2009 - February 2011 | : Teaching assistant in the chemistry department at Sudan University of Science and Technology |

## Training and Applied Courses :

- ✓ Quality Control of water processing and soft drinks in Nile soft drinking factory, duration (05.12.2009-20.12.2009) and Dal Foodstuffs Company from (01.03.2010- 30.03.2010).
- ✓ Ministry of science and technology central labs (Sudan) in the analytical chemistry department mastering different techniques, with adequate specificity with atomic absorption spectroscopy "AAS" Gas Chromatography –Mass Spectrometry "GC-MS"

High Performance Liquid Chromatography “HPLC” & “UV-VIS” Spectroscopy From 25.4.2010 up to 04.05.2010.

- ✓ The Research Institute (R.I) at the King Fahad University of Petroleum and Minerals as a part-time research assistant in water and environment center, my job was on soil and water samples pretreatment and analysis of trace metals by ICP-MS & ICP-OES instruments from (01.02.2013-31.07.2013).